

Detection of Nonstructural Protein NSm1 in Rift Valley Fever Virus
Virions Assembled in Insect but not Mammalian Cells

by

Alan McGreevy

A Thesis submitted to the Faculty of Graduate Studies of
The University of Manitoba

In partial fulfilment of the requirements of the degree of

MASTER OF SCIENCE

Department of Medical Microbiology

University of Manitoba

Winnipeg, MB

Copyright © 2012 by Alan McGreevy

Abstract

Rift Valley fever virus is a zoonotic pathogen that is transmitted between mosquitoes and mammals such as sheep, cattle and humans. It is an enveloped negative-sense single-stranded RNA virus, which is a member of the family *Bunyaviridae* and the genus *Phlebovirus*. During replication, RVFV produces a 78 kDa glycoprotein NSm1 of unknown function, believed to be nonstructural. Here I show that NSm1 is incorporated into RVFV virions assembled in C6/36 mosquito cells, but not in virions assembled in Vero E6 mammalian cells. The presence of NSm1 in insect-amplified virions was demonstrated through repeated immunoblots of purified virions and further supported by mass spectrophotometric confirmation of the identity of immunoblot-positive protein bands. This research appears to be the first evidence that distinct viral protein profiles are correlated to the host cell in which replication occurred.

Acknowledgments

I could not have achieved this tremendous accomplishment without the love, support, encouragement and advice of my family and friends. I know that this document cannot possibly encapsulate everything that I have learned during this degree: there are so many jewels of planning and scientific technique now filling my academic treasure chest that I almost wish I could do it over again to show how much better my work would be. Almost.

Thank you to my supervisor Hana Weingartl for giving me the opportunity to do this research; I have appreciated her experience and insight. Thank you to my advisory committee Kevin Coombs and Klaus Wrogemann for their support, understanding and guidance.

I've learned so much from many friends and teachers at the National Centre for Foreign Animal Disease. Yohannes Berhane was an incredible support and I hope I've learned enough to make him proud. This work would not have been possible without the patience, support and expertise of Peter Marszal and Greg Smith, and the supporting work of Jieyuan Jiang and Shunzhen Zhang. Thank you to Kathy Handel and Tamiko Hisanaga for their expertise with DNA and to Marsha Leith and Tim Salo for their formidable molecular biology skills. Thank you to Lynn Burton for lending her electron microscopy expertise to my cause and to Mike Carpenter and Xiaojie Hu of the National Microbiology Laboratory for sharing with me a glimpse of their world of mass spectrometry.

All the guidance, advice, encouragement and support made this document possible. Thank you.

Table of Contents

Abstract.....	i
Acknowledgements.....	ii
Table of Contents.....	iii
List of Tables.....	vi
List of Figures.....	vii
Abbreviations.....	ix
Chapter 1: Introduction.....	1
1.1 History.....	1
1.2 Pathogenesis and pathology in the natural mammalian host.....	3
1.2.1 Sheep.....	3
1.2.2 Cattle.....	4
1.2.3 Goats.....	4
1.2.4 Camels.....	5
1.2.5 Humans.....	5
1.3 Genetics of host resistance.....	6
1.4 Mosquitoes.....	8
1.5 Genome and proteome.....	11
1.6 Virus structure.....	13
1.7 RVFV replication in C6/36 cells and in Vero E6 cells.....	15
1.8 Differences in RVFV replication between C6/36 and Vero E6 cells.....	16
1.9 Structural proteins.....	18
1.9.1 RNA-dependent RNA polymerase L.....	18
1.9.2 Nucleocapsid protein.....	18
1.9.3 Glycoproteins Gn and Gc.....	19
1.10 Accessory proteins.....	19
1.10.1 Nonstructural protein NSs	19
1.10.2 Nonstructural M segment proteins.....	22
1.10.3 Nonstructural protein NSm2.....	22
1.10.4 Nonstructural protein NSm1.....	24
1.11 Overview of objectives and statement of hypothesis.....	25
Chapter 2: Methodology.....	28
2.1 Cells.....	28
2.1.1 Vero E6 cells.....	28
2.1.2 C6/36 cells.....	29
2.2 Production of virus stocks.....	30
2.3 Plaque titration.....	30
2.4 Antibodies.....	31

2.5 Recombinant NSm1.....	33
2.6 Immunoblotting.....	38
2.6.1 Protein separation and transfer.....	38
2.6.1 Chromogenic immunoblots.....	39
2.6.2 Enhanced chemiluminescence immunoblots.....	41
2.7 RVFV proteins expressed in mammalian or insect cells.....	41
2.8 Virus preparation and concentration.....	42
2.8.1 Viral growth curves.....	42
2.8.2 Virus purification with ultracentrifugation through a sucrose cushion.....	42
2.8.3 Virus concentration using filtration.....	43
2.9 Virus purification.....	44
2.9.1 Virus purification with polyethylene glycol precipitation and ultracentrifugation.....	44
2.9.2 Virus purification using filtration and gradient ultracentrifugation.....	46
2.9.3 Dialysis for removal of iodixanol.....	48
2.10 Mass spectrometry.....	48
2.11 Electron microscopy.....	50
2.12 Comparative serum neutralization.....	50
Chapter 3: Results.....	51
3.1 Expression and purification of recombinant NSm1.....	51
3.2 Development of NSm1-specific antibodies.....	56
3.3 Preparation of RVFV stocks.....	57
3.4 Selected RVFV proteins expressed in mammalian or insect cells.....	60
3.5 Virus growth and purification.....	62
3.6 RVFV virions assembled in mammalian or insect cells.....	65
3.7 To confirm presence of virions in preparations – N immunoblots.....	66
3.8 To confirm purity of the virions preparations – NSs immunoblots.....	70
3.9 Detection of NSm1 in virions.....	70
3.10 Mass spectrometry detection of NSm1.....	73
3.11 Virion glycoproteins Gn and Gc.....	79
3.12 Electron microscopy of virions.....	79
3.13 Comparative serum neutralization.....	81
Chapter 4: Discussion.....	85
4.1 Summary of findings.....	85
4.2 RVFV production and titration.....	85
4.3 RVFV replication in Vero E6 and C6/36 cells.....	87
4.4 RVFV virions produced in Vero E6 and C6/36 cells.....	89
4.5 Possible effects of incorporating NSm1 into C6/36-amplified virions...	92

4.6 Significance of findings.....	94
4.7 Significance for potential research.....	95
4.8 Conclusion.....	97
References.....	99
Appendixes.....	109
Appendix A: DNA sequences.....	109
Appendix B: Buffers and media.....	110
Appendix C: Protocols.....	117
Appendix D: Supplemental figures.....	143

List of Tables

Table 1: Proteins expressed by RVFV.....	14
Table 2: Primary and secondary antibodies used in immunoblots.....	40

List of Figures

Figure 1 - Proteins translated from the RVFV M-segment.....	12
Figure 2 - The 38 N-terminal amino acids of NSm1 analyzed for antigenicity, hydrophobicity and tertiary structure by residue.....	32
Figure 3 - Agarose gel of the DNA products of RT-PCR of the RVFV ZH501 NSm1 gene.....	52
Figure 4 - Agarose gel of PCR screening of TOP10 bacterial colonies transformed with pET-100 RVFV NSm1.....	53
Figure 5 - Agarose gel of pET-100 RVFV NSm1 plasmids following restriction endonuclease digestion.....	54
Figure 6 - Immunoblots for the detection of rNSm1 expression in the soluble and insoluble cell lysate fractions following IPTG-induced expression of pET-100 RVFV NSm1.....	55
Figure 7 - Detection of recombinant NSm1 using R1108 rabbit anti-NSm1 polyclonal serum.....	58
Figure 8 - Agarose gel of the PCR amplification of the <i>Aedes albopictus</i> mitochondrial DNA cytochrome C species marker gene.....	59
Figure 9 - Infection of C6/36 with RVFV at multiple MOI, images taken at 4 dpi.....	61
Figure 10 - Immunoblots of Vero E6 or C6/36 cell lysates over a 21 hour time course.....	62
Figure 11 - Production of RVFV in cell culture over time.....	64
Figure 12 - Immunoblot of Vero E6 RVFV and C6/36 RVFV with anti-nucleocapsid (N) rabbit serum.....	67
Figure 13 - Immunoblot of Vero E6 RVFV and C6/36 RVFV following polyethylene glycol precipitation, resuspension and ultracentrifugation through a sucrose or iodixanol gradient.....	68
Figure 14 - Immunoblot of Vero E6 RVFV and C6/36 RVFV following polyethylene glycol precipitation, resuspension and ultracentrifugation through a sucrose or iodixanol gradient, bound with rabbit R1108 polyclonal anti-NSm1 serum.....	69
Figure 15 - Immunoblot of Vero E6 RVFV and C6/36 RVFV following polyethylene glycol precipitation, resuspension and ultracentrifugation through an iodixanol gradient.....	72
Figure 16 - ECL western blots of purified RVFV virions from Vero E6 or C6/36 cells.....	74

Figure 17 - Denaturing PAGE of Vero E6 RVFV and C6/36 RVFV with numbered boxes indicating gel slices excised for mass spectrometry following PEG precipitation, resuspension and continuous gradient ultracentrifugation, stained using Coomassie G-250 SimplyBlue protein stain.....	75
Figure 18 - Mass spectrometry coverage of NSm1 following Mascot analysis of detected ions.....	77
Figure 19 - Liquid chromatography electrospray ionization tandem mass spectrometry.....	78
Figure 20 - A composite of Figures 16 and 17 showing denaturing PAGE of Vero E6 RVFV and C6/36 RVFV following polyethylene glycol precipitation and resuspension.....	80
Figure 21 - Electron micrographs of RVFV virions produced in Vero E6 or C6/36 cell cultures.....	82
Figure 22 - Serum neutralization assays of Vero E6 RVFV and C6/36 RVFV performed with final bleed polyclonal sheep sera raised against Vero E6 RVFV.....	84

Abbreviations

A280	spectrophotometric absorbance at 280nm wavelength
BSA	bovine serum albumin
BSL-2	Biosafety Level 2
BSL-3	Biosafety Level 3
BSL-3E	Biosafety Level 3 – Enhanced
cfu	colony-forming unit
CMC	carboxymethyl-cellulose
CPE	cytopathic effect or cytopathogenic effect
DIC	disseminated intravascular coagulation
DMEM	Dulbecco's modification of Eagle's medium
DNA	deoxyribonucleic acid
dpi	days post-infection
ECL	enhanced chemiluminescence
EDTA	ethylenediaminetetraacetic acid
ELISA	enzyme-linked immunosorbent assay
EMEM	Eagle's minimal essential medium
ER	endoplasmic reticulum
FBS	fetal bovine serum
HEPES	4-(2-hydroxyethyl)-1-piperazineethanesulfonic acid
hpi	hours post-inoculation
IFN	interferon
IPTG	isopropyl β -D-1-thiogalactopyranoside

kDa	kiloDaltons
KLH	keyhole limpet hemocyanin
KPL	Kirkegaard & Perry Laboratories
LB	lysogeny broth
LC-ESI-MS/MS	liquid chromatography electrospray ionization tandem mass spectrometry
LEW	Lewis strain rats
MES	2-(N-morpholino)ethanesulfonic acid
MOI	multiplicity of infection
MOPS	3-(N-morpholino)propanesulfonic acid
NaCl	sodium chloride
NMWL	nominal molecular weight limit
Nt	nucleotides
PAGE	polyacrylamide gel electrophoresis
PBMC	peripheral blood mononuclear cell
PBS	phosphate-buffered saline
PCR	polymerase chain reaction
PEG	polyethylene glycol
pfu	plaque-forming unit
PVDF	Polyvinylidene fluoride
rpm	revolutions per minute
rcf	relative centrifugal force
RNA	ribonucleic acid
RT-PCR	reverse transcriptase polymerase chain reaction

RVF	Rift Valley fever
RVFV	Rift Valley fever virus
SDS	sodium dodecyl-sulfate
VLP	virus-like particle
v/v	volume per volume
WF	Wistar-Furth strain rats
w/v	weight per volume

Chapter 1: Introduction

Rift Valley fever virus (RVFV) is a negative sense single-stranded RNA virus (Baltimore Group V), which is a member of the family *Bunyaviridae* and the genus *Phlebovirus*. The virus is a zoonotic pathogen that causes Rift Valley fever (RVF) in humans, as well as in sheep, cattle and other ruminants. It is transmitted by a variety of mosquito vectors and is considered to be one of the most important viral zoonoses in Africa (Daubney *et al.* 1931, Flick and Bouloy 2005).

1.1 History

The most recent common ancestor of sequenced RVFV strains appears to have existed in the late 1800s, during a period in which non-indigenous animals were introduced to the Great Rift Valley and agricultural practices changed (Bird *et al.* 2007a). Retrospective analysis of agricultural records suggests an outbreak in 1912-1913 (Findlay 1931, Bird *et al.* 2007a). The virus was first isolated following a seven-week outbreak of acute disease causing the death of 3500 lambs and 1200 ewes at a single farm on the shores of Lake Naivasha in the Great Rift Valley of Kenya (Daubney *et al.* 1931). The disease appeared mildly pathogenic in humans, and was associated with several laboratory-acquired infections during research immediately following the outbreak.

In addition to the disease in sheep that led to the initial discovery of the virus, Daubney *et al.* found during a natural outbreak at a dairy farm that goats and cows were also susceptible (1931). Working with the virus experimentally in England, rats, mice and a number of wild rodents were found highly susceptible to intraperitoneal inoculation with RVFV (Findlay and Daubney 1931). Rabbits, guinea pigs and birds were found insusceptible, and monkeys were not immune but the virus did not replicate to sufficiently high titres in their blood to subsequently infect sheep (Daubney and Hudson 1932).

The disease was originally believed to be limited to the eastern Rift Valley region of Africa, but in 1951 a severe outbreak occurred in South Africa involving the death of 100,000 sheep and an abortion storm affecting 500,000 ewes. The disease was not initially recognized as RVFV and was only identified after a veterinarian and several assistants became infected during the necropsy of a bull (Bird *et al.* 2009). Another outbreak in South Africa between 1974 and 1976 resulted in an estimated 10,000 to 20,000 human cases (WHO 2010).

A novel arbovirus named Zinga virus, endemic to the Central African Republic, was isolated from mosquitoes in 1969 and from humans in 1974 (Georges *et al.* 1983). It was later discovered through serology that this virus was actually RVFV (Meegan *et al.* 1983).

The first outbreak of RVFV outside of sub-Saharan Africa occurred in 1977 along the Nile delta in Egypt. There are no records of RVFV outbreaks in this area prior to this outbreak, and it is the largest outbreak to date. There were estimates of over 200,000 human infections and 594 confirmed deaths among hospitalized victims (Bird *et al.* 2009). The Egypt outbreak was also the first major zoonotic event, illustrating the full range of RVF pathology in humans. There have been several theories raised regarding the route by which the virus was introduced to Egypt, including the movement of infected camels along Sudanese trade routes, windblown mosquitoes and travel by infected humans.

The first epidemic of RVFV outside of Africa occurred in 2000 in Saudi Arabia and Yemen, along the Red Sea. There were an estimated 2,000 human infections with 245 reported deaths, along with the deaths of thousands of sheep and goats (CDC 2000). In the months before the outbreak, exceptionally heavy rainfall was documented, likely resulting in increased local mosquito populations (Jupp *et al.* 2002). Phylogenies based on the sequence of the virus suggested similarity to an outbreak in Kenya in 1997 and 1998, and an east African origin for the virus

(Shoemaker *et al.* 2002, Jupp *et al.* 2002). This similarity may have been caused by wind-blown mosquitoes or transportation of infected livestock across the Red Sea, as occurs annually for the Muslim pilgrimage of the Hajj (Fagbo 2002). In 2007 and 2008, a series of RVFV outbreaks were detected in Kenya, Tanzania, Somalia, Sudan, South Africa and Madagascar (LaBeaud *et al.* 2008). Case fatality rates in these outbreaks varied from 41% in Tanzania and 32% in Sudan to 29% in Kenya and Somalia, to 4% in Madagascar (WHO 2007, WHO 2008a, WHO 2008b). The reported cases in Madagascar were suspected rather than confirmed, which may decrease the reported case fatality rate due to misdiagnosis of other febrile illnesses. An outbreak in South Africa in 2010 resulted in 186 confirmed cases and 18 deaths (WHO 2010).

1.2 Pathogenesis and pathology in the natural mammalian host

1.2.1 Sheep – The mortality rate in adult sheep is approximately 10 to 30%. Lambs of less than one month of age are highly susceptible to RVFV with mortality rates of 90% or higher. The disease produces an abortion rate approaching 100% (Erasmus and Coetzer 1981).

Abortuses show necrosis and multiple organ infection of the fetus, with necrosis of the placenta, and viral titres of up to 10^9 pfu/mL (Flick and Bouloy 2005). In adult sheep, RVFV travels through the lymphatic system and blood, and begins to replicate to high virus titres in the liver, spleen and kidneys, causing thrombocytopenia and leucopenia. In cases of encephalitis, the virus is evident in the brain (Flick and Bouloy 2005).

RVF in adult sheep in field is characterized by febrile illness, lethargy, vomiting blood, bloody stool and nasal discharge (Daubney *et al.* 1931, Erasmus and Coetzer 1981). The liver shows multifocal to diffuse areas of necrosis, and subcutaneous, visceral and serosal haemorrhages are evident (WHO 2009).

Necrosis is also evident in the lymph nodes and within the white pulp of the spleen. Some animals develop pulmonary congestion and oedema with multifocal necrosis of alveolar and pleural lymphatic tissue (Bird *et al.* 2009).

1.2.2 Cattle – RVFV infection in cattle presents as a febrile illness with loss of appetite, lethargy, bloody stool and, in some animals, nosebleeds (Bird *et al.* 2009). Abortions are common and may be the only indicator of infection in pregnant cattle. Among adult cattle, the case fatality ratio is between 5 and 10% (Erasmus and Coetzer 1981). During active infection there is a decrease in milk production and some reports have indicated the potential for virus transmission to humans through infected milk (Erasmus and Coetzer 1981).

Neonatal calves show greatly increased susceptibility to RVFV compared to adult cattle, but are less susceptible than lambs. The disease course and histopathology are similar in calves and lambs (Bird *et al.* 2009). Various studies have found mortality rates between 10 and 70% (Nabeth *et al.* 2001, Bird *et al.* 2009).

The gross and histopathology of infection are similar between sheep and cattle. Hepatic lesions are prominent and occasionally consistent with disseminated intravascular coagulation (Erasmus and Coetzer 1981). Both sheep and cattle show depletion of lymphocytes and lymphoid tissue necrosis (Bird *et al.* 2009).

1.2.3 Goats – The clinical signs of severe disease in goats are abortion, lethargy and inappetite, similar to sheep and cows (Bird *et al.* 2009). Outbreaks in Senegal, Mauritania and Cameroon have shown goats to be highly susceptible to infection but less prone to mortality than sheep (Nabeth *et al.* 1998). There appears to be a 2 to 10% seropositivity during enzootic periods, rising to greater than 70% following epizootics (Bird *et al.* 2009). Studies of goat flocks following the Mauritania outbreak in 1998 found that an average of 47% of the pregnant female goats within each flock experienced abortion, stillbirth or death within a 48 hour

period (Nabeth *et al.* 2001). During the 2006-2007 outbreak in Kenya, RVFV infections in goats were about half the level seen in cattle and sheep (Bird *et al.* 2008).

1.2.4 Camels – The majority of research on the effects of RVFV on camels comes from an outbreak of an abortive disease in Kenya in 1961 (Scott *et al.* 1963). No causative agent was definitively proven, but 45% of 60 animals sampled were IgG-seropositive for RVFV. Following the report of abortions in camels during the RVFV outbreaks in Egypt between 1977 and 1979, 466 animals were screened as 21% IgG positive and virus was successfully isolated from at least one animal (Meegan 1981). During the 1998 outbreak in Mauritania, one of 39 camels screened were positive for anti-RVFV IgM and none for anti-RVFV IgG, but the perinatal mortality rate was 21% (Nabeth *et al.* 2001).

1.2.5 Humans – In humans, the virus has an incubation period of two to six days: the shortest of the viral haemorrhagic fevers (Jahriling *et al.* 2007). During this replication period, some common symptoms, collectively known as the RVF prodrome, are fever, headache, photophobia and retro-orbital pain. After this point there are generally four clinical patterns the disease may follow. The first, which occurs in more than 90% of cases, is a Dengue-like illness of undifferentiated fever lasting two to seven days, associated with headache, nausea, vomiting and abdominal pain. The second, appearing in approximately 10% of cases, is marked by retinitis and temporary or permanent loss of vision that appears one to four weeks after the onset of the fever. The third clinical pattern appears in less than 1% of cases and is characterized by encephalitis, an inflammation of the brain, appearing one to four weeks after the onset of fever. The fourth pattern, also appearing in less than 1% of cases, is haemorrhagic fever appearing two to four days after the onset of the fever. It is marked by severe liver necrosis and

disseminated intravascular coagulation with a high mortality rate (Madani *et al.* 2003, Gerdes 2004).

The mortality rate of the 2001 Saudi Arabia outbreak was 13.9% (Madani *et al.* 2003). Jaundice occurred in 18.1% of cases, which is most likely a symptom of liver necrosis, but can also be caused by the destruction of red blood cells (Madani *et al.* 2003). Neurological manifestations, such as confusion, lethargy, ataxia, seizures or coma, occurred in 17.1% of cases (Madani *et al.* 2003). Haemorrhagic manifestations occurred in 7.1% of cases and were most commonly seen as gastrointestinal bleeding or nosebleeds (Madani *et al.* 2003).

Disseminated intravascular coagulation (DIC) is the mechanism of bleeding in viral haemorrhagic fevers, including RVF (Geisbert and Jahrling 2004). In cases of DIC, the clotting system is unintentionally activated, resulting in the deposition of fibrin inside blood vessels which can cause necrosis due to lack of blood flow (Levi and ten Cate 1999). Fibrin blockages can also cause haemolysis from the shredding of red blood cells squeezing past clots, and thrombocytopenia from the sequestering of platelets. The lack of platelet availability can then lead to systemic haemorrhages. Lesions are generally not extensive enough to cause terminal shock and death in cases of viral haemorrhagic fever; the most commonly cited mechanisms of death in RVF are DIC and liver necrosis (Geisbert and Jahrling 2004).

1.3 Genetics of host resistance

Experiments using American inbred rat strains (mai rats) showed that Lewis rats (LEW), but not Wistar-furth rats (WF), were resistant to RVFV-induced hepatitis (Peters and Slone 1982, Anderson *et al.* 1987). When these experiments were repeated with rats from a European breeding colony (mol rats), all LEW/mol rats became progressively ill and died of acute hepatitis within 3 dpi, while all WF/mol rats survived with no signs of infection (Ritter *et al.* 2000).

Breeding experiments between WF/mol and LEW/mol rats demonstrated resistance in all first-generation progeny (P1) and in half of second-generation progeny back-crossed with LEW/mol rats, showing the ratios predicted for a single Mendelian locus with a dominant resistance allele (Ritter *et al.* 2000).

Rapid invasion of the liver is a key feature of RVFV infection in mice (McGavran and Easterday 1963). Primary cell culture of rat hepatocytes showed that WF/mol hepatocytes produced less than 1% of the progeny virus of LEW/mol hepatocytes (Ritter *et al.* 2000). However, the virus is capable of causing encephalitis at 2 to 3 weeks post infection even in animals that are resistant to virus-induced hepatitis and intracranial inoculation is uniformly lethal across rat strains (Peters and Slone 1982, Anderson *et al.* 1987). A similar result was seen using an attenuated R-ΔNSm-ZH501 virus, a recombinant virus lacking RVFV accessory proteins NSm1 and NSm2 (Gerrard *et al.* 2007). R-ΔNSm-ZH501 was lethal in 61% of Wistar-furth rats, regardless of challenge dose, compared to 100% lethality with wildtype virus (Bird *et al.* 2007b), suggesting that the outcome may be based on such host-specific issues as early viral load, tissue-specific replication and host immune factors (Bird *et al.* 2007b).

To investigate tissue specificity of the resistance gene, Ritter used primary hepatocyte culture and primary glial (immune cells of the CNS) cell culture from the two rat strains and found resistance to CPE in WF/mol hepatocytes but not in LEW/mol hepatocytes or glial cells of either rat strain (Ritter *et al.* 2000). Resistance to RVFV infection appears to correlate significantly with an IFN-induced antiviral response (Anderson and Peters 1988). Pre-treatment with IFN does not have a significantly different effect on resistance to RVFV in resistant or susceptible strain hepatocyte primary cell culture, suggesting that the resistance gene is not under IFN regulation (Ritter *et al.* 2000).

1.4 Mosquitoes

Rift Valley fever virus is an arthropod-borne virus and its transmission has been associated with mosquitoes of the genera *Aedes*, *Culex*, *Anopheles*, *Eretmapodites* and *Masonia* (reviewed by Flick and Bouloy 2005). The virus has been isolated from more than 30 different species of mosquito, and laboratory studies suggest additional possible hosts outside of its endemic region (Turell *et al.* 1990, Bird *et al.* 2009). RVFV has also been isolated from *Culicoides* (biting midges), *Simuli* (black flies) and *Rhipicephalus* (ticks), although some of these host species are likely dead-end hosts for the virus (Turell *et al.* 1990). The virus is capable of transovarial transmission in mosquitoes and has been documented to lay dormant in mosquito eggs for up to seven years between flood seasons (White *et al.* 1987). It is unknown if there is a vertebrate reservoir that contributes to the maintenance or propagation of the virus (Turell *et al.* 1990).

As a result of its association with mosquitoes, RVFV outbreaks are cyclical and are significantly correlated with periods of unusually heavy rainfall or the construction of dams within the endemic region. The rainfall during 1930 in the Naivasha region of Kenya was over 45 inches, compared to the mean annual rainfall of 25 inches, leading to the proliferation of RVFV in the region (Daubney *et al.* 1931). The outbreak in Egypt in 1977 followed the flooding of the Aswan dam and the outbreak along the Senegal River in 1987 followed the flooding of the Diama dam. Outbreaks were observed in 1997 and 1998, following *El Niño* rains and flooding along the horn of Africa. Based on average rainfall and vegetative indices, it is possible to use satellite imagery to predict RVFV outbreaks in East Africa up to five months in advance (Linthicum *et al.* 1999).

The primary reservoir of the virus appears to be *Aedes* mosquitoes, with transovarial transmission first documented in *Aedes lineatopennis* (Linthicum *et al.* 1985). During relatively dry periods, the virus engages in an enzootic cycle of

transmission between *Aedes* mosquitoes and local wildlife, such as African buffalo species, that are relatively asymptomatic (Bird *et al.* 2009). Following periods of heavy rain, there can be an emergence of transovarially-infected *Aedes* mosquitoes that infect humans and livestock. When the virus replicates to high titres within these hosts, it can be transmitted to secondary vectors such as *Culex* mosquitoes, which will continue to infect new mammalian hosts (Bird *et al.* 2009).

Following the 1977 outbreak of RVFV in Egypt, *Culex pipiens* was identified as a potential vector (Meegan *et al.* 1980). *Aedes* and *Culex* mosquitoes consume approximately 5 μ L of blood per feeding (Turell *et al.* 2008). Initial experimental infections found that over 80% of *C. pipiens* females became infected after feeding on blood that contained at least $10^{4.5}$ pfu/mL of RVFV, but only 25% of infected females transmitted the virus to susceptible hamsters during feeding (Gargan *et al.* 1983). Research on the transmission of arboviruses, specifically western equine encephalitis, found similar results and suggested that there are two barriers within mosquitoes that must be overcome to act as a vector: escape from the mesenteron (midgut) and infection of salivary glands (Kramer *et al.* 1981). Escape from the mesenteron is correlated with greater amounts of virus ingested by mosquitoes, with all mosquitoes infected through intrathoracic injection developing systemic infections (Turell *et al.* 1984a). Median viral titres were $10^{3.1}$ pfu/mosquito for mesenteric infections and $10^{5.5}$ pfu/mosquito for systemic infections, and, in this study, all mosquitoes with systemic infections successfully transmitted the virus to suckling mice or hamsters by bite (Turell *et al.* 1985). Systemic mosquito infections result in mean viral titres 10- to 1000-fold higher than infections that have not disseminated (Turell *et al.* 2008).

The traditional view of arboviruses was that infection was not deleterious to the arthropod vector. However, systemic RVFV infection in *Culex pipiens* following oral exposure results in a 21% reduction in refeeding rate and a 20% reduction in

the number of eggs laid compared to uninfected mosquitoes (Turell *et al.* 1984b, Turell *et al.* 1985). Mosquitoes with non-disseminated infections show reductions in these behaviours, but not to the same degree as those with systemic infections (Turell *et al.* 1985). All *Culex pipiens* larvae infected with RVFV failed to mature to adulthood (Turell *et al.* 1985). Mosquitoes with systemic infections derived from oral exposure or intrathoracic inoculation did not have significantly different transmission rates (Turell *et al.* 2008).

Culex pipiens and *Aedes fowleri* adult mosquitoes are less susceptible to RVFV when held at lower temperatures (13–19°C) (Turell *et al.* 1985, Turell *et al.* 1988, Brubaker *et al.* 1998). One of the factors in this decreased susceptibility may be reduced virus fusion at lower temperatures, as has been shown for Uukuniemi virus (Rönkä *et al.* 1995).

Tissue-specific examinations of RVFV in different mosquitoes of the genera *Aedes* and *Culex* found that different species had varying levels of resistance to infection at different barrier points, such as midgut infection, midgut escape and salivary gland infection (Turell *et al.* 2008). Once the virus has escaped the midgut, it can produce a systemic infection in the mosquito, which can be detected by testing for the presence of RVFV in the mosquito's legs. In order to transmit the virus by bite, the virus must pass through the salivary gland barrier so that it can be injected into a new host during feeding. The viral titre in mosquitoes with systemic infections is not predictive of whether the virus has infected the salivary glands and can be transmitted through biting. Infection in *Culex* mosquitoes is more limited by the midgut barrier than *Aedes* mosquitoes, which is more limited by the salivary gland barrier (Turell *et al.* 2008). A higher viral dose increases the rate of midgut escape, even without the infection of the midgut epithelium (Turell *et al.* 2008).

Transovarial transmission in mosquitoes has been observed in field-collected larvae (Linthicum *et al.* 1985). Vertical transmission of RVFV has not been observed

in laboratory studies (McIntosh *et al.* 1980, Jupp and Cornel 1988, Turell *et al.* 2008).

1.5 Genome and proteome

The virus carries a tripartite single-stranded negative-sense RNA genome of 12 kilobase size in total. Each of the three RNA segments maintains a circular panhandle shape with complementary regions at the ends of each strand. The 6.4kb L segment encodes viral RNA-dependent RNA polymerase protein L (237 kDa).

There is evidence that the three RNA segments have undergone reassortment in nature during co-infection between seven distinct lineages (Bird *et al.* 2007a). Mutation rates within RVFV appear consistent across lineages (Bird *et al.* 2007a) and largely consistent with other negative sense single stranded RNA viruses (Drake and Holland 1999, Jenkins *et al.* 2002). The 3.9 kilobase M segment encodes a set of four nested polyproteins arising from a single open reading frame with five in-frame methionine codons (Figure 1), although the virus appears to use only four of these as translation start codons (Won *et al.* 2007).

Based on the initiating methionine, the translated polyprotein precursors are subsequently processed as follows:

Protein synthesis starting with the first methionine (M1, nt 21) results in a polyprotein which is cleaved between Ala153 and Glu154 into NSm1 and Gc proteins;

Protein synthesis starting at the second methionine (M39, nt 135) results in NSm2, Gn and Gc proteins: with two cleavage sites between Ala153 and Glu154 and between Ala97 and Ser698;

The third methionine (M51, nt 174) does not initiate translation;

Protein synthesis starting at the fourth or fifth methionines (M130, nt 411 and M135, nt426) result in Gn and Gc (Suzich *et al.* 1990, Bird *et al.* 2007a).

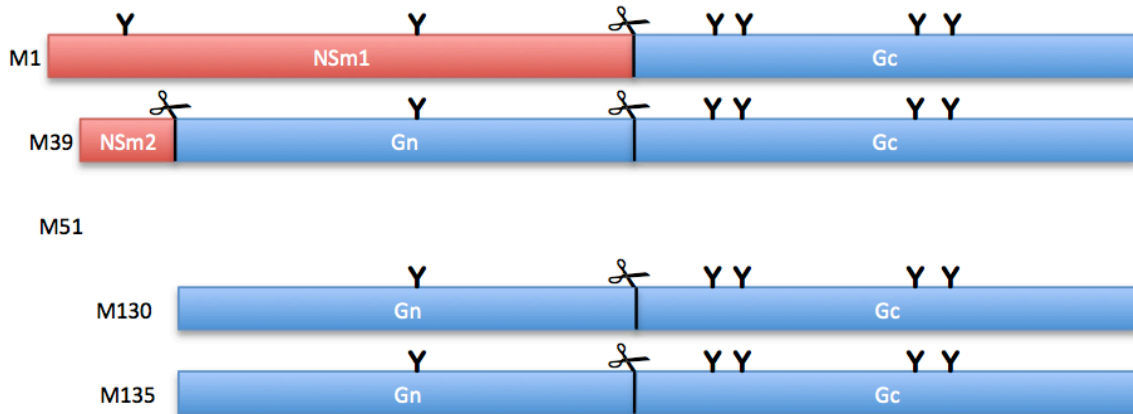


Figure 1. Proteins translated from the RVFV M-segment. Translation initiated at the first methionine, M1, produces NSm1 and Gc. Translation initiated at the second methionine, M39, produces NSm2, Gn and Gc. The third methionine, M51, does not appear to initiate translation. Translation initiated at the fourth or fifth methionines, M130 and M135, produce Gn and Gc. Known structural glycoproteins Gn and Gc are shown in blue and non-structural proteins NSm1 and NSm2 are shown in red. The scissors symbols indicate proposed cleavage sites (between Ala153 and Glu154 and between Ala97 and Ser698 on M1). The branching stick symbols indicate N-linked glycosylation (positions 88, 438, 794, 829, 1035 and 1077 on M1).

The molecular weights of resulting proteins are as follows: NSm1+Gc (130 kDa), NSm2+Gn+Gc (126kDa), Gn+Gc (110 kDa), glycoproteins Gn (54 kDa) and Gc (56 kDa) and non-structural proteins NSm1 (78 kDa) and NSm2 (14 kDa) (Kakach *et al.* 1989, Gerrard and Nichol 2007). The N-terminus of Gn arising from the second, fourth or fifth methionine is cleaved to have the same N-terminus (Gerrard and Nichol 2007). These predicted cleavage sites are consistent with the experimentally determined N-termini of the glycoproteins (Collet *et al.* 1985).

All 33 of the RVFV strains collected between the years 1944 and 2000 maintained five methionine/initiation codons in the NSm region, including the third AUG start codon, which does not appear to be expressed in cells (Bird *et al.* 2007a).

There is one N-linked glycosylation site at position 88 that is glycosylated in NSm1 but not in NSm2. There is one N-linked glycosylation site at position 438 that is used in both NSm1 and Gn (Kakach *et al.* 1989). There are four N-linked glycosylation sites, positions 794, 829, 1035 and 1077, used within Gc (Kakach *et al.* 1989).

The 1.7kb S segment employs an ambi-sense encoding strategy with nucleocapsid protein N (27 kDa) being encoded in a negative orientation and non-structural protein NSs (31 kDa) being encoded in a positive-sense orientation, separated by a short noncoding region.

Functions of the individual RVFV proteins are summarized below (Table 1).

1.6 Virus structure

RVFV is an enveloped icosahedral particle (Sherman *et al.* 2009), 100 nm in diameter. The envelope has no matrix protein and is composed of glycoproteins Gn and Gc in heterodimers across the 4nm-thick lipid membrane, with the C-terminus of Gn internal to the virus and interacting with nucleocapsid N protein. The lipid envelope is acquired by budding through the Golgi apparatus of the host cell. The

Table 1. Rift Valley fever virus proteins and their known functions.

Protein	Genome segment	Molecular weight	Function
L	L	237 kDa	RNA-dependent RNA polymerase. Transcribes viral RNA from negative- to positive-sense for translation, replicates viral genomic RNA.
NSm1	M	78 kDa	Unknown.
NSm2	M	14 kDa	Suppresses host cell apoptosis.
Gn	M	54 kDa	Envelope glycoprotein.
Gc	M	56 kDa	Envelope glycoprotein.
N	S	27 kDa	Encapsidates viral RNA in virion and binds glycoproteins for virus assembly, facilitates RNA-dependent RNA polymerase function.
NSs	S	31 kDa	Prevents host innate immune response. Inhibits host DNA transcription, downgrades PKR activity.

core of the virion is comprised of nucleocapsid N, viral RNA and a viral RNA-dependent RNA polymerase L (Freiberg *et al.* 2008, Huiskonen *et al.* 2009).

Virus-like particles (VLPs) have been assembled using a variety of plasmid systems *in vitro* (Liu *et al.* 2008, Habjan *et al.* 2009a, Piper *et al.* 2011). These systems have been used to explore the requirements for virion assembly and release.

There is limited evidence of differences in arbovirus virions produced in mammalian or insect hosts. N-linked glycosylation, and thus glycoprotein maturation, can differ between mammalian and insect cells (Altmann *et al.* 1999). Mammalian cells contain high-density lipoproteins, such as cholesterol, that are not found in insect cells and can affect virus assembly (West *et al.* 2006). West Nile viruses amplified in mammalian or insect cells have different infectivity for, and induce different innate immune activation of, monocytes and dendritic cells *in vitro* (Davis *et al.* 2006, Silva *et al.* 2007). No differences were detected in tissue tropism, infectivity, clinical disease or mortality *in vivo* during infections of mice, although differences in viral load and IFN- α/β activation were consistent with previous reports for WNV (Lim *et al.* 2010).

1.7 RVFV viral entry and replication in Vero E6 cells

Cell entry by RVFV requires only the glycoproteins Gn and Gc. As a member of the family *Bunyaviridae*, it employs a class II fusion mechanism activated by low pH following endocytosis (Rönkä *et al.* 1995, Garry and Garry 2004). The virus binds dermal dendritic cells through a C-type lectin called DC-SIGN (Lozach *et al.* 2011). DC-SIGN interactions with high-mannose *N*-glycans found on viral glycoproteins and leads to virus attachment and endocytosis. RVFV disassociates with DC-SIGN following internalization and the virus is trafficked to the late endosome (Lozach *et al.* 2011).

The first viral transcript produced upon cell entry is NSs, the only gene carried by RVFV in anti-genomic (positive) sense encoding (Parker *et al.* 1984, Ikegami *et al.* 2005). The first visible feature of viral replication in Vero cells is the development of filamentous nuclear inclusion bodies (Ellis *et al.* 1988), polymerizations of NSs with nuclear transcription factors (Swanepoel and Blackburn 1977, Billecocq *et al.* 2004). These appear at 5 hpi, while other viral proteins begin to aggregate at 7 to 9 hpi, and virion assembly begins with budding through the membrane of the Golgi at 11-13 hpi (Ellis *et al.* 1988). The first cell deaths occur at 13 hpi, at which point the replication cycle is complete, and most replication has ceased by 17 hpi (Ellis *et al.* 1988). The virions are sequestered to the Golgi cisternae or smooth walled vesicles and remain encapsulated, singly or within a vacuole, for at least four hours prior to release. Peak releases of virus occur at 19 hpi and at 25 hpi from cells that acquired secondary infection (Ellis *et al.* 1988). Apoptosis appears to occur significantly earlier in cells infected with virus lacking the NSm2 protein (Won *et al.* 2007).

1.8 Differences in RVFV replication between C6/36 cells and Vero E6 cells

Following the determination that *Aedes albopictus* cells are as effective as newborn mice for isolating Dengue fever virus infection (Chappell *et al.* 1971), the C6/36 cell line was developed in 1978 from a primary cell line developed by Singh in 1967 (Igarashi 1978). Clone C6/36 of *Aedes albopictus* cells ("SAAR" Singh cells) showed the highest yield of Chikungunya virus and Dengue virus types 1-4 (Igarashi 1978). C6/36 cells have also been used for the growth of RVFV (White 1987).

C6/36 cells are able to produce RVFV particles for a greater length of time post-infection than Vero E6 cells. Following infection with RVFV, C6/36 cells have been shown to remain viable but fail to proliferate at 72 hpi (Streeter and Gerrard in Vaughn *et al.* 2010). Even with the anti-apoptotic function of NSm2, fewer than 35%

Vero E6 cells infected with RVFV remain viable by 72 hpi, based on a measurement of mitochondrial dehydrogenases compared to mock-infected controls (Won *et al.* 2007).

Compared to Vero E6 cells, a higher percentage of C6/36 cells were initially infected with RVFV (Vaughn *et al.* 2010). Collectively, glycoproteins Gn, Gc and nucleocapsid protein N accumulate at comparable levels in insect and mammalian cells, while NSs expression was significantly lower in insect cells. Radiolabelling showed that this was indeed due to lower levels of NSs synthesis in the insect cells, not higher levels of NSs degradation (Vaughn *et al.* 2010). The deletion of NSs in recombinant RVFV resulted in attenuated infections in mammalian hosts but not in mosquito hosts *in vivo*, suggesting that NSs is dispensable in insect hosts (Muller *et al.* 1995).

NSs forms polymerizing filaments in both mammalian and insect cells. These filaments are intranuclear in mammalian cells but cytoplasmic in insect cells (Vaughn *et al.* 2010). It is unknown if this difference is because the nuclear-targeting signal peptide is not functional in insect cells, or if a cytosolic protein in insect cells triggers the polymerization normally carried out in the presence of mammalian TFIIH. When NSs is over-expressed in insect cells using an expression plasmid, it does localize to the nucleus and functions to inhibit gene expression (Vaughn *et al.* 2010).

It was previously accepted that the pathways inhibited by NSs in vertebrates, such as the induction of interferon and dsRNA-dependent protein kinase, have no invertebrate homologues. Although there has been recent evidence to the contrary, these mechanisms are poorly understood and the detected homologous genes may serve different functions in invertebrates (Robalino *et al.* 2004, Neyhba 2009).

In mammalian or insect cell lines grown at 28°C, NSs fails to localize to the nucleus and remains in the cytoplasm (Vaughn *et al.* 2010). NSs is expressed at

higher levels when RVFV is grown in mammalian cells at 35°C than when grown in insect cells at 28°C (Vaughn *et al.* 2010). When mammalian cells are grown at 28°C, to control for any temperature effects between mammalian and insect cells, they continued to produce significantly higher levels of NSs than insect cells (Vaughn *et al.* 2010).

Aedes aegypti and *Culex quinquefasciatus* mosquitoes are less susceptible to infection with recombinant RVFV lacking NSm1 and NSm2 than to infection with wildtype RVFV (Crabtree *et al.* 2012). This effect was more pronounced in *Ae. aegypti*, with significant decreases in systemic dissemination of the virus and salivary transmission of the virus. Because RVFV transmission in *Aedes* mosquitoes is generally limited by midgut escape compared to *Culex* mosquitoes where transmission is limited by salivary gland barriers, this suggests that the NSm proteins may play a significant role in midgut escape (Crabtree *et al.* 2012).

1.9 Structural proteins

1.9.1 RNA-dependent RNA polymerase L is the largest protein in the RVFV proteome. It is recruited to the Golgi apparatus for viral assembly by the glycoprotein Gn and is found within the core of the assembled virion associated with viral RNA (Piper *et al.* 2011). *Bunyaviridae* require both L and nucleocapsid N proteins to perform “cap-snatching” of host mRNA-derived cap structures to use as primers. During infection, L protein undergoes oligomerization, which is required for the L protein to function as an RNA-dependent RNA polymerase (Zamoto-Niikura *et al.* 2010).

1.9.2 Nucleocapsid protein is the most abundant viral component in the virion and the most abundantly expressed viral protein in infected cells (Liu *et al.* 2008). It associates with the three viral RNA strands in a helical fashion forming

nucleocapsids within the icosahedral virion. It interacts with L, Gn and Gc (Liu *et al.* 2008), although the interaction with Gc appears to be mediated through Gn (Ferron *et al.* 2011). The basic oligomeric shape is a dimer, but more complex structures can be formed (Liu *et al.* 2008). Electron microscopy and resonance spectroscopy suggest that N forms ring-shaped hexamers, although N appears able to form oligomers with different subunit organization that support the observation of filamentous ribonucleocapsids *in vivo* (Ferron *et al.* 2011). N localizes to the cytoplasm and is recruited by glycoprotein Gn for virus assembly in the Golgi apparatus (Piper *et al.* 2011).

1.9.3 Glycoproteins Gn and Gc are *Bunyaviridae* glycoproteins G2 and G1, respectively. When expressed individually in recombinant viruses, Gn is targeted to the Golgi apparatus and Gc is retained in the endoplasmic reticulum (Wasmoen *et al.* 1988). When expressed as part of the complete M-segment, they appear to form a complex shortly after expression and co-localize to the Golgi (Gerrard and Nichol 2007).

Experimentally, over-expression of the glycoproteins using an alphavirus vector results in their localization directly to the cell membrane (Filone *et al.* 2006). In various mammalian cell lines, these glycoproteins promote cell-cell fusion between 24°C and 37°C, behaving optimally between 28°C and 37°C and failing to promote fusion at 42°C (Filone *et al.* 2006). Cell-cell fusion was initiated at low pH, suggesting that virus fusion is mediated through endocytosis (Filone *et al.* 2006).

1.10 Accessory Proteins

1.10.1 Nonstructural protein NSs is encoded in the only RVFV positive-sense open reading frame (Ihara *et al.* 1984, Parker *et al.* 1984). The 265 amino acid

NSs protein is expressed in infected cells and is post-translationally phosphorylated (Swanepoel and Blackburn 1977).

As with most highly pathogenic viruses, RVFV has a means of suppressing the immune response (Bouloy *et al.* 2001). The non-structural protein NSs is able to suppress the production of type I IFN by binding p44, a subunit of transcription factor TFIID, which is essential for the transcription of type I IFN as well as many other cellular proteins (Billecocq *et al.* 2004, Bird *et al.* 2007b). While this process frees up ribosomal activity for the translation of viral proteins, NSs does not appear to be essential for the replication of the virus. RVFV lacking the NSs encoding region is avirulent in healthy mice, but virulent in IFN-deficient mice, suggesting that it is important in maintaining the life cycle of the virus in the wild (Frese *et al.* 1996).

The NSs protein's inhibition of TFIID also suppresses the host cell's ability to respond to external stimuli such as hormones (Bird *et al.* 2007b). This insensitivity may trigger the maternal controls responsible for the high abortion rate caused by the virus, but that mechanism would fail to explain the very high mortality rate in newborn animals, which are no longer responding to maternal development signals (Flick and Bouloy 2005).

By preventing host cell transcription, NSs suppresses the production of type I IFN (α/β), and thus the host's activation of an antiviral state. RVFV replication is severely inhibited by dsRNA-dependent protein kinase (PKR) but, to combat this, viral NSs degrades PKR (Habjan *et al.* 2009). Pre-treatment with INF- α has been shown in rhesus monkeys to protect against RVFV viremia and liver damage (Peters *et al.* 1988), demonstrating that interferon is effective against RVFV and that viral infection is significantly attenuated in the absence of NSs (Billecocq *et al.* 2004).

Investigation of the role of NSs has been facilitated by using a naturally occurring variant strain of RVFV known as Clone 13, isolated from the heterozygous RVFV strain 74HB59 that was collected from a human patient in the Central African

Republic (Muller *et al.* 1995). Clone 13 lacks approximately 70% of the NSs sequence but contains both the N and C termini, resulting in a protein product that is not expressed, is quickly degraded by the host cell, or is not recognized by antisera (Muller *et al.* 1995). This NSs-deficient Clone 13 appears to replicate normally in Vero cells (deficient in interferon-(IFN) induction) and in *Culex pipiens* mosquitoes (Muller *et al.* 1995).

NSs protein forms multiple filamentous structures in the nuclei of infected cells (Mansuroglu *et al.* 2010). These strands associate with pericentromeric γ -satellite sequences of host genomic DNA (Mansuroglu *et al.* 2010). This association is subject to heritable DNA traits and therefore may be a basis for genetic differences in susceptibility that have been observed in rats (Rosebrock and Peters 1982).

Immunofluorescent co-localization experiments have demonstrated that almost all cellular DNA is excluded from NSs filaments, but some particularly dense centromere regions did co-localize with the filaments (Mansuroglu *et al.* 2010). This association occurred at 5hpi (before significant polymerization of NSs into filaments) and at 7hpi (with NSs nuclear inclusion filaments), although the larger amount of NSs in the nucleus at the later time point was associated with higher levels of DNA binding. This is the first report of a DNA-binding domain in NSs (Mansuroglu *et al.* 2010). The host protein SAP30, which interacts directly and indirectly with host DNA, is necessary for NSs to inhibit the IFN- α promoter, although the mechanism is unknown (Le May *et al.* 2008).

Nuclear imaging has shown that NSs significantly increases the frequency of nuclear anomalies such as micronuclei, lobulated nuclei and intranuclear DNA bridges (Mansuroglu *et al.* 2010). These nuclear anomalies can be associated with virus-induced apoptosis (Roulston *et al.* 1999), but were not correlated with a significant increase of apoptosis in RVFV infection (Mansuroglu *et al.* 2010),

possibly because of the anti-apoptotic properties of NSm2 (Won *et al.* 2007). There was a marginal increase in apoptosis in cells infected with Clone 13, suggesting that the PKR-induced antiviral state increases cell death even in the absence of NSs. Mansuroglu *et al.* observed that NSs arranges around mitotic DNA in a "cage-like" structure in murine fibroblastic and fetal sheep kidney cell lines infected with RVFV ZH548, preventing entry into prophase and significantly reducing mitosis (Mansuroglu *et al.* 2010). The increase in nuclear anomalies may be a mechanism for the high rate of fetal mortality seen with RVFV (Mansuroglu *et al.* 2010).

1.10.2 Nonstructural M segment proteins RVFV replication using NSm1- and NSm2-deletion viruses *in vitro* and *in vivo* suggests that the non-structural M-segment proteins are not necessary for the processing, transport or assembly of viral structural glycoproteins Gn and Gc (Wasmoen *et al.* 1988, Gerrard *et al.* 2007, Won *et al.* 2007). Several experiments have been performed using RVFV R-ΔNSm-ZH501 strain, a recombinant virus lacking NSm1 and NSm2 due to a deletion of M-segment nucleotides 22-408 (Gerrard *et al.* 2007). Using this model, differences between the recombinant virus and RVFV R-ZH501 could be due to the loss of NSm1 or NSm2, but are generally consistent with the known effects of NSm2. Pathogenic strain ZH501 with an NSm region deletion was used to confirm that NSm1 and NSm2 are not required for the correct localization of glycoprotein Gn or nucleocapsid protein N *in vitro* in mammalian cells (Gerrard *et al.* 2007).

1.10.3 Nonstructural protein NSm2 suppresses caspase-induced apoptosis in mammalian host cells (Won *et al.* 2007). A recombinant strain lacking NSm1 and NSm2, arMP-12-del21/384, produces larger plaques after 24 hours than the control strain (Won *et al.* 2007).

With an initial MOI of 1 or higher, efficient release of RVFV occurs within the first 24 hours, with most of the progeny being released prior to apoptosis (Ikegami *et al.* 2006, Won *et al.* 2006). RVFV suppresses host cell transcription and translation, a state in which the host cell is particularly susceptible to apoptosis by tumour necrosis factor alpha (Won *et al.* 2007). A reduction in apoptosis-sensitivity may allow for increased production of progeny virus by RVFV (Won *et al.* 2007), a theory that is supported by the observation of decreased pathogenesis in rats by virus lacking the pre-Gn region (Bird *et al.* 2007b). Cysteine-aspartate proteases (caspases) are regulatory proteins involved in a variety of cell pathways, including programmed cell death. Caspase-9 is the initiator of the intrinsic pathway, while caspase-8 is the initiator of the extrinsic apoptotic pathway.

NSm2 expression appears to suppress the activity of caspase-8, an extrinsic death receptor-pathway protein (Won *et al.* 2007). It is also capable of inhibiting staurosporine-induced caspase-8 and caspase-9 activities. Activated caspase-8 is capable of activating caspase-9 through the release of cytochrome *c* from the mitochondria through the cleavage of intermediary protein Bid. It may be that the inhibition of the activation of caspase-8 by NSm2, or the inhibition of activated caspase-8 by NSm2, suppresses caspase-9 activation or activity. It is also possible that NSm2 may act directly to suppress executioner caspases such as caspase-9 and -3 (Won *et al.* 2007).

In addition to its role as death-cycle initiator, caspase-8 is involved in the development and differentiation of embryonic cells, monocytes, T and B cells, and in the activation of NFκB. Disruption of caspase-8 appears to be lethal in embryonic mice through disruption of vascular formation and hyperemia in most major blood vessels and many organs (Varfolomeev 1998). Possibly because of the redundancy between caspase-8 and -10, humans do not show the developmental defects seen in

caspase-8 deficient mice, limiting human symptoms primarily to immune function deficiencies and not embryonic or vascular malformations.

RVFV R-ΔNSm-ZH501 was found to retain virulence in rats, but was significantly less lethal than RVFV R-ZH501 (Bird *et al.* 2007b). Infection with RVFV R-ΔNSm-ZH501 shows a much lower initial mortality rate with severe neurological signs (ataxia, head tilt, head tremors, lethargy) appearing in some animals at two weeks post-infection. These signs are more consistent with the human presentation of RVFV than is normally seen in rats (Bird *et al.* 2007b). The redundancy of caspase-8 and -10 in humans compared to mice and rats may explain why the deletion of NSm2 produces an illness in rats that more closely mimics the neurological pathology of RVFV seen in humans.

1.10.4 Nonstructural protein NSm1 is a 78 kDa fusion protein comprised of NSm2 and the glycoprotein Gn with 38 unique amino acids at the N-terminus (Figure 1). Its role is unknown, although it has been shown to have no anti-apoptotic function *in vitro* (Won *et al.* 2007). Recombinant plasmid expression of NSm2 or a 73 kDa protein beginning from the third methionine of the M-segment ORF significantly reduce caspase-3 activity, while plasmid expression of NSm1 was not significantly different from an empty expression vector in reducing caspase-3 activity and apoptosis (Won *et al.* 2007).

NSm1 has two N-linked glycosylation sites, one of which is also carried but not used in NSm2 protein (Kakach *et al.* 1988). Protein cleavage appears independent of glycosylation (Kakach *et al.* 1989). Both NSm1 and NSm2 have transmembrane domains expected to sit across the endoplasmic reticulum (Gerrard and Nichol, 2007). N-linked glycosylation takes place within the lumen of the endoplasmic reticulum, suggesting that the proteins may be oriented differently across its transmembrane domains such that the site is accessible in NSm1

conformation but not NSm2 conformation (Gerrard and Nichol 2007). Because caspases are cytoplasmic proteins, NSm2 would have an active site able to effect the apoptotic pathway while NSm1 would not (Won *et al.* 2007).

NSm1 glycoprotein forms a complex with Gc (Gerrard and Nichol 2007), leading to speculation that NSm1 may be packaged into the virion through this association (Gerrard *et al.* 2007). The NSm1 protein does not appear to play a role *in vivo* in mammals, but it has been speculated without any proposed mechanism that NSm1 may be functional during infection in insects (Gerrard *et al.* 2007).

1.11 Overview of objectives and statement of hypothesis

The RVFV proteome is highly conserved and contains relatively little noncoding RNA (Bird *et al.* 2007a). While there was abundant evidence that NSm2 was dispensable *in vitro*, its role in pathogenesis has been demonstrated (Won *et al.* 2007). Efforts, to this point, have failed to demonstrate the function of NSm1: suggestions have included incorporation into virions (Gerrard and Nichol 2007), or to function during replication in insect hosts (Gerrard *et al.* 2007). Despite having no known function, the 38 amino acid region unique to NSm1 is highly conserved between strains of RVFV, suggesting that it is a functional coding region for the virus (Bird *et al.* 2007a).

Hypothesis 1: Viral protein expression during infection differs between mammalian and insect cells.

Objective: To determine whether protein expression profile is the same in Vero E6 cells and the C6/36 cells with a particular focus on the expression of NSm1.

To demonstrate through viral protein-specific immunoblots of RVFV-infected cell lysate from mammalian and insect cell lines that viral proteins are expressed at

significantly different quantities or are first detected at demonstrably different time points following infection.

Rationale: RVFV infection follows a significantly different course in insect cells than in mammalian cells, with insect cell infection being non-lytic and having slower viral kinetics than is observed in mammalian cells (Vaughn *et al.* 2010). The RVFV non-structural protein NSs shows differences in expression levels, cellular localization and function between infections in mammalian or insect cells. During infection of mammalian cells, RVFV NSs localizes to the nucleus (Billecocq *et al.* 2004). In C6/36 insect cells, NSs appears to remain in the cytoplasm, forming filamentous structures but not associated with the nucleus (Vaughn *et al.* 2010). NSs is also expressed at significantly lower levels in C6/36 cells than in Vero E6 cells, even when controlling for temperature (Vaughn *et al.* 2010). NSs is expressed at different levels and localizes to different regions of the cell between Vero E6 and C6/36 cells. Additionally, NSs is a significant virulence factor during RVFV infection in mammalian cells (Bouloy *et al.* 2001), but its attenuation only impacts transmission in *Aedes aegypti* mosquitoes, not infection or systemic dissemination of RVFV (Crabtree *et al.* 2012). The mechanisms of host-recognition that elicit these differences in the expression, localization and function of NSs between mammalian and insect cells may also be affecting other viral proteins such as NSm1.

The deletion of non-structural proteins NSm1 and NSm2 has a significant impact on *in vivo* infection of *Aedes aegypti* mosquitoes, reducing virus dissemination within the mosquito host and reducing bite transmission rates (Crabtree *et al.* 2012). This work has used a recombinant virus with a deletion of both NSm1 and NSm2, although the effects were attributed to NSm2.

Hypothesis 2: The protein profiles of assembled virions differ between mammalian and insect cells.

Objective: To demonstrate through viral protein-specific immunoblots of concentrated, purified RVFV grown in mammalian or insect cell cultures that the profiles of viral proteins incorporated into the respective virions are demonstrably different and/or the quantities of the individual virion proteins are demonstrably different. Immunoblots will focus in particular on the detection of NSm1 which has no known function but may be incorporated into virions. The presence of nucleocapsid N in immunoblots will be used to confirm the presence of virions and the absence of accessory protein NSs in immunoblots will be used to confirm that the purified samples do not contain non-structural proteins.

Rationale: Differences in the viral protein expression based on host cells have been reported, with decreased expression of glycoprotein Gn in C6/36 cells compared to Vero E6 (Vaughn *et al.* 2010). Because both NSm1 and Gn associate with Gc (Gerrard and Nichol 2007), it is possible that NSm1 may be associated into virions through its association with Gc. To our knowledge, it has not previously been reported for an arbovirus to have a demonstrably different virion structure based on replication in a mammalian or insect host. However, differences in the levels of structural proteins, as well as long-standing speculation on the role of NSm1, suggest that it may be possible, since mammalian and insect cells differ in their post-translational processing of proteins and the protein and lipid content of membranes through which RVFV buds.

Chapter 2: Methodology

2.1 Cells

All non-infectious cell culture work was performed in a Biosafety Level-3 (BSL-3) laboratory with the use of a Class II Biological Safety Cabinet (BSC).

2.1.1 Vero E6 cells

Vero E6 cells were grown in media (Appendix B) composed of 90% DMEM (Wisent), 10% fetal bovine serum (Wisent 080-450) and were grown in vented-capped flasks at 37°C in humidified air with 5% CO₂.

Cells in a T-75 flask (Corning 430641) were passaged by removing the growth media, gently washing the cells in 5 mL phosphate-buffered saline (PBS) for 30 seconds and trypsinizing the cells with a 0.25% (w/v) Trypsin 0.53 mM ethylenediaminetetraacetic acid (EDTA) solution for 6 minutes at 37°C with periodic gentle rocking. Cells were then rinsed from wall of the flask with fresh growth media at 37°C, collected from the bottom of the flask and suspended in a sufficient volume of fresh growth media to be seeded into new flasks. The cells of each flask were commonly suspended in 80 to 160 mL of fresh media and seeded into four to eight T-75 flasks, each containing 20 mL media.

Cells were suspended in the growth medium and transferred to new T75 flasks in a split ratio from 1:4 up to 1:8. The procedure for growing and passaging Vero E6 cells in T-150 flasks (Corning 430825) was the same with all volumes doubled.

2.1.2 C6/36 cells

C6/36 cells were grown in media (Appendix B) composed of 46% Expression Systems Formula (ESF) 921 (Expression Systems 96-001), 46% Eagle's minimum essential medium (EMEM) (Wisent 320-036-CL), 2.5% heat-inactivated fetal bovine serum (FBS) (Wisent 080-450), 1mM final concentration sodium pyruvate (Sigma Aldrich S8636), 25mM final concentration 4-(2-hydroxyethyl)-1-piperazineethanesulfonic acid (HEPES) (Sigma Aldrich H0887) and non-essential amino acid stock solution for final concentrations of 17.8 mg/L L-alanine, 30 mg/L L-asparagine monohydrate, 26.6 mg/L L-aspartic acid, 29.4 mg/L L-glutamic acid, 15 mg/L glycine, 23 mg/L L-proline and 21 mg/L L-serine (Sigma Aldrich 58572C).

Cells were passaged by removing the growth media and using a Sarstedt cell scraper (Fisher Scientific 50101128) to detach the cells from the flask. The cells were then suspended in equal volumes of conditioned and fresh growth media and seeded in 20 mL volumes into plug-seal capped T-75 flasks (Corning 430725). Each flask was commonly split into five to ten new flasks. The flasks were incubated at 28°C. The procedure for growing and passaging C6/36 cells in T-150 flasks (Corning 430823) was the same with all volumes doubled.

C6/36 cells are normally grown in 5% CO₂ atmospheric conditions. However, no 5% CO₂ 28°C incubators were available at the time of these experiments. After comparing various techniques, the use of plug seal flasks to contain and accumulate CO₂ released by cellular respiration, along with the use of HEPES buffer, was found to be the most effective way of maintaining C6/36 growth and stabilizing the pH of the media.

2.2 Production of virus stocks

The RVFV used in these experiments was the Zagazig Hospital 501 (ZH-501) strain, originally isolated from a fatal human haemorrhagic fever case in the Sharqiya governate in Egypt, 1977 (Meegan *et al.* 1979). It was provided by Heinz Feldmann of the National Microbiology Laboratory, Winnipeg, Canada. All work with infectious virus was performed in a Biosafety Level 3 – Enhanced (BSL-3E) laboratory with the use of a Class II BSC and personal protective equipment including HEPA filtered respirator.

Stock virus was produced in Vero E6 cells that were infected at 95% confluence at MOI 0.1 and harvested after apparently complete cell death by 5 days post-infection (dpi). Infectious supernatant was transferred from flasks without intentionally lysing the cells. The supernatant was then clarified through centrifugation at 3,000 *g* for 30 minutes at 4°C and the clarified product was transferred and frozen in 1 mL aliquots at -70°C. Virus stocks were thawed and plaque titrated on Vero E6 cells as described below with a titre of 10^{6.9}pfu/mL.

C6/36 cells were infected at 95% confluence at MOI 0.1 and the virus was harvested at 7 dpi. The supernatant was clarified as for Vero E6 supernatant. C6/36-amplified virus stocks were plaque titrated on Vero E6 cells as described below with a titre of 10^{8.2}pfu/mL.

2.3 Plaque titration

Plaque titration assays were performed in twenty-four-well plates of Vero E6 cells, prepared by seeding 130,000 cells/cm² using Dulbecco's Modification of

Eagle's Medium (DMEM) with 10% FBS one day prior to infection. On the day of infection, each plate well was washed with 0.5 mL of phosphate-buffered saline (PBS) and incubated with 800 μ L infectious media for 1.5 hours before the media was removed and replaced with 1 mL 2% carboxymethyl-cellulose (CMC) overlay (Appendix B). The plates were incubated at 37°C with 5% CO₂ for 4 to 6 days before being fixed with 1 mL 10% buffered formalin for a minimum of one hour, washed, and stained with 5% (w/v) crystal violet (Tris(4-(dimethylamino)phenyl)methyl chloride) (Fisher C581-100) in methyl alcohol (Sigma Aldrich 322415). Each plate contained three uninfected control wells and three wells each for dilutions 10⁻² through 10⁻⁸ of the stock virus.

2.4 Antibodies

Rabbit polyclonal anti-N and rabbit polyclonal anti-NSs sera were developed by Dr. Markus Czub at the University of Calgary, Calgary, Canada. Sheep anti-RVFPV sera were developed at the National Centre for Foreign Animal Disease, Winnipeg, Canada. The sera were collected from animals designated 11, 12, 13 and 14 at -1 dpi and 29 dpi with RVFPV ZH-501 that had been produced in Vero E6 cells.

The peptide SSTREETCFGDSTNPE (Figure 2) was commercially synthesized by EvoQuest (Carlsbad, California, USA) and used to produce polyclonal rabbit sera (Invitrogen M0300). Control serum was collected on the same day that two animals were injected subcutaneously with the synthetic peptide that had been conjugated with keyhole limpet hemocyanin (KLH) as a carrier protein to stimulate an immune response. Sera were collected from the two rabbits, R1108 and R1109, at 36 dpi.

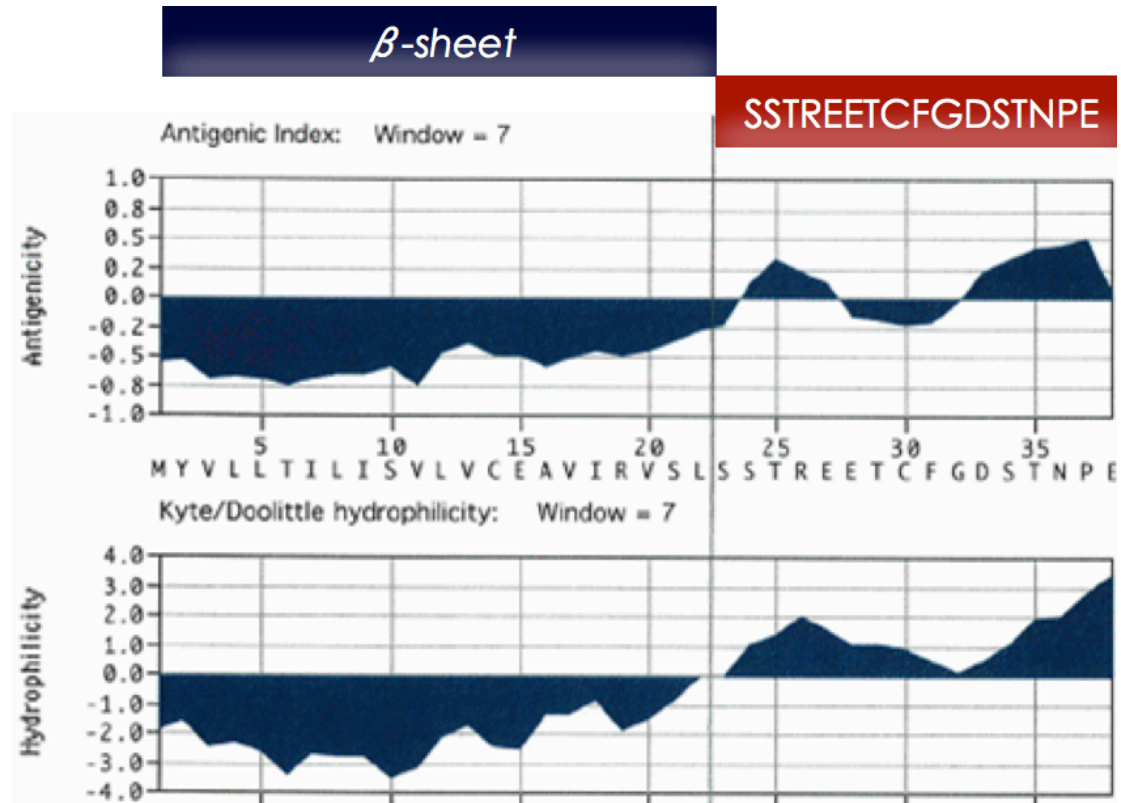


Figure 2. The 38 N-terminal amino acids of NSm1 analyzed for antigenicity, hydrophobicity and tertiary structure by residue. The first 22 amino acids are predicted to form a B-sheet structure. Amino acids 23 through 38 were selected for peptide synthesis and polyclonal antibody development because they fell outside of the predicted B-sheet structure and had a higher predicted antigenicity. Figure modified from EvoQuest antibody development suite.

2.5 Recombinant NSm1

Rift Valley fever virus ZH501 RNA was isolated using TriPure isolation reagent (Roche Applied Science 11667165001) following manufacturer's instruction. RT-PCR was performed using Superscript III Reverse Transcriptase in the One-Step RT-PCR System with Platinum *Taq* DNA Polymerase (Invitrogen 12574-030) to amplify the NSm1 gene (nt 20-2080 of the M segment). RT-PCR was carried out using forward primer CACCATGTATGTTTTATTAACAATTCTAA and reverse primer TGCTGATGCATATGAGACAA at 10pmol each with 5µL template RNA, 25 µL 2× reaction mix containing 0.4 µM of each dNTP and 3.2 µM MgSO₄, 1 µL of additional 5 µM MgSO₄ and 1µL enzyme mixture containing SuperScript III reverse transcriptase and Platinum *Taq* proofreading DNA polymerase (Invitrogen 12574-030) with distilled water to a total volume of 50µL per reaction. SuperScript III is a modified Moloney Murine Leukemia Virus Reverse Transcriptase. The DNA polymerase used was Platinum *Taq*, a hot-start *Pyrococcus* species GB-D strain DNA polymerase. The RNA was reverse transcribed to cDNA at 50°C for 30 minutes and was subsequently denatured at 95°C for 2 minutes. DNA was amplified over 40 cycles of DNA melting at 94°C for 15 seconds, annealing at 57°C for 35 seconds and extension at 68°C for 150 seconds. The final extension phase was at 68°C for ten minutes. The reactions were carried out in a Biometra T1 Thermal Cycler. From each reaction, 10 µL of PCR product was mixed with 1 µL BlueJuice gel loading buffer (Invitrogen 10816-015) and run, along with TrackIt 1kb Plus DNA ladder (Invitrogen 10488-085), on 1% agarose gels with 1:50,000 SYBR-SAFE (Invitrogen

S33102) in TE running buffer at 100V constant for 60 minutes before being visualized on a Bio-Rad Gel Doc 2000.

The resulting PCR product was scalpel-excised from the agarose gel, visualized using UV trans-illumination, and purified with a Promega Wizard SV Gel and PCR Clean-Up System (Promega A9282). The purified product was cloned into a pET-100/D-TOPO (Invitrogen K100-01) directional topoisomerase-ligated bacterial expression vector with an N-terminal HIS-tag, ampicillin resistance gene and *lac* operon using the TOPO Gateway topoisomerase ligation system (see Appendix). The plasmid was transformed into One-Shot TOP10 chemically competent *E. coli* (Invitrogen C4040-03) and the cells were plated on LB agar with ampicillin (Invitrogen 11593-027) and X-gal (Invitrogen 15520-018) to select for successful plasmid ligation and transformation (see Appendix).

Plasmid clones were screened using PCR and restriction endonuclease digestion. Purified plasmids were collected from transformed TOP10 and purification was performed using QIAGEN Mini-Prep kit (QIAGEN 217193) according to manufacturer's directions. DNA concentrations were determined using a NanoDrop 1000 spectrophotometer (Thermo).

PCR screening was carried out using forward primer CACCATGTATGTTTTATTAACAATTCTAA and reverse primer TGCTGATGCATATGAGACAA at 10pmol each in 12.5 μ L HotStarTaq Master Mix (QIAGEN 203446) with distilled water to a total volume of 30 μ L per reaction. Colonies showing x-gal expression were picked using sterile inoculating loops, mixed gently in each PCR tube and then transferred to 1 mL volumes of LB broth

and incubated at 37°C overnight at 300rpm aeration. The PCR reactions were carried out in a Biometra T1 Thermal Cycler. The DNA was denatured at 95°C for 15 minutes, followed by thirty cycles of DNA melting at 95°C for 30 seconds, annealing at 45°C for 30 seconds and extension at 72°C for 120 seconds. The final extension phase was 72°C for five minutes. From each reaction, 10 µL PCR product was mixed with 2 µL BlueJuice loading buffer and run, along with TrackIt 1kb Plus DNA ladder, on a 1% agarose gel with 1:50,000 SYBR-SAFE (S33102) at 100V constant for 60 minutes in TBE running buffer before being visualized on a Bio-Rad Gel Doc 2000.

Restriction endonuclease digestions were performed using *XbaI* (Roche) to linearize the plasmid or *NdeI* (Roche) to cut the plasmid into three distinct bands in the respective buffers supplied by the manufacturer. Digestion reactions contained approximately 80 µg of purified pET-100 RVFV NSm1 clone 02 plasmid, 2 µL enzyme (10,000 U/mL concentration) reaction buffer and water to a final volume of 20 µL (see Appendix C). Digestions were carried out in 1.5 mL microcentrifuge tubes for two hours at 37°C and products were mixed with BlueJuice gel loading buffer (Invitrogen 10816-015) and separated on a 1% agarose gel with 1:50,000 SYBR-SAFE (S33102) at 80V constant for 70 minutes in TBE running buffer. Gels were visualized on a Bio-Rad Gel Doc 2000.

Following confirmation through PCR screening and restriction endonuclease digestions, DNA sequencing was carried out on clones of the pET-100D/TOPO RVFV NSm1 plasmid using BigDye Terminator cycle sequencing approach (Invitrogen) on a 3130xl Genetic Analyzer (Applied Biosystems) by Tamiko Hisanaga of the National Centre for Foreign Animal Disease, Winnipeg, Canada. Properly constructed clones

were transformed into expression-specialized One-Shot BL21 Star DE3 (Invitrogen K100-01) chemically competent *E. coli* (see Appendix C).

Following transformation, bacteria were plated on LB agar and incubated overnight at 37°C. Colonies were selected, PCR-screened and grown in 1 mL LB broth at 37°C. Following PCR screening, plasmids were purified using a QIAGEN Mini-Prep kit and subjected to restriction endonuclease digestion as described above for TOP10 cells to confirm that clones of the transformed expression cells continued to carry the correctly ligated plasmid.

A pilot study was performed in which bacteria were grown in 5 mL LB broth cultures (BD 244510) to an OD₆₀₀ of 0.5 and induced with 0.1mM isopropyl β-D-1-thiogalactopyranoside (IPTG) hourly for three to six hours. Following protein induction, bacterial cells were pelleted by centrifugation at 16,000 *g* for 20 minutes at 4°C and lysed using BugBuster Protein Extraction Reagent (Novagen 70584-4) with lysozyme and HALT protease inhibitors (Thermo Scientific). The soluble and insoluble protein fractions of bacterial cell lysate were separated using the Inclusion Body BugBuster protocol (see Appendix); the insoluble cell pellet was resuspended in 5% of the original culture volume of deionized water with lysozyme and incubated for five minutes and pelleted by centrifugation at 16,000 *g* for 20 minutes at 4°C. Following centrifugation, the insoluble pellet was resuspended in 10% of the original culture volume of BugBuster protein extraction reagent, incubated with lysozyme at room temperature for five minutes, diluted in an equal volume of 10% concentration BugBuster Protein Extraction Reagent in distilled water and pelleted by centrifugation at 5,000 *g* for 15 minutes. This pellet was resuspended in 20% of

the original culture volume of 10% BugBuster Protein Extraction Reagent in distilled water and centrifuged at 5,000 *g* for 15 minutes at 4°C. The wash step was performed a total of three times with the final spin at 16,000 *g* and the remaining pellet was suspended in NuPAGE lysis buffer for PAGE (polyacrylamide gel electrophoresis).

Soluble and insoluble protein fractions were analysed using NuPAGE SDS denaturing electrophoresis Bis-Tris polyacrylamide gels. The gels were stained with Coomassie G-250 SimplyBlue SafeStain (Invitrogen LC6065). Following the separation of the cell lysate into soluble and insoluble fractions using BugBuster Protein Extraction Reagent, the induced recombinant NSm1 was detected in the lysate insoluble fraction using immunoblots with Nickel (Ni-NTA) anti-His antibody (QIAGEN 34530). The immunoblot protocol is described in Section 2.6.

The proteins in the insoluble protein fraction of expression-induced bacterial cell lysate were separated by NuPAGE lithium dodecyl-sulfate denaturing PAGE, performed using Invitrogen NuPAGE Bis-Tris gels (NP0323PK2) and transferred onto Polyvinylidene fluoride (PVDF) membranes (Bio-Rad 162-0177) using a semi-dry transfer (see Appendix C) in a Bio-Rad Trans-Blot SD Semi-Dry Electrophoretic Transfer Cell (Bio-Rad 170-3940). The presence of the induced protein was confirmed on immunoblots with Ni-NTA anti-His antibody and anti-RVFPV sheep sera (29 dpi, -1 dpi control).

Large-scale production of rNSm1 was performed using six 500 mL volumes of LB broth grown in 2L flasks at 300 rpm orbital shaking for aeration at 37°C. Volumes were inoculated with bacteria to an initial OD_{600nm} of 0.2. IPTG was added

to a final concentration of 1M at an OD_{600nm} of 0.6. Bacteria were harvested at 6 hours post induction and purified as described above with all volumes adjusted to reflect the 3L total volume.

Immunoblots were repeated as described above to confirm the induced expression of rNSm1. Mass spectrometry was performed as described below (Section 2.10) to confirm the amino acid sequence of rNSm1.

2.6 Immunoblotting (Western Blots)

2.6.1 Protein separation and transfer

SDS-PAGE was performed on protein samples mixed 1:1 in 4×NuPAGE sample buffer (Invitrogen) with 10×NuPAGE antioxidant (Invitrogen).

Dithiothreitol was added to a final concentration of 0.1M. Samples were then heated to 95°C for five minutes prior to loading into NuPAGE 4-12% Bis-Tris precast gels (Invitrogen). Gels were submerged in 800 mL NuPAGE MOPS buffer (Invitrogen) in XCell SureLock mini-cell electrophoresis tanks (Invitrogen). Samples were run at 150V constant voltage for 50 minutes.

Following electrophoresis, gels were washed in Milli-Q water (Millipore). Gels were blotted onto PVDF membranes using an iBlot gel transfer device (Invitrogen) at 20V constant voltage for 13 minutes. Membranes were blocked in 10 mL of 5% skim milk (Bio-Rad) Tris-buffered saline with Tween-20 (TBS-T) at room temperature for one hour with gentle rocking prior to probing with primary antibodies.

Novex Sharp (Invitrogen LC5800) protein standard was used as a visible indicator of protein band progress during PAGE and as a protein membrane transfer control. MagicMarkXP (Invitrogen LC5603) was used as a chemiluminescent protein standard.

Primary antibodies used for detection of respective proteins are listed in Table 2, along with working dilutions, secondary antibodies and their dilutions.

2.6.2 Chromogenic immunoblots

The proteins blotted on the PVDV membrane were incubated with primary antibodies diluted in 5 mL of 5% skim milk TBS-T per blot overnight at 4°C with gentle rocking. Membranes were then washed three times in 10 mL TBS-T for 10 minutes each at room temperature. All secondary antibodies were acquired from Kirkegaard & Perry Laboratories (KPL). Blots were incubated with secondary antibodies with horseradish peroxidase conjugates (HRP) in 5 mL of 5% skim milk TBS-T per blot for one hour at room temperature with gentle rocking. Membranes were once again washed three times in 10 mL TBS-T for 10 minutes each at room temperature. Chromogenic signals were developed using SIGMAFAST 3,3'-Diaminobenzidine tablets in 5 mL Milli-Q water (Millipore). The reaction was stopped by rinsing in Milli-Q water and blots were dried overnight in the dark at 37°C.

Novex Sharp (Invitrogen LC5800) protein standard used as a visible indicator of protein band progress during PAGE and as a protein membrane transfer control did not require chromogenic detection.

Table 2. Primary and secondary antibodies used in immunoblots.

Figure	Primary antibody (dilution)	Secondary antibody (dilution)
Figure 6B	NiNTA anti-His conjugate HRP (1:500)	None
Figure 6C	Sheep pre-bleed (1:1000)	Rabbit anti-sheep IgG HRP (1:2500)
Figure 6D	Sheep anti-RVFV (1:1000)	Rabbit anti-sheep IgG HRP (1:2500)
Figure 7B	Rabbit R1108 pre-bleed	Goat anti-rabbit IgG HRP (1:2000)
Figure 7C	Rabbit R1108 anti-NSm1	Goat anti-rabbit IgG HRP (1:2000)
Figure 10A	Rabbit anti-N (1:1000)	Goat anti-rabbit IgG HRP (1:2000)
Figure 10B	Rabbit anti-NSs (1:1000)	Goat anti-rabbit IgG HRP (1:2000)
Figure 12	Rabbit anti-N (1:1000)	Goat anti-rabbit IgG HRP (1:2000)
Figure 13A	Rabbit anti-N (1:1000)	Goat anti-rabbit IgG HRP (1:2000)
Figure 13B	Rabbit anti-NSs (1:1000)	Goat anti-rabbit IgG HRP (1:2000)
Figure 14B	Rabbit R1108 anti-NSm1 (1:1000)	Goat anti-rabbit IgG HRP (1:2000)
Figure 15B	Rabbit R1109 anti-NSm1 (1:1000)	Goat anti-rabbit IgG HRP (1:2000)
Figure 15C	Sheep anti-RVFV (1:100)	Goat anti-rabbit IgG HRP (1:2000)
Figure 16A	Rabbit R1109 pre-bleed (1:100)	Goat anti-rabbit IgG HRP (1:500)
Figure 16B	Rabbit R1109 anti-NSm1 (1:100)	Goat anti-rabbit IgG HRP (1:500)
Figure 16C	Rabbit R1109 anti-NSm1 (1:100)	Goat anti-rabbit IgG HRP (1:500)
Figure 20	Rabbit R1109 anti-NSm1 (1:1000)	Goat anti-rabbit IgG HRP (1:2000)

2.6.3 Enhanced chemiluminescence immunoblots

Blots were incubated with primary antibodies in 5 mL of 5% skim milk TBS-T per blot and incubated overnight at 4°C with gentle rocking. Membranes were then washed three times in 10 mL TBS-T for 10 minutes each at room temperature. Blots were incubated with HRP secondary antibodies in 5 mL of 5% skim milk TBS-T per blot for one hour at room temperature with gentle rocking. Membranes were once again washed three times in 10 mL TBS-T for 10 minutes each at room temperature. Blots were covered with Amersham ECL Plus western blotting reagents (GE RPN2132), sealed in plastic wrap and images were captured on Kodak BioMax Maximum Resolution film (Fisher Scientific 05-728-24) in a dark room. MagicMark XP (Invitrogen LC5603) was used as a chemiluminescent protein standard.

2.7 RVFV protein expression in mammalian or insect cells

To investigate the timeline of RVFV protein expression during primary virus replication in cells, T-25 flasks of Vero E6 or C6/36 cells were infected at MOI 2 and harvested at 3, 6, 9, 12, 15, 18 and 21 hours post infection (hpi) with uninfected control flasks harvested at 3 hpi, 12 hpi and 21 hpi. To harvest cells, media were decanted from the bottles and the cell monolayer were covered with 1 mL of 25% NuPAGE 4× sample buffer in distilled water. Cells were collected using a cell scraper into 2 mL microcentrifuge tubes. Prior to removal from BSL-3E, samples were heated to 95°C for 30 minutes. Samples were stored frozen at -20°C.

Cell lysates in NuPAGE lysis buffer were diluted to protein concentration of 2.0 µg/µL as measured on a NanoDrop 1000 spectrophotometer (Thermo) at 280 nm wavelength. The samples were analysed using chromogenic HRP immunoblotting with rabbit polyclonal anti-N, anti-NSs, commercial anti-NSm1 sera and sheep anti-RVSV sera, as described above in section (2.6).

2.8 Virus preparation and concentration

2.8.1 Viral growth curves

Thirty T-25 flasks each of Vero E6 cells or C6/36 cells were infected with C6/36-amplified RVSV ZH-501 at an MOI of 0.1. Vero E6 cells were grown in vented T-25 flasks (Corning 3056) with 7 mL DMEM/2% FBS at 37°C in 5% CO₂. C6/36 cells were grown in plug-capped T-25 flasks (Corning 430168) in 7 mL ESF-MEM/2% FBS at 28°C. Samples were collected daily for 1 to 8 dpi.

At each time point, three flasks of each cell type were harvested with 1.0 mL supernatant collected from each flask in a 1.5 mL sterile microcentrifuge tube and frozen at -70°C for plaque titration assay. Prior to the titration, samples were thawed, clarified by centrifugation at 3,000 *g* for 30 minutes at 4°C, and tenfold serially diluted (300 µL infectious media in 2.7 mL) in DMEM. Virus growth was evaluated by titrating the plaque forming units per mL of supernatant taken from infected cell cultures as described in section (2.3).

2.8.2 Virus semi-purification by ultracentrifugation through a sucrose cushion

Two T-75 flasks of Vero E6 and two T-75 flasks of C6/36 were infected with

RVFV at an MOI of 0.1. Supernatant was collected from Vero E6 cells and C6/36 cells at 4 dpi. Infectious supernatant was clarified by centrifugation at 3,000 *g* for 30 minutes at 4°C and the clarified supernatant was concentrated by pelleting of the clarified samples through a 2 mL 30% sucrose cushion at 150,000 *g* for two hours. The residual media and sucrose cushion were decanted off and the pelleted virus was resuspended in TN buffer (see Appendix) overnight at 4°C. Virus samples were mixed in equal volumes with NuPAGE sample buffer and heat-inactivated at 95°C for 30 minutes prior to removal from BSL-3E.

Concentrated virus was diluted to 2.0 µg/µL A280 protein concentration as measured using a NanoDrop 1000 spectrophotometer (Thermo Scientific) at 280nm wavelength to detect amino acids, particularly aromatic ring amino acids.

2.8.3 Virus concentration using filtration

Vero E6 and C6/36 cells were infected at an MOI of 0.1. Cells were harvested and the supernatant collected from C6/36 cells at 5 dpi and from Vero E6 at 7dpi. This purification technique was performed concurrently to purification through a sucrose cushion using the same clarified infectious supernatant described above (2.8.2). Filtration purification was performed using the same clarified supernatant. The supernatant was pre-filtered through a 0.45 µm syringe filter and the retentate was discarded. The filtrate was then passed through a 100 kDa NMWL filter (Amicon UFC910024). Retentate was collected and filtrate was passed through a 10 kDa NMWL filter (Amicon UFC901024). The 100 kDa and 10 kDa filter retentates were mixed with equal volumes of NuPAGE sample buffer, heat inactivated at 95 °C

for 30 minutes prior to removal from BSL-3E and stored at -20°C. Protein retentates were run on denaturing PAGE and tested for the presence of RVFV proteins using immunoblots.

2.9 Virus purification

2.9.1 Virus purification with polyethylene glycol precipitation and ultracentrifugation

Vero E6 cells and C6/36 cells were seeded into two Corning M HyperFlasks (Corning 10030) for virus replication. HyperFlasks were seeded using the cells from five confluent T-150 flasks, collected as described above (Sections 2.1.1 and 2.1.2) and resuspended in 560 mL of cell-specific growth media (Appendix B). The media with suspended cells were then transferred into HyperFlasks and incubated as normal for the respective cell line. HyperFlasks contain gas-permeable plastic spacing between layers to facilitate gas exchange, preventing them from mimicking the plug cap sealed flask used to grow C6/36 cells. In order to simulate the growth conditions in plugged flasks, a HyperFlask containing C6/36 cells was placed in a close-fitting airtight plastic bag to provide a fixed volume of air for gas exchange analogous to the air space within a plugged flask, without allowing gas exchange with the room air, which could result in alkalinisation of the growth medium.

During cell growth and following infection, cells within HyperFlasks were observed at 400× magnification. A HyperFlask is composed of ten layers, each with 172 cm² of surface area. A standard light microscope can be focused on either of the bottom two layers of the HyperFlask and inverting the flask allows the microscope

to be focused on the other two outside-most layers, allowing viewing of 40% of the total growing surface within the flask. Gas exchange spaces sit between each layer so that each layer is equally exposed to air conditions within the incubator. Based on the design of the HyperFlask, there is no evidence that the six middle layers of the HyperFlask would be subject to any different conditions from the observable four external layers.

At confluence, each 560 mL HyperFlask was infected approximately at an MOI of 0.01 with RVFV-ZH501 virus stocks that had been grown in either Vero E6 cells or C6/36 cells. The seeding media was decanted out of the HyperFlasks, replaced with the FBS-free infectious media and the flasks were incubated with RVFV for one hour, at 37°C for Vero E6 and at 28°C for C6/36. After one hour, infectious media was removed from the HyperFlask and replaced with fresh media containing 1.8% FBS. Virus was harvested at 2dpi for Vero E6 and 6 dpi for C6/36 cells, shown to be the minimum times for peak virus production based on virus growth curves (Section 2.8.1). Supernatant was decanted off into a separate container without lysing the RVFV infected cells and clarified by centrifugation at 3,000 *g* for 30 minutes at 4°C in a Sorvall Legend RT Plus centrifuge.

Following centrifugation, sodium chloride (NaCl) was added to the clarified supernatant to increase molarity to 0.5 Molar (58.4 g/L). The volumes were refrigerated at 4°C for 2 hours. PEG-6000 was added slowly to a final concentration of 10% w/v while stirring. Glycerol was added to a final concentration of 3% v/v and the volume was stirred overnight at 4°C.

The precipitated supernatant was subsequently centrifuged at 3,000 *g* for 60 minutes at 4°C. Following centrifugation, the supernatant was discarded and the precipitated pellet was resuspended in 10mL solution of 100mM NaCl 10mM HEPES. A sample of this solution was taken as a purification control. Some solid material could not be dissolved and was discarded after a sample of this material was collected for immunoblot analysis as an indicator of the purification progress by testing for the presence of RVFV N, NSs and NSm1 at this step in the process.

PEG-soluble fractions were collected after PEG-resuspension but prior to ultracentrifugation as a control. Resuspended virus samples were purified by sucrose or iodixanol gradient ultracentrifugation at 40,000 rpm (200,000 *g*_{avg}) in a Beckman Coulter SW-Ti-41 swinging bucket rotor for two hours, described below in section 2.9.2. Visible protein bands were syringe-aspirated and examined on immunoblots.

2.9.2 Virus purification using filtration and gradient ultracentrifugation

Vero E6 cells and C6/36 cells were grown into two Corning M HyperFlasks (Corning 10030) for virus replication. At confluence, each 560 mL HyperFlask was infected at a MOI of 0.01 with RVFV-ZH501 virus stocks that had been grown in either Vero E6 cells or C6/36 cells, as described above (Section 2.8.3).

Supernatant was collected without lysing the RVFV infected cells and clarified by centrifugation at 3,000 *g* for 30 minutes at 4°C in a Sorvall Legend RT Plus centrifuge. Supernatant was gravity-filtered through a 0.2 µm polyether-sulfone filter (Millipore SCGPU11RE) with two glass fibre pre-filters (Millipore

AP2507500 and AP1507500) at 4°C overnight. Filtrate was concentrated through repeated use of Amicon Ultra-15 100,000 (100k) NMWL cellulose centrifugal filter units (Millipore UFC910024) at 4,000 *g* for 15 minutes at room temperature to concentrate the virus approximately 100-fold.

Ultracentrifuge gradients were created using 10-40% OptiPrep iodixanol solutions (Sigma-Aldrich D1556) that were allowed to diffuse for one hour at room temperature. Concentrated virus was layered over the gradient and centrifuged at 14,200 rpm (25,000 g_{avg}) in a SW Ti 32 Beckman-Coulter swing-bucket rotor for 16 hours at 4°C or centrifuged at 40,000 rpm (200,000 g_{avg}) in a SW Ti 41 Beckman-Coulter swing-bucket rotor for 2 hours at 4°C. The ultracentrifuge was a Beckman-Coulter Optima L-100K. Visible bands were collected through bottom-puncture aspiration and collected in 1 mL volumes in sterile 1.5 mL microcentrifuge tubes. Each 1000 μ L sample was mixed with 333 μ L NuPAGE 4 \times sample buffer and heat-inactivated at 95°C for 30 minutes before being removed from BSL-3E. Samples were frozen at -20°C prior to PAGE and immunoblotting.

2.9.3 Dialysis for removal of iodixanol

Samples collected following gradient ultracentrifugation through an iodixanol gradient could not be analyzed for protein content using absorption of 280nm wavelength light (Simonian and Smith 2006). Iodixanol gradient solutions have an overwhelming level of optical interference when analyzed using this technique and virus samples collected through iodixanol gradient ultracentrifugation were approximately equalized by aspirating the gradient sample

in equal volumes. The protein load was compared using the apparent proteins visible in Coomassie-stained protein gels.

Attempts were made to remove the iodixanol from gradient ultracentrifuge-purified samples through dialysis in sterile phosphate-buffered saline (PBS). Samples were dialyzed in 3 mL volume 10 kDa molecular weight cut-off (MWCO) Thermo Scientific Slide-A-Lyzer G2 dialysis cassettes (Thermo 87730) in 4L volumes of PBS at 4°C with stirring. PBS was changed after two hours and after four hours of dialysis, and dialysis was allowed to continue overnight. The osmosis of water across the dialysis membrane diluted the sample to the point of possibly damaging the membrane due to over-inflation, which could have resulted in the loss of sample into the PBS. Because the large volume of PBS required was prepared and autoclaved in 2 L glass bottles, it was difficult to transport safely in and out of BSL-3E.

2.10 Mass spectrometry

Proteins from purified virus preparations (VE6-RVFPV and C6/36 RVFPV) were separated using denaturing SDS-PAGE on Invitrogen NuPAGE Bis-Tris gels (NP0321BOX). Bands of interest were excised with a scalpel and transferred into Protein Lo-Bind 0.5 mL microcentrifuge tubes (Invitrogen) and refrigerated at 4°C prior to >2.5MRad gamma-irradiation at 4°C. Samples bands were cut into 1mm³ cubes and vortexed for 30 minutes at 700 rpm at room temperature in 1:1 100mM ammonium bicarbonate and acetonitrile buffer to destain the gel. Buffer was discarded and the wash was repeated. Gel slices were dehydrated in 500 µL

acetonitrile at room temperature for five minutes. Acetonitrile was discarded and the dehydration was repeated before the gel slices were allowed to air dry. Gel slices were rehydrated in 50 μ L of 1M dithiothreitol (Fluka 43819) at 55°C for 30 minutes. After being allowed to cool to room temperature, dithiothreitol was discarded and replaced with 500 μ L acetonitrile for 10 minutes at room temperature. Acetonitrile was discarded and replaced with 50 μ L of 50mM iodoacetamine (Sigma I6125), then incubated in the dark at room temperature for 30 minutes. Supernatant was discarded and gel plugs were washed twice in 500 μ L of 1:1 100mM ammonium bicarbonate and acetonitrile buffer while being vortexed at 700 rpm for 10 minutes at room temperature. Gel slices were dehydrated twice in 500 μ L acetonitrile for 5 minutes at room temperature before being dried completely in a SpeedVac. The dried gel slices were rehydrated in 45 μ L ice cold 50mM acetic acid (Sigma 320099) 1.0 μ g/ μ L trypsin (Promega V5280) solution on ice for 2 hours in the dark. Samples were then incubated at 37°C overnight in the dark.

Following overnight incubation, supernatant was transferred to fresh Protein Lo-Bind 0.5 mL microcentrifuge tubes (Invitrogen). Gel slices were vortexed twice in 100 μ L 5% formic acid, 50% acetonitrile solution at 700 rpm for 25 minutes at room temperature, with supernatant being added to the collection tubes after each vortexing. Supernatant was dried in a SpeedVac and stored at -80°C. Prior to liquid chromatography electrospray ionization tandem mass spectrometry, samples were resuspended in 15 μ L of 2% acetonitrile 1% formic acid solution. BSA blanks were run between each sample to reduce protein carryover between samplings. Data

were analyzed using Mascot mass spectrometry software (Matrix Science) and viewed using Scaffold3 (Proteome Software).

2.11 Electron microscopy

Electron microscopy was performed by Lynn Burton at the National Microbiology Laboratory, Winnipeg, Canada. Samples were mixed with fixative to a final concentration of 2% glutaraldehyde overnight at 4°C to fix the virus prior to removal from BSL-3E.

2.12 Comparative serum neutralization

Serum neutralization assays were performed using sheep sera raised against Vero E6-grown RVFV ZH501, collected at 28 dpi or 33 dpi, with virus that had been grown in either Vero E6 or C6/36 cells. Sheep sera from animals experimentally infected with RVFV ZH-501 were serially diluted at a factor of 2 in serum-free 1X DMEM (Wisent 319-005) and dilutions were mixed with 100 pfu of virus and incubated for one hour at 37°C. The virus/serum mixture was then further diluted at a factor of 2 in FBS-free DMEM and added to confluent 24-well plates of Vero E6 cells volume. Each dilution was plated in triplicate. One hour incubation at 37°C 5% CO₂ was allowed for virus adsorption before the infectious media was replaced with 1.75% carboxymethyl cellulose media overlay (Appendix B). Plates were incubated for 5 days, fixed with 10% phosphate buffered formalin (Fisher Scientific SF100-4) and stained with 5% crystal violet in methanol (Sigma-Aldrich C0775-100G).

Chapter 3: Results

3.1 Expression and purification of recombinant NSm1

Viral RNA from RVFV ZH501 grown in Vero E6 cells was isolated for RT-PCR to amplify the NSm1 gene region. The resulting PCR products were separated through agarose gel electrophoresis (Figure 3), excised and extracted from the gel, cloned into the pET-100/D-TOP0 expression vector and transformed into chemically competent cells. Plasmids were screened using direct PCR of bacterial colonies (Figure 4), plasmid purification and restriction endonuclease digestion (Figure 5) and DNA sequencing (see Appendix). Restriction endonuclease digestion of pET-100 RVFV NSm1 plasmids: *XbaI* linearizes the 7834nt plasmid, and *NdeI* cuts the plasmid into fragments of 5662, 1509 and 658nt length. Clones that appeared to contain the correct sequence, based on PCR screening, restriction endonuclease digestion and DNA sequencing, were transformed into expression-specialized chemically competent *E. coli* BL21 Star cells and screening was repeated (Figure 5).

The expressed recombinant NSm1 was detected in the insoluble fraction of cell lysate (Figure 6) employing Bis-Tris denaturing polyacrylamide gel electrophoresis and immunoblotting. The identity of the expressed protein was confirmed through immunoblotting with Ni NTA anti-HIS antibody (Figure 6.B) and anti-RVFV sheep sera (Figure 6.D). rNSm1 was found to be insoluble and washed using BugBuster protein extraction reagent. The apparent molecular weight of rNSm1 was approximately 60 kDa; 20 kDa smaller than predicted. There is an apparent size discrepancy between the rNSm1 shown in frames B and D, although the discrepancy is small. Each blot was produced from

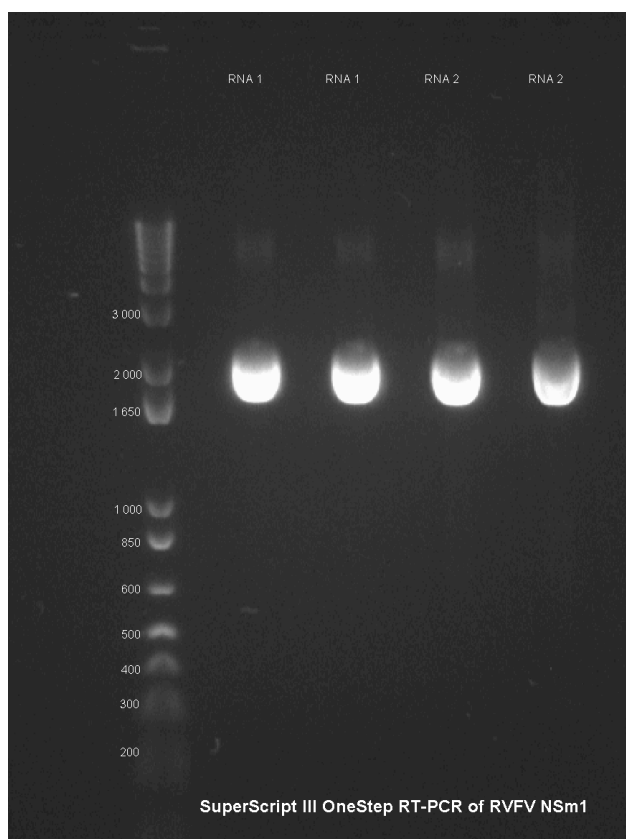


Figure 3. Agarose gel of the DNA products of RT-PCR of the RVFV ZH501 NSm1 gene (nt 20-2080) using SuperScript III OneStep reagents. The DNA products were separated by size through gel electrophoresis through a 1% agarose gel containing 1:50,000 SYBR-SAFE and trans-illuminated with ultraviolet (UV) light. The four DNA products seen are approximately 2000nt in size, which is consistent with the expected size of the amplified DNA products.

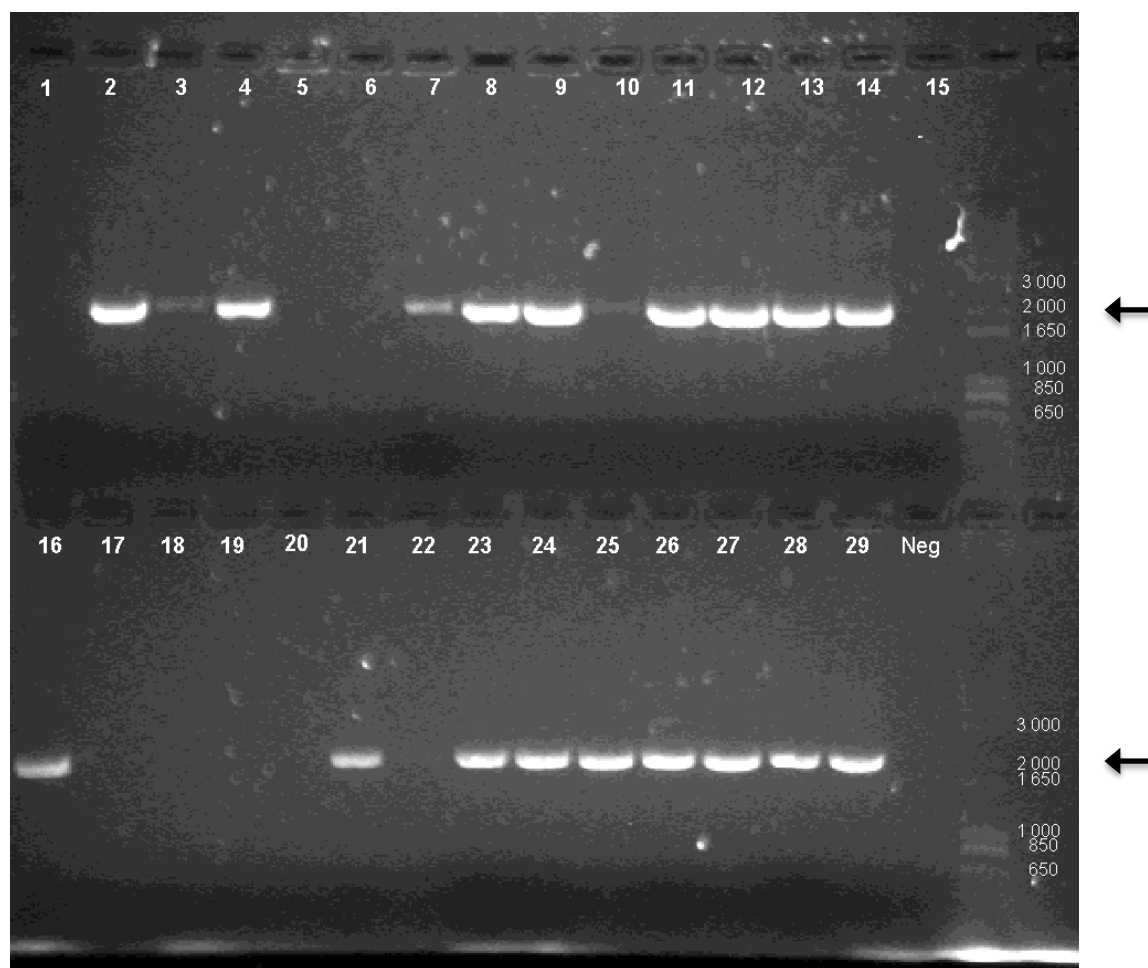


Figure 4. Agarose gel of PCR screening of TOP10 bacterial colonies transformed with pET-100 RVFV NSm1. The expected size of the NSm1 insert amplified is 2060nt (indicated by arrows).

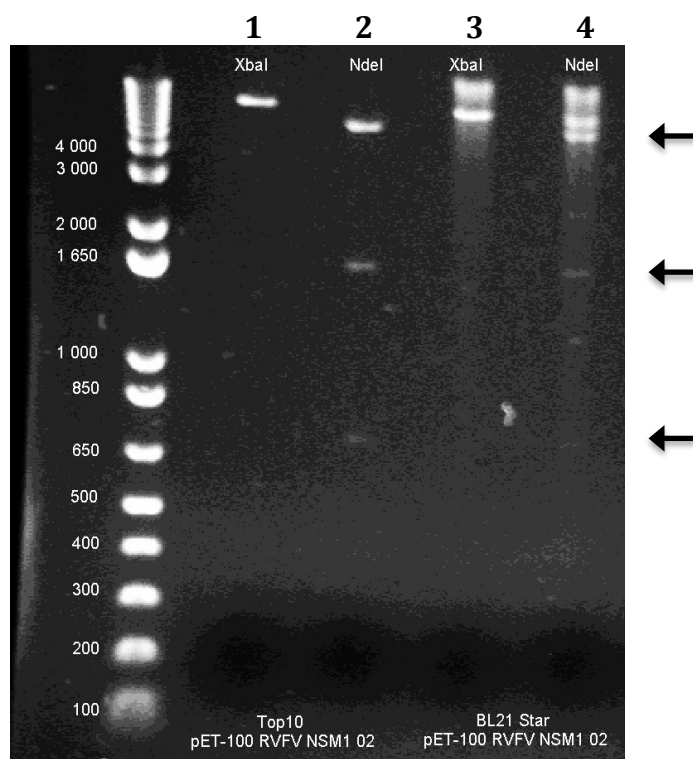


Figure 5. Agarose gel of pET-100 RVFV NSm1 plasmids following restriction endonuclease digestion. Lanes 1 and 3: digestion with XbaI linearizes the 7834nt plasmid. Lanes 2 and 4: Digestion with NdeI cuts the plasmid into fragments of 5662, 1509 and 658nt length (indicated by arrows). Lanes 1 and 2 contain plasmids purified from TOP10 cloning cells while lanes 3 and 4 contain the same plasmid after transformation into BL21 Star expression cells.

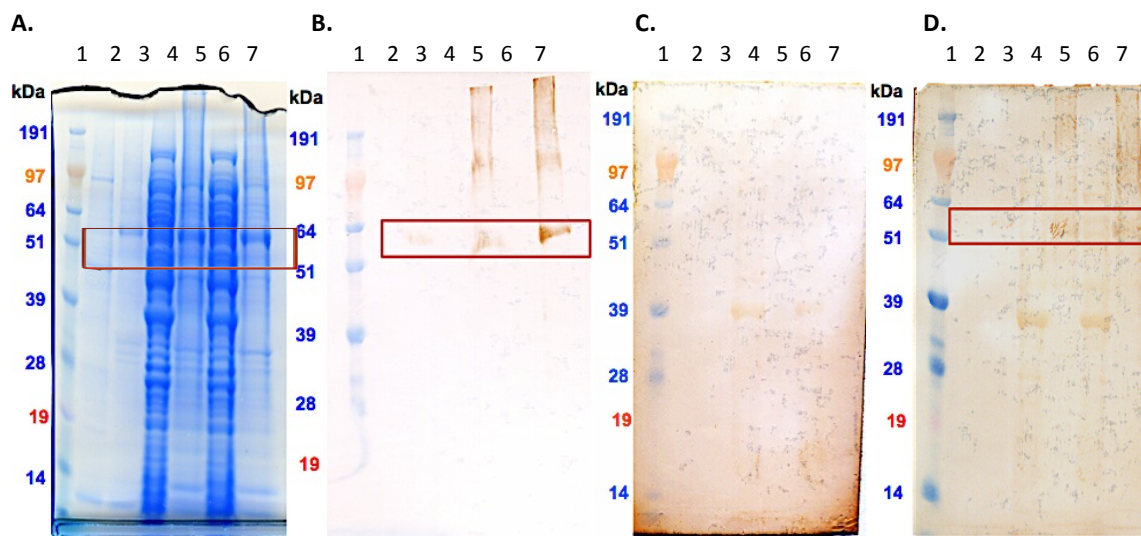


Figure 6. Immunoblots for the detection of rNSm1 expression in the soluble and insoluble cell lysate fractions following IPTG-induced expression of pET-100 RVFV NSm1 in One-Shot BL21 Star *E. coli* cells. Lanes, left to right: 1. SeeBlue Plus 2 pre-stained protein standard. 2. Uninduced control without IPTG. 3. +1mM IPTG. 4. 0.25mM IPTG soluble fraction. 5. 0.25mM IPTG insoluble fraction. 6. 0.75mM IPTG soluble fraction. 7. 0.75mM IPTG insoluble fraction. (A) Protein gel stained with Coomassie G-250 SimplyBlue Safestain. (B) NiNTA anti-HIS conjugate HRP. (C) Sheep negative control sera -2 dpi. (D) Sheep anti-RVSV sera 29 dpi. rNSm1 is detected by anti-HIS and sheep anti-RVSV sera in the insoluble fractions only.

half of a single gel that was loaded and run; the apparent molecular weights of rNSm1 and non-specifically bound visible proteins appear similar between A and D and between B and C. Thus, the size differences seen between rNSm1 samples in immunoblots B and D are likely a gel- or buffer-effect based on PAGE conditions.

Repeated DNA sequencing of the plasmid showed a single nucleotide deletion in a seven guanine repeat (nt 1620-1626). This frameshift mutation resulted in a stop codon one amino acid downstream (nt 1630-1632), truncating the recombinant protein at 79% of the expected length (Appendix A), but maintaining the NSm1-specific antigenic region at the N-terminus of the protein intact and expressed correctly.

Proteomic predictive modelling of the truncated recombinant protein using ExPASy ProtParam (Swiss Institute of Bioinformatics) generated an expected molecular weight of 62.6 kDa (Appendix A), which is consistent with the apparent molecular weight (Figure 6). Mass spectrometry identified rNSm1 amino acid sequences to more than 75% of the protein's length (Appendix A). The rNSm1 was suitable to be used as a positive control for antibodies directed at the N-terminal 545 amino acids of the 690 amino acids of NSm1, including antibodies specifically generated against the very N-terminus of the NSm1 protein.

3.2 Development of NSm1-specific antibodies

Concurrent to the recombinant protein development, a synthetic peptide polyclonal antibody development was commissioned. The peptide SSTREETCFGDSTNPE was synthesized and used to produce polyclonal monospecific

rabbit sera. These rabbit polyclonal sera specifically recognized rNSm1 on immunoblots (Figure 7).

3.3 Preparation of RVFV stocks

Typical mammalian cells used for RVFV infection are Vero E6, an immortalized cell line of African green monkey kidney epithelium, an interferon production-deficient line frequently used for virus growth (Desmyter *et al* 1968). Cells were infected at 95% confluence with RVFV previously grown in Vero E6 cells at an MOI 0.1 and the supernatant was collected after extensive cell death at 5 dpi. The virus was collected in clarified supernatant; plaque titration on Vero E6 cells showed $10^{6.9}$ pfu/mL.

C6/36 is an immortalized line of Asian tiger mosquito larva epithelium, isolated for its susceptibility to dengue virus that has previously been used to culture RVFV (Ellis et al. 1988). Species identity of the cell line was confirmed using PCR of the *Aedes albopictus* mitochondrial DNA cytochrome C species marker gene (Figure 8).

Mosquito cell lines have been reported not to show cytopathic effects (CPE) with RVFV infection (Peters and Anderson 1981). C6/36 cultures do not show visible cellular debris and do not adhere firmly to cell culture flasks, making it difficult to perform plaque assays or 50% tissue culture infectious dose (TCID₅₀) assays, but they do manifest a stressed phenotype in which cells detach from the support and form clumps. This phenotype can be initiated through a variety of stressors such as virus infection, changes in pH or osmolarity. Higher MOIs increase

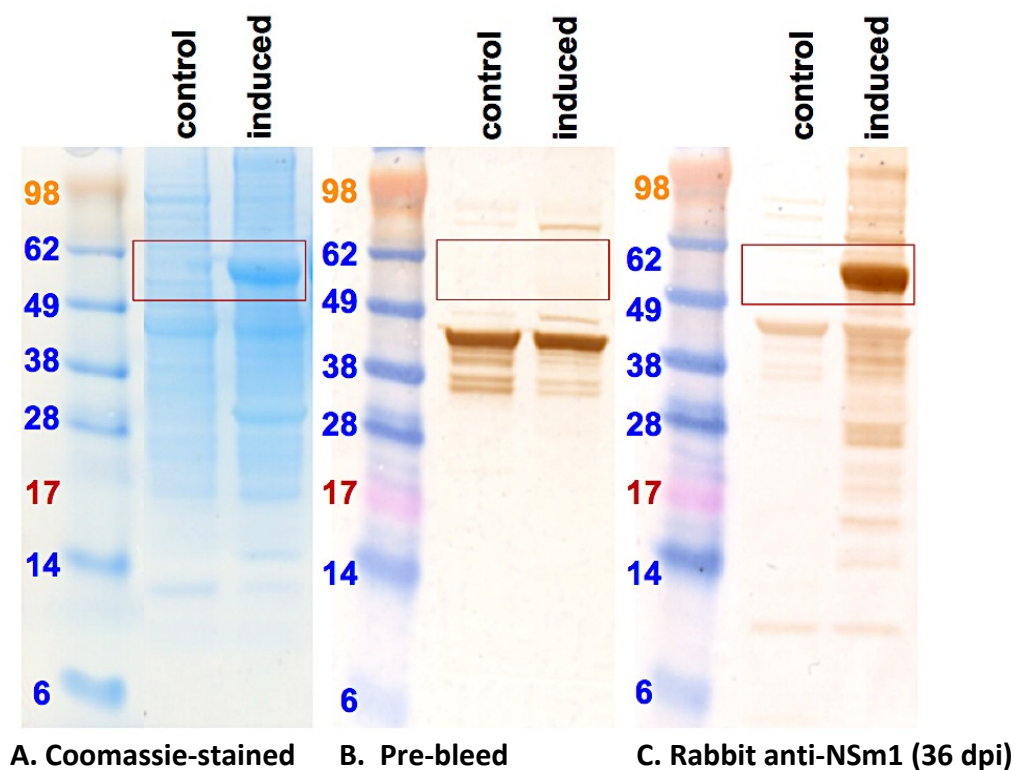


Figure 7. Detection of recombinant NSm1 using R1108 rabbit anti-NSm1 polyclonal serum. The first panel shows the protein gel stained with Coomassie G-250 SimplyBlue SafeStain. Immunoblots were performed with pre-bleed and anti-RVSV rabbit R1108 anti-NSm1 sera (1:250 dilution) with secondary goat anti-rabbit IgG HRP antibodies (1:2000 dilution). The red box between 65 kDa and 50 kDa indicates the expression of a protein induced by IPTG that is prominently bound by the serum at 36 dpi but not detected by pre-bleed serum.

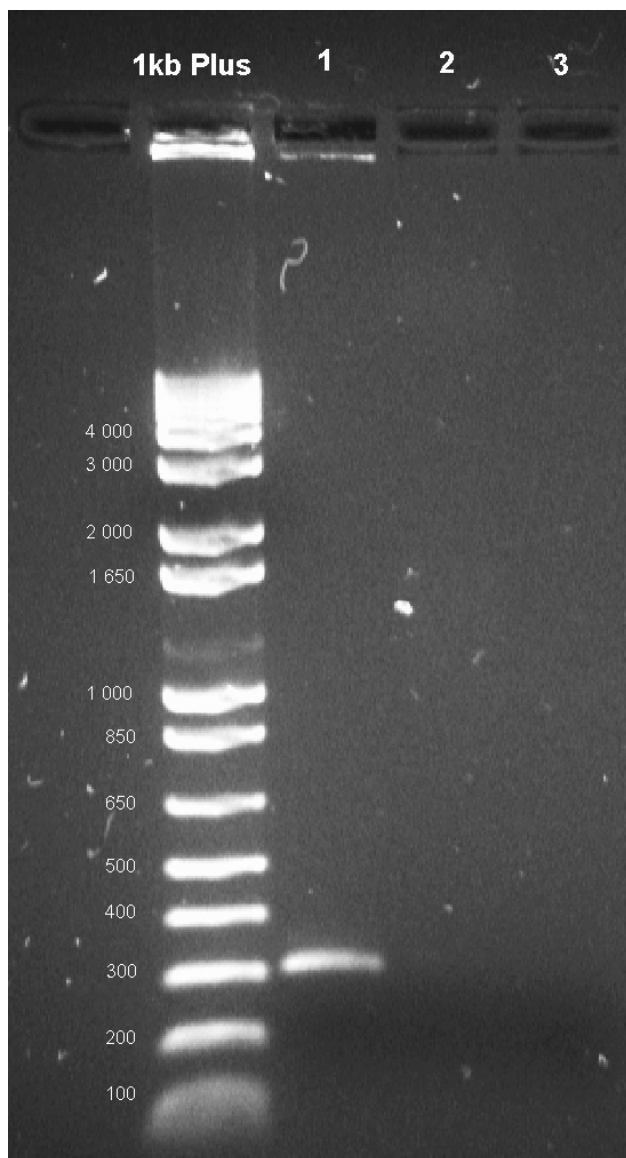


Figure 8. An agarose gel of the PCR amplification of the *A. albopictus* mitochondrial DNA cytochrome C species marker gene. The confirmatory amplicon is 300nt in size. Lane 1 contains *Aedes albopictus* cell line C6/36 lysate. Lane 2 contains sterile C6/36 culture media. Lane 3 is a negative control lane containing only PCR master mix and primers.

this stress response and may kill the cells, but infection of up to 50 MOI do not show visible debris from lysed cells at 4 dpi (Figure 9). Because C6/36 cells are weakly adherent to growth surfaces, they cannot be washed effectively when grown in multi-well plates.

C6/36 cells were infected at 95% confluence at MOI 0.1 and harvested at 7 dpi. Despite the lack of apparent cellular debris, the supernatant was clarified using the same protocol as for Vero E6 supernatant. TCID₅₀ titration of virus stocks on C6/36 cells were found to be subjective, based on other factors possibly leading to the stressed phenotype. C6/36-amplified virus stocks were titrated on Vero E6 cells yielding a titre of $10^{8.2}$ pfu/mL for the stock virus.

3.4 Selected RVFV proteins expressed in mammalian or insect cells

To examine the expression of viral proteins during infection, time course studies were performed for the first round of replication in Vero E6 or C6/36 cells (Figure 10). For both anti-N and anti-NSs antibodies, viral proteins in C6/36 cells crossed the detection threshold at approximately three hours later than in Vero E6 cells. C6/36 cells are typically grown at 28°C, 9°C colder than the incubation temperature for Vero E6 cells. Within the functional temperature range of most biological enzymes, there is a doubling in the rate of reaction when the temperature is increased 10°C (the Q10 rule); this rate of reaction is consistent with the observation of nucleocapsid protein N reaching detectable levels at 3 hpi in Vero E6 cells and 6 hpi in C6/36 cells. NSs reaches visible levels at 6 hpi in Vero E6 cells and 9 hpi in C6/36 cells, but the three-hour time points using in this experiment the

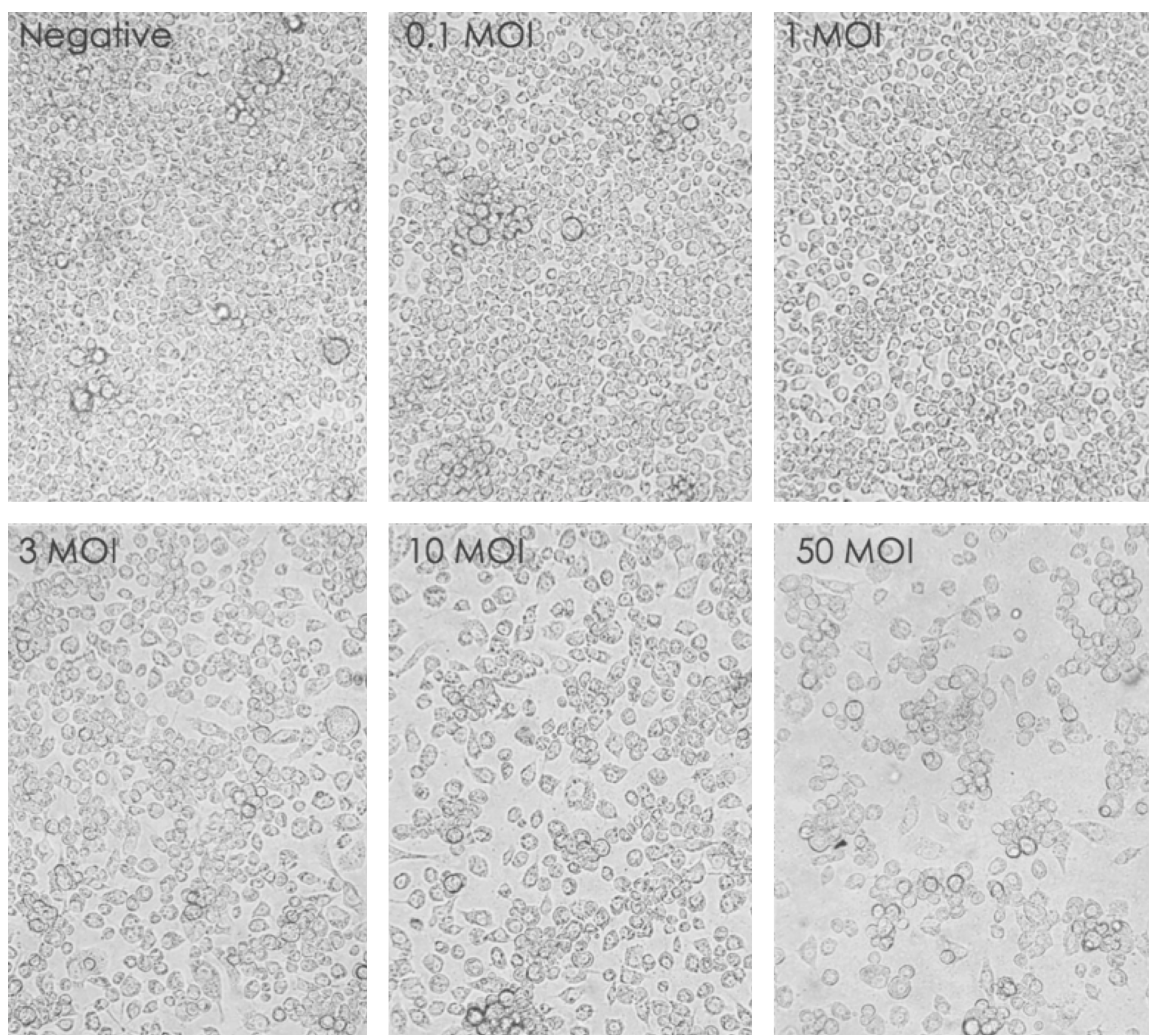


Figure 9. Infection of C6/36 with RVFV at multiple MOI, images taken at 4 dpi. Despite obvious CPE correlating with increased MOI, there is no visible evidence of lysed cellular debris.

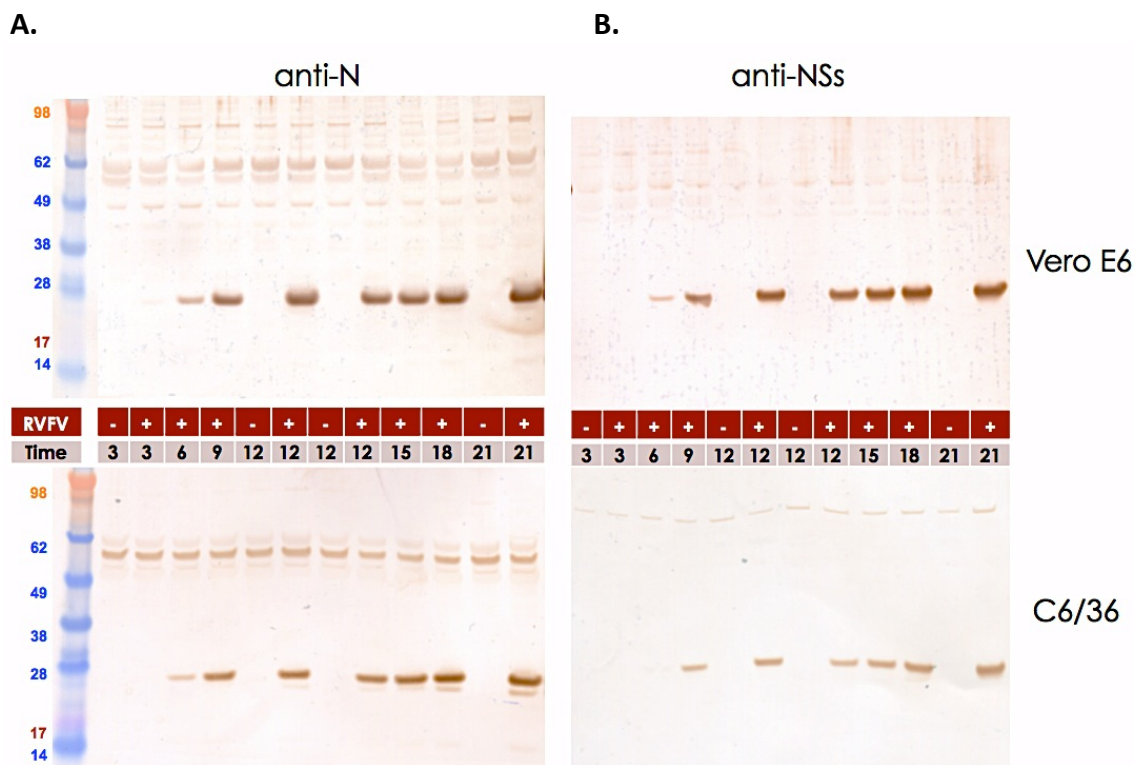


Figure 10. Immunoblots of Vero E6 or C6/36 cell lysates over a 21 hour time course. Time is given in hour post infection. Samples were diluted to a concentration of 2.0 $\mu\text{g}/\mu\text{L}$ based on spectrophotometric absorbance at 280nm wavelength. Uninfected lysates were collected as negative controls at 3, 12 and 21hpi. **A.** Immunoblot using anti-N (nucleocapsid protein) rabbit serum. Nucleocapsid N protein is first detectable in Vero E6 cells at 3 hpi and in C6/36 cells at 6 hpi. **B.** Immunoblot using anti-NSs (non-structural NSs protein) rabbit sera. Accessory protein NSs is first detectable in Vero E6 cells at 6 hpi and in C6/36 cells at 9 hpi. Based on an incubation temperature difference of 9°C (37°C for Vero E6 and 28°C for C6/36), these differences are not significant.

limits the resolution of these data. Sheep polyclonal anti-RVFPV sera only bound to a protein in the size of nucleocapsid N, and with much less sensitivity than the anti-N rabbit serum (not shown). Anti-NSm1 failed to bind any detectable viral protein in the cell lysates even at the latest time point of 21 hrs post infection (not shown). Non-denatured proteins in infectious supernatant were concentrated using 100 kDa nominal molecular weight limit (NMWL) filtration and immunoblot assayed but the positive signals detected were not confirmed by mass spectrometry (see Appendix D).

3.5 Virus growth and purification

The optimum time point for collection of virions for purification was determined by titrating cell culture supernatant collected daily over a period of 8 days post infection using plaque assay (Figure 11). The titre in Vero E6 cells did not significantly vary after the first 24 hours. This curve was consistent for two complete replicates infected with different aliquots of virus. The titre in C6/36 cells increased over several days, reaching its highest level at 6 dpi. In subsequent experiments, Vero E6-amplified RVFPV was collected at 2 dpi and C6/36-amplified RVFPV was collected at 6 dpi.

To investigate phenotypic differences in cell cultures infected with virus stock of either Vero E6 or C6/36 origin, HyperFlasks of Vero E6 cells and C6/36 cells were infected with VE6-RVFPV and C6-RVFPV in duplicate. HyperFlasks were observed daily for four days at 400× magnification and inoculated Vero E6 or C6/36 cells did not show significantly different CPE following infection with insect- or

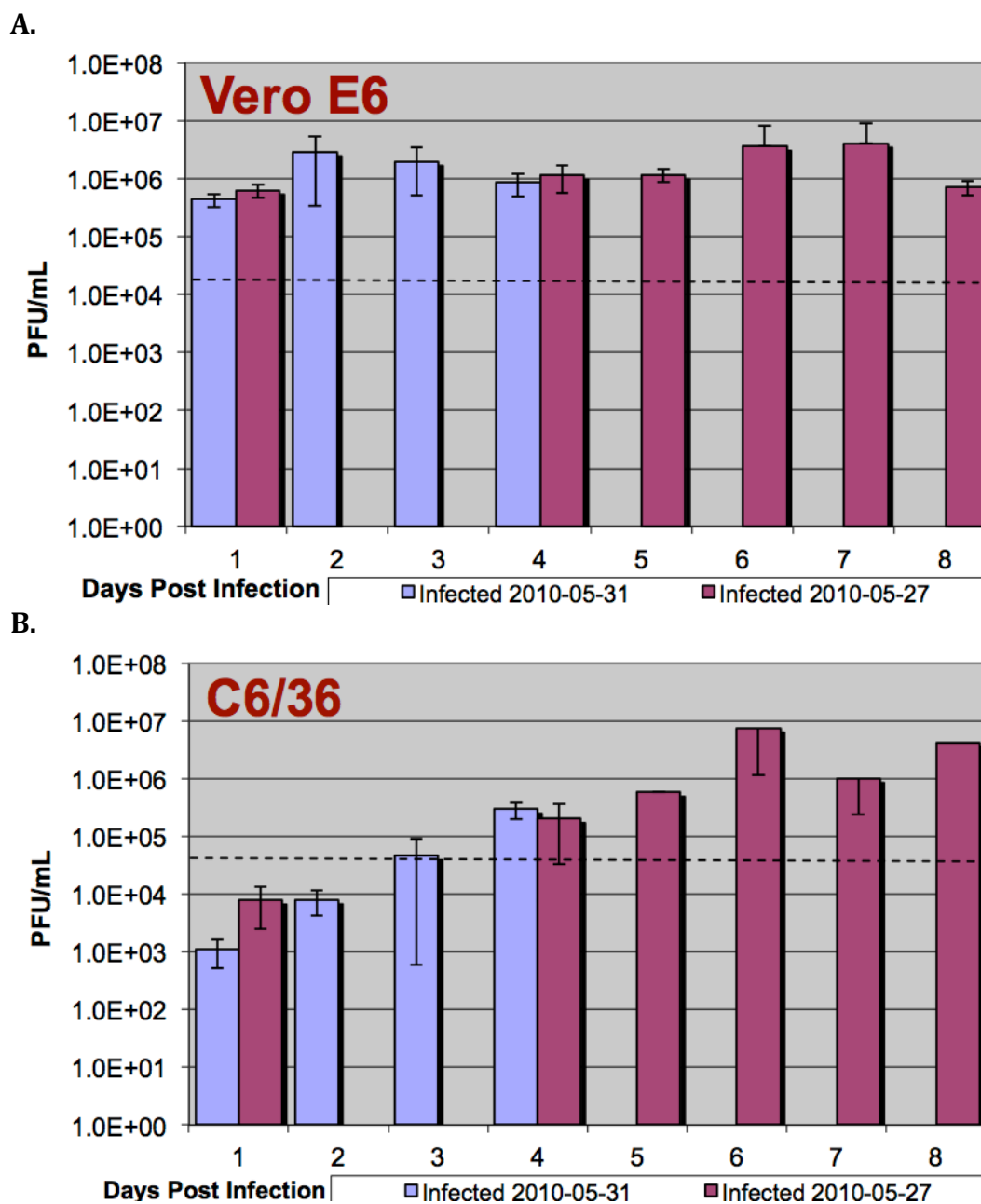


Figure 11. Production of RVFV in cell culture over time. Cells were incubated with virus for one hour before the infectious media was removed. Supernatant was collected, centrifuge-clarified at 3,000 *g* and frozen at -70°C. Virus was thawed and titrated on Vero E6 cells. Each collection was performed in triplicate and titrated separately. Error bars indicate variation between the averages calculated for each replicate. The horizontal line indicates the input titre of MOI 0.1. **A.** Growth of RVFV in Vero E6 cells following infection at MOI 0.1 with virus produced in Vero E6 cells at 37°C in 5% CO₂. **B.** Growth of RVFV in C6/36 cells following infection at MOI 0.1 with virus produced in C6/36 cells at 28°C in sealed flasks without exposure to room air.

mammalian-derived RVFV (not shown). Complete cell death was observed in Vero E6 HyperFlasks at 4 dpi. HyperFlasks containing C6/36 cells did not show detectable cell lysis even at 14 dpi.

3.6 RVFV virions assembled in mammalian or insect cells

In order to establish comparable levels of protein concentration, Vero E6 and C6/36 supernatants containing RVFV were diluted to 2.0 µg protein/µL as measured using 280nm wavelength light. Because iodixanol gradients inhibit the calculation of protein concentrations through spectrophotometry (Simonian and Smith 2006), the protein load from samples collected following ultracentrifugation were compared using the apparent proteins visible in Coomassie-stained protein gels.

Dialysis in sterile phosphate-buffered saline (PBS) was attempted to remove the iodixanol from ultracentrifuge-purified samples of virus. Due to the technical complications and loss of concentration of the samples, dialysis was not continued on subsequent iodixanol purification procedures and relative protein levels were visually compared in PAGE gels using Coomassie staining.

Clarified virus preparations were concentrated and purified through a variety of techniques including 100 kDa NMWL filter concentration and polyethylene glycol precipitation prior to ultracentrifugation into sucrose or iodixanol gradients (Section 2.9.1). PEG-soluble and PEG-insoluble fractions were collected following PEG resuspension but prior to ultracentrifugation.

Following ultracentrifugation, two bands were visible in each iodixanol gradient. The approximate iodixanol concentration around these bands were

estimated based on bottom-puncture aspiration and measurement of the volumes removed compared to the volumes initially layered to produce the gradient. The dense band of each virus preparation were collected at a depth into the gradient estimated to be approximately 25% iodixanol, based on the volume of bottom-puncture aspirant removed to reach the band. This is the gradient density expected for optimal purification of *Bunyaviridae* (AXIS-SHIELD 2011).

3.7 To confirm presence of virions in preparations – N immunoblots

Immunoblots against nucleocapsid N were used to confirm the presence of RVFV in purified samples. A second N band was visible at approximately 56 kDa and mass spectrometric analysis (not shown) detected the presence of 28 kDa N, suggesting that this is an N dimer.

Virus amplified in Vero E6 cells showed higher levels of N protein on immunoblots (Figures 12 and 13A), based on the intensity of the protein bands viewed on Coomassie blue stained denaturing PAGE (Figure 14A). A comparison of the levels of nucleocapsid protein in Vero E6 and C6/36 cell lysate, standardized to a total protein concentration of 2.0 µg/µL (Figure 10), shows a marginally larger signal from Vero E6 cell lysate but also shows a greater amount of nonspecific binding than C6/36 cells. Based on these factors, there does not appear to be a significant difference in the level of nucleocapsid protein incorporated into virions assembled in Vero E6 compared to C6/36 cells during RVFV replication up to 21 hpi.

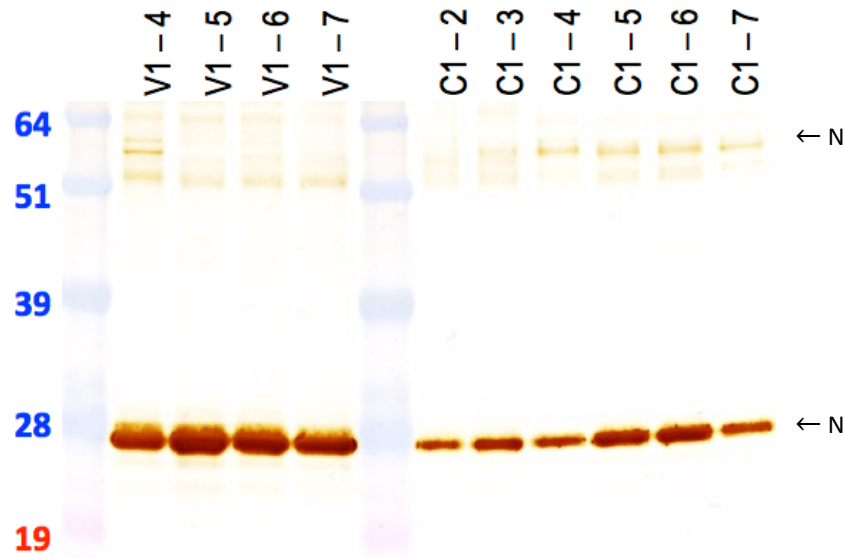


Figure 12. Immunoblot of Vero E6 RVFV (V1) and C6/36 RVFV (C1) with anti-nucleocapsid (N) rabbit serum (1:2500 dilution). Virus from clarified supernatant was pelleted through a 20-40% iodixanol discontinuous gradient interface at 25,000 *g* for 16 hours at 4°C and 0.5 mL fractions were collected from bottom-puncture aspiration. Numbers next to each lane indicate the millilitre volume collected sequentially through bottom-puncture aspiration. Arrows indicate N at 28 kDa and an N-dimer at 56 kDa. There appears to be more nucleocapsid protein detected in the preparations from Vero E6 cells than from C6/36 cells in the immunoblot.

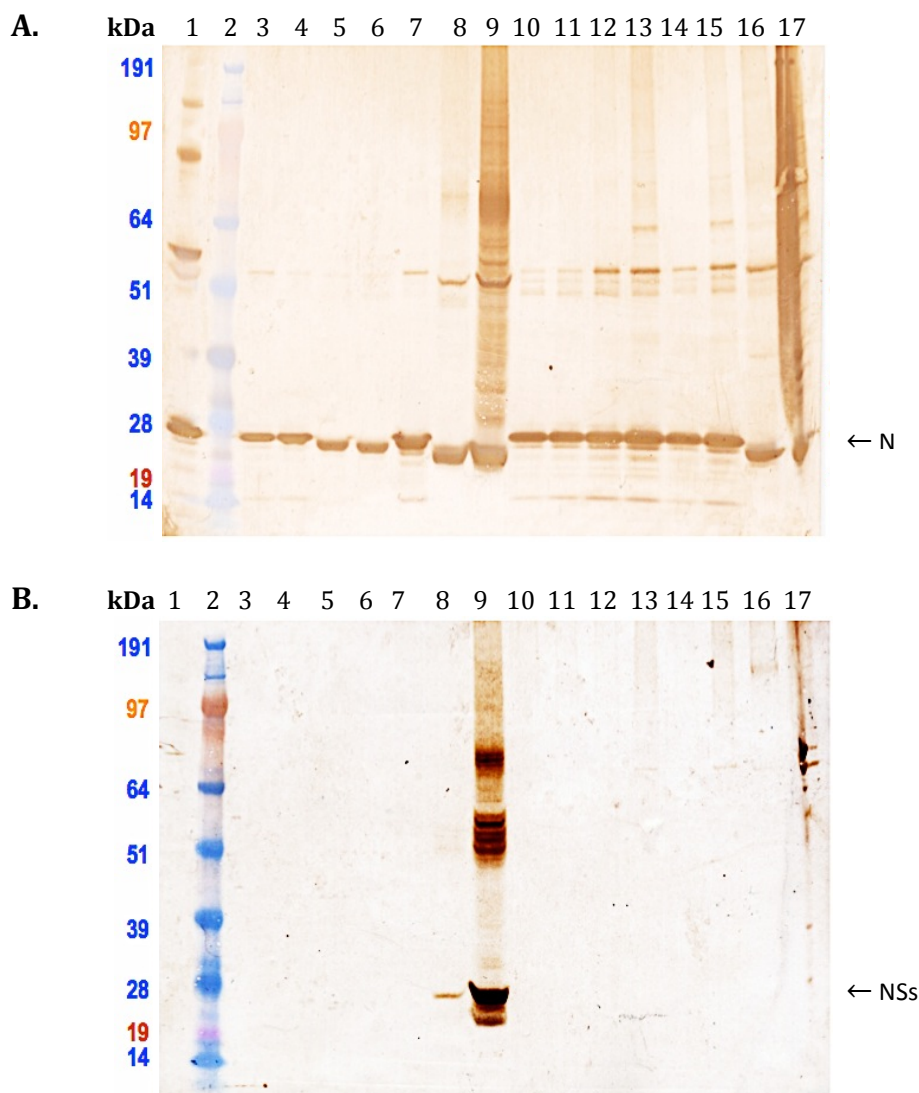


Figure 13. Immunoblot of Vero E6 RVFV and C6/36 RVFV following polyethylene glycol precipitation and ultracentrifugation through sucrose or iodixanol gradients (Section 2.9.1). Lanes, left to right: 1. rNSm1 recombinant bacterial protein positive control. 2. SeeBlue Plus 2 pre-stained protein standard. 3-4. Replicates of Vero E6-derived RVFV collected from a sucrose gradient. 5-7. Replicates of Vero E6-derived RVFV collected from an iodixanol gradient. 8. Vero E6-derived RVFV resolubilized following polyethylene glycol (PEG) precipitation, prior to gradient ultracentrifugation. 9. Vero E6-derived RVFV that remained insoluble following PEG precipitation. 10-12. Replicates of C6/36-derived RVFV collected from a sucrose gradient. 13-15. Replicates of C6/36-derived RVFV collected from an iodixanol gradient. 16. C6/36-derived RVFV resolubilized following PEG precipitation. 17. C6/36-derived RVFV that remained insoluble following PEG precipitation. **A.** Immunoblot probed with anti-N antibodies from rabbit anti-N serum at 1:1000 dilution. Arrow indicates nucleocapsid protein at 31 kDa. **B.** bound with rabbit anti-NSs serum at 1:1000 dilution. Arrow indicates NSs at 28 kDa. Figures 13 and 14 were prepared concurrently from the same samples.

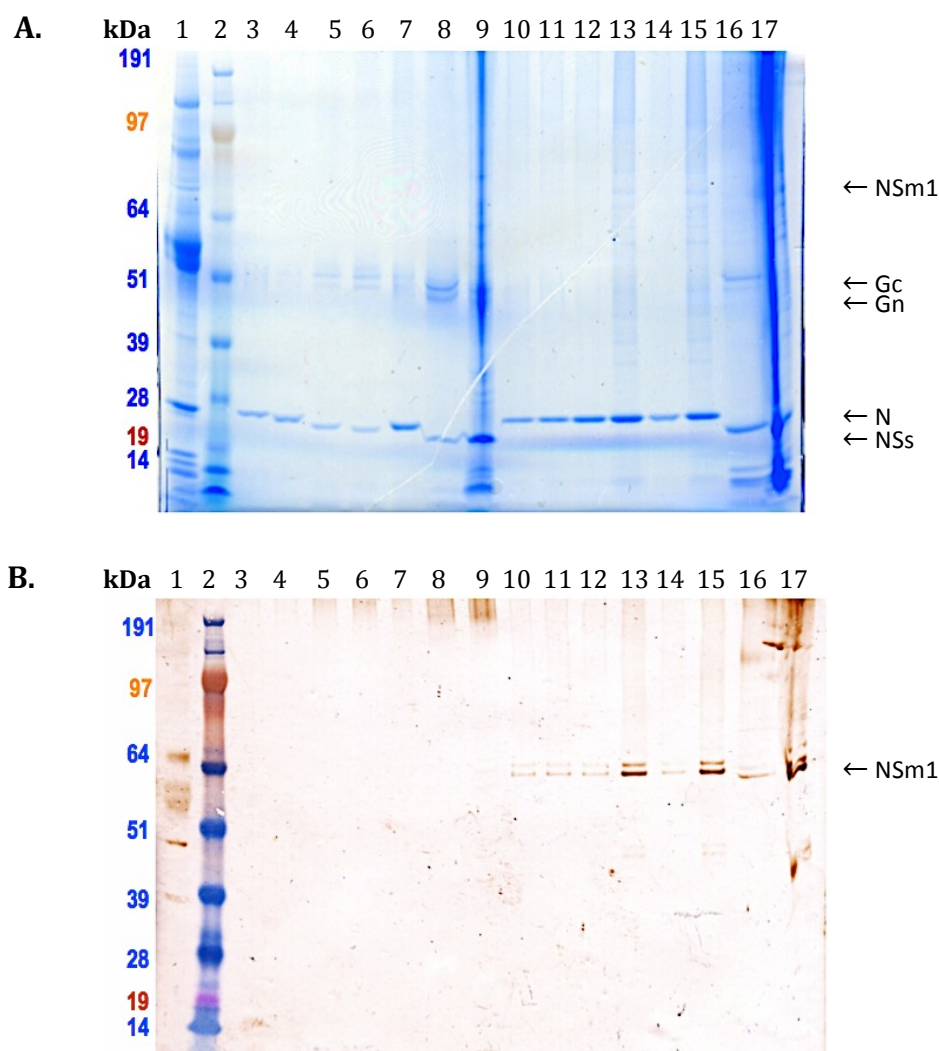


Figure 14. Immunoblot of Vero E6 RVFV and C6/36 RVFV following polyethylene glycol precipitation, resuspension and ultracentrifugation through a sucrose or iodixanol gradient. Lanes, left to right: 1. rNSm1 recombinant bacterial protein positive control. 2. SeeBlue Plus 2 pre-stained protein standard. 3-4. Replicates of Vero E6-derived RVFV collected from a sucrose gradient. 5-7. Replicates of Vero E6-derived RVFV collected from a iodixanol gradient. 8. Vero E6-derived RVFV resolubilized following polyethylene glycol (PEG) precipitation. 17. Vero E6-derived RVFV that remained insoluble following PEG precipitation. 10-12. Replicates of C6/36-derived RVFV collected from a sucrose gradient. 13-15. Replicates of C6/36-derived RVFV collected from an iodixanol gradient. 16. C6/36-derived RVFV resolubilized following PEG precipitation. 17. C6/36-derived RVFV that remained insoluble following PEG precipitation. **A.** SimplyBlue safestain Coomassie G-250 stained gel. **B.** PVDF membrane bound with rabbit R1108 polyclonal anti-NSm1 serum and goat anti-rabbit HRP conjugate. Figures 13 and 14 were prepared concurrently from the same samples.

3.8 To confirm purity of the virion preparations – NSs immunoblots

Immunoblots using rabbit anti-NSs detects significant levels of NSs in the insoluble fraction of polyethylene glycol-precipitated Vero E6-derived virus but not from the gradient ultracentrifuge-purified virus samples (Figure 13B). Both the PEG-soluble and PEG-insoluble fractions were collected prior to gradient ultracentrifugation. The PEG-insoluble fraction in particular appears to contain significant levels of non-virion proteins (Figure 14A lanes 9 and 17).

NSs is an intracellular non-structural protein, so the lack of detection of NSs in purified virion samples suggests that the samples are relatively pure. Cells were not lysed during the collection of supernatant (section 2.9) and NSs localizes to the nucleus of Vero E6 cells or the cytoplasm of C6/36 cells (Vaughn *et al.* 2010), which suggests that there has been a greater quantity of intracellular material released into the supernatant during the infection of Vero E6 cells than during the infection of C6/36 cells. A greater level of cellular debris following Vero E6 infection with RVFV is consistent with cell lysis being observed in Vero E6 but not C6/36 cells.

3.9 Detection of NSm1 in virions

Following PEG precipitation and gradient ultracentrifugation of RVFV-infectious supernatant collected from C6/36 cells, immunoblots probed with R1108 rabbit anti-NSm1 serum detected two protein bands at approximately 65 kDa (Figure 14). The two protein bands were visible in virus produced in C6/36 cells but not in virus produced in Vero E6 cells. Based on the positive immunoblot signal and apparent molecular weight, the bands are believed to both be NSm1, with the

difference in apparent molecular weight arising from the use of two N-linked glycosylation sites. From the size of prominent protein bands, there is an apparent molecular weight effect that varies between virion samples (Figure 14A). This variance is most likely an artefact from polyethylene glycol precipitation of the proteins, which can significantly affect the apparent molecular weight of proteins (Yan *et al.* 1984, Kurfürst 1992).

Based on the initial putative detection of NSm1 in only C6/36 cells, infection and purification of virions from both cell types was repeated. Supernatant from Vero E6 and C6/36 cells for this experiment were collected at 2 dpi and 6 dpi respectively, clarified at 3,000 *g* and passed through a 0.22 μ m filter prior to PEG precipitation. Precipitate was subsequently dissolved and layered over an iodixanol gradient for ultracentrifugation and bands were collected through bottom-puncture aspiration in 0.5 mL fractions. Protein samples were then run on denaturing PAGE and immunoblotted. R1109 rabbit anti-NSm1 serum detected a prominent protein band at approximately 70 kDa that appears in the C6/36 virion preparation but not the Vero E6 virion preparation (Figure 15). The apparent molecular weight of 70 kDa for NSm1, rather than the expected 78 kDa, is consistent with the continued use of PEG precipitation. In the low density bands collected from gradient ultracentrifugation (Figure 15B lanes 4 and 5), the proteins detected at approximately 55 kDa in VE6-RVFPV are present in fractions that do not appear to contain nucleocapsid N, as seen on the Coomassie stained gel, and are not unique to intact virions and may be a host protein or intracellular NSm1 that is not

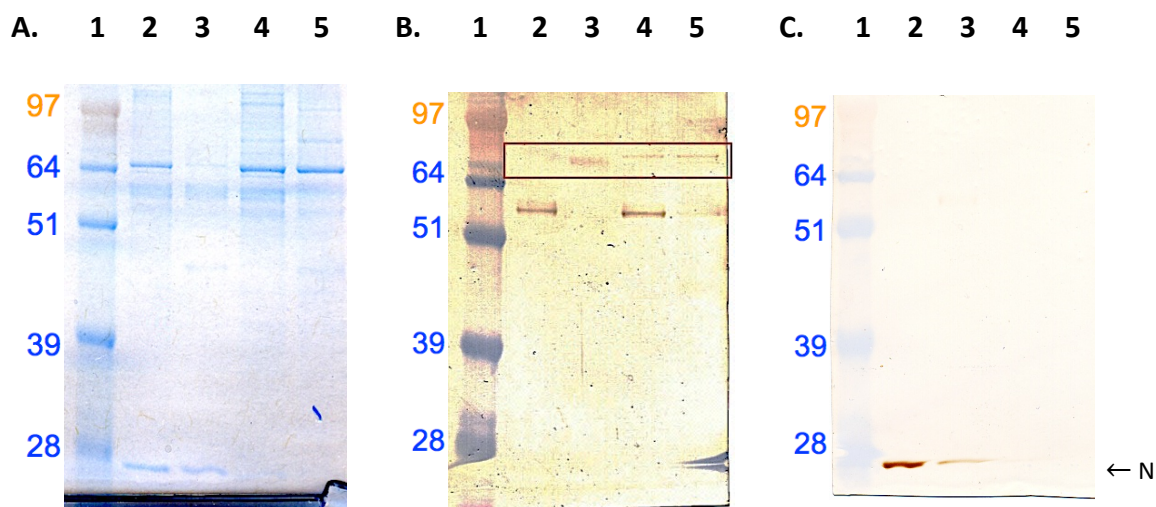


Figure 15. Immunoblot of Vero E6 RVFV and C6/36 RVFV following polyethylene glycol precipitation, resuspension and ultracentrifugation through an iodixanol gradient. Lanes, left to right: 1. SeeBlue Plus 2 prestained protein standard. 2. Vero E6-derived RVFV, dense band. 3. C6/36-derived RVFV, dense band. 4. Vero E6-derived RVFV, lighter band. 5. C6/36-derived RVFV, lighter band. **A.** Denaturing PAGE stained with SimplyBlue safestain G-250 coomassie protein stain. **B.** Immunoblot using rabbit R1109 anti-NSm1 serum (1:1000 dilution). In the red box, NSm1 is detected in the virion produced by C6/36 cells but not in those produced by Vero E6 cells. **C.** Immunoblot using sheep anti-RVFV serum. Based on size, the bound protein is most likely nucleocapsid N.

incorporated into the virion. The rabbit serum shows a lack of specificity, binding at least two proteins that are not believed to be NSm1 (Figure 15B lanes 2 and 4), and mass spectrometry of these fractions can provide greater confidence in these identifications. Immunoblots with anti-NSs serum did not bind proteins in any fractions following ultracentrifugation (not shown), which is consistent with the results seen previously (Figure 14B).

Subsequent immunoblots, using enhanced chemiluminescence (ECL) detection, showed the putative NSm1 band in the C6/36- but not the Vero E6-derived virus purification sample (Figure 16). Even when the ECL immunoblot is overexposed, showing a prominent signal from NSm1 in C6/36-derived RVFV, no comparable signal is detectable in Vero E6-derived RVFV (Figure 16C).

Separated immunoblots of the two densities of protein bands collected following gradient ultracentrifugation provide additional information as to their composition (Figure 15). In addition to evidence based on the density at which each sample was collected, the less dense bands of each virus preparation, approximately 15-20% iodixanol, do not contain any proteins that are detected by sheep anti-RVFV serum. The heavy band also contains a protein consistent in size with nucleocapsid protein that was not seen in the lighter band, suggesting that the heavy band contained intact RVFV virions.

3.10 Mass spectrometry detection of NSm1

Following PAGE separation of proteins, gel bands were excised (Figure 17) and gamma-irradiated for mass spectrometry analysis at biosafety level 2 (BSL-2).

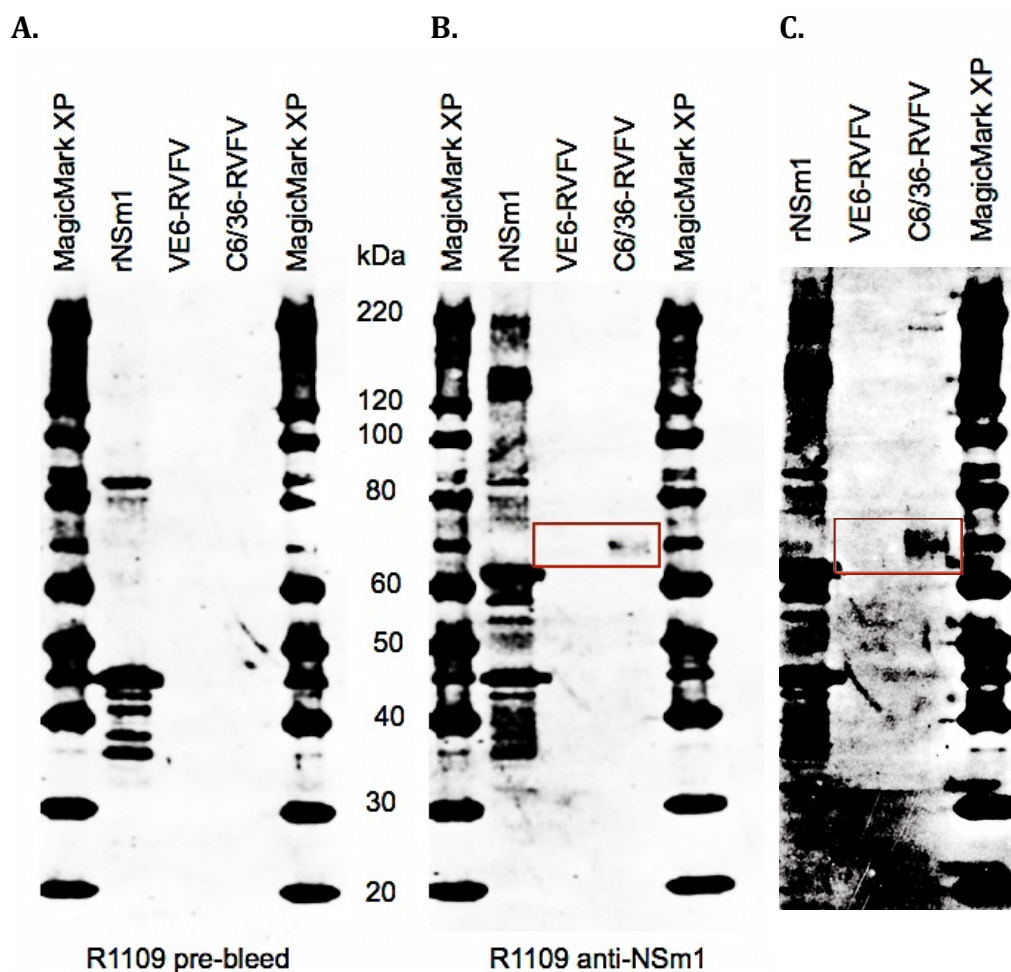


Figure 16. ECL western blots of purified RVFV virions from Vero E6 or C6/36 cells. Lanes, left to right: MagicMark XP protein standard, rNSm1 positive control, Vero E6 purified virions, C6/36 purified virions, MagicMark XP protein standard. **A.** R1109 rabbit pre-bleed serum was used as primary antibodies (1:100 dilution) with KPL goat anti-rabbit IgG conjugate HRP (1:500 dilution) secondary antibodies and imaged on a BioRad ChemiDoc. **B.** R1109 rabbit anti-NSm1 serum was used as primary antibodies (1:100 dilution) with KPL goat anti-rabbit IgG conjugate HRP (1:500 dilution) secondary antibodies and imaged on a BioRad ChemiDoc. **C.** An overexposed view of the R1109 anti-NSm1 immunoblot shown in panel A, showing that NSm1 is prominent in C6/36-derived RVFV and no comparable signal is detectable in Vero E6-derived RVFV. The red box highlights the NSm1 protein band that is visible in the C6/36-derived RVFV but not in the Vero E6-derived RVFV.

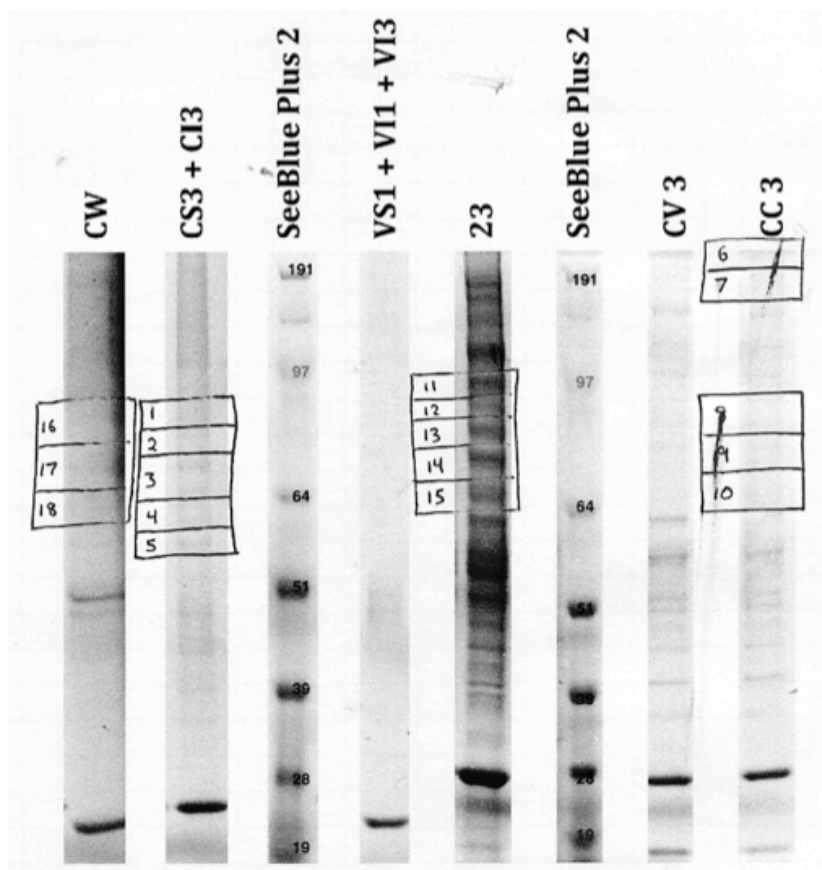


Figure 17. Denaturing PAGE of Vero E6 RVFV and C6/36 RVFV with numbered boxes indicating gel slices excised for mass spectrometry following PEG precipitation, resuspension and continuous gradient ultracentrifugation, stained using Coomassie G-250 SimplyBlue protein stain. Evidence of NSm1 was detected by mass spectrometry in samples 3, 4, 6, 7, 17 and 18. (CW) C6/36 RVFV polyethylene glycol precipitate. (CS3+CI3) contains a mixture of C6/36 RVFV sucrose and iodixanol gradient purified samples to increase total loading volume. (VS1+VI1+VI3) Vero E6 RVFV sucrose and iodixanol gradient purified samples to increase total loading volume. (23) Vero E6 RVFV iodixanol gradient purified sample. (CV3) C6/36 RVFV infected from Vero E6 RVFV, iodixanol purified sample. (CC3) C6/36 RVFV infected from C6/36 RVFV, iodixanol purified sample.

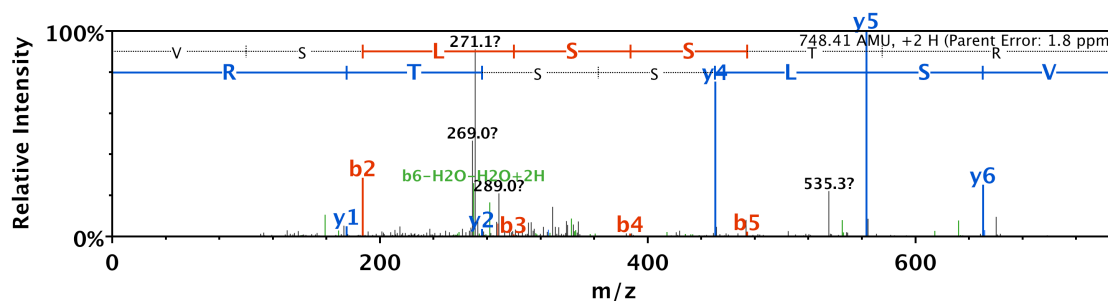
Protein samples were trypsin-digested and run on liquid chromatography electrospray ionization tandem mass spectrometry (LC-ESI-MS/MS), with samples of purified bovine serum albumin (BSA) run between each virus sample to reduce possible false-positive detection of residual viral proteins from previous samples. The peptide fragment VLSSTR was detected with 54% confidence in protein sample 03 that had also indicated a positive immunoblot for NSm1 (Figure 14B). The statistical confidence is lower for this fragment in part because it is short and therefore more likely to occur randomly than a longer fragment. The VLSSTR sequence is unique within RVFV (BLAST taxid:11588) proteome for NSm1 and not found within the proteomes of Vero E6 (BLAST taxid:9534) or C6/36 (BLAST taxid:7160). In total, 353 of 697 amino acids were detected, which is 51% coverage of NSm1 (Figure 18). The slightly larger fragment TSSQELYR, unique to NSm1 and NSm2, was also detected with 95% confidence in samples 04, 06, 07 and 18. VLSSTR or TSSQELYR were detected in samples 3, 4, 6, 7 and 18 from the C6/36 cells. Neither peptide was detected in samples 11, 12, 13, 14 or 15, all of which had been sampled from Vero E6-derived virus. Samples of the detected spectra are shown (Figure 19).

There is a gap of 135 amino acids between TSSQELYR and the next peptide fragment detected, which is the largest gap in the NSm1 sequence. Because of this, particularly due to the low confidence in VLSSTR, it is possible that the N-terminal fragments are cellular proteins or mismatches and that the majority of the positive signal comes from glycoprotein Gn. However, Gn would not contain the confidently identified TSSQELYR sequence and, while this scenario would explain the mass

1	MYVLLTILIS	VLVCEAVIRV	<u>SLSSTR</u> EETC	FGDSTNPEMI	EGAWDSLREE
51	EMPEELSCSI	SGIREVK <u>TSS</u>	<u>QELYR</u> ALKAI	IAADGLNNIT	CHGKDPEDKI
101	SLIKGPPHKK	RVGIVRCERR	RDAKQIGRET	MAGIAMTVLP	ALAVFALAPV
151	VFAEDPHLRN	RPGKGHNYID	GMTQEDATCK	PVTYAGACSS	FDVLLEKGKF
201	PLFQSYAHR	<u>TLLEAVHDTI</u>	<u>IAKADPPSCD</u>	<u>LQSAHGNPCM</u>	<u>KEKLVMTKTHC</u>
251	<u>PNDYQSAHYL</u>	NNDGKMASVK	CPPKYELTED	CNFCRQMTGA	<u>SLKKGSYPLQ</u>
301	<u>DLFCQSSDD</u>	GSKLKTKMKG	VCEVGVQALK	KCDGQLSTAH	EVVPFAVFKN
351	SKKVYLDKLD	LK <u>TEENLLPD</u>	SFVCFEHKGQ	YKGTMDSGQT	KRELK <u>SFDIS</u>
401	<u>QCPK</u> IGGHGS	KKCTGDAAFC	SAYECTAQYA	NAYCSHANGS	GIVQIQVSGV
451	WKKPLCVGYE	RVVVKRELSA	KPIQRVEPCT	TCITKCEPHG	<u>LVVRSTGFKI</u>
501	<u>SSAVACASGV</u>	<u>CVTGSQSPST</u>	<u>EITLKYPGIS</u>	<u>QSSGGDIGVH</u>	<u>MAHDDQSVSS</u>
551	<u>KIVAHCPPQD</u>	PCLVHGCIVC	AHGLINYQCH	TALSAFVVVF	VFSSIAIICL
601	AVLYRVLKCL	KIAPRKVLNP	LMWITAFIRW	IYKKMVARVA	<u>DNINQVNREI</u>
651	<u>GWMEGGQLVL</u>	<u>GNPAPIPRHA</u>	PIPRYSTYLM	LLLIVSYASA	CSELIQASSR
701	<u>ITTCSTEGVN</u>	<u>TKCRLSGTAL</u>	<u>IRAGSVGAEA</u>	<u>CLMLKGVKED</u>	<u>QTKFLKIKTV</u>
751	<u>SSELSCREGO</u>	<u>SYWTGSFSPK</u>	<u>CLSSRRCHLV</u>	<u>GECHVNRCLS</u>	WRDNETS

Figure 18. Mass spectrometry coverage of NSm1 following Mascot analysis of detected ions. The 353 of 697 amino acids detected (51% coverage) are highlighted in yellow. Analysis suggested 54% probability of the identity of VLSSTR (underlined), which is unique to NSm1, and greater than 95% probability of TSSQELYR (double-underlined), which is unique to NSm1 and NSm2. The relatively low confidence in VLSSTR is based in part on it being a short sequence, thus increasing the possibility of other sequences having similar mass spectrometry profiles. Based on approximate molecular weight, this band is more likely to be the 68 kDa NSm1 than the 14 kDa NSm2.

A.



B.

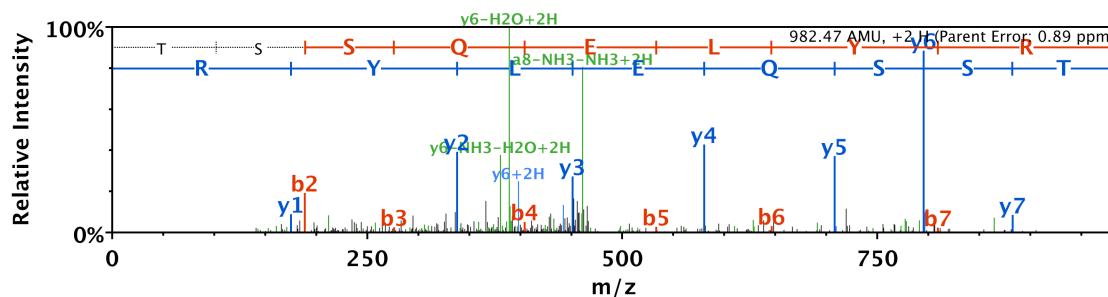


Figure 19. Liquid chromatography electrospray ionization tandem mass spectrometry. Mass spectrometry spectra of gel-excised protein bands from gradient ultracentrifuge-purified RVFV from C6/36 cells. **A.** Spectra for VLSSTR (amino acids 20-26 of NSm1) with 54% confidence on MASCOT analysis. **B.** Spectra for TSSQELYR (amino acids 68-75 of NSm1, 30-37 of NSm2) with 95% confidence on MASCOT analysis.

spectrometry data, it would not explain the immunoblots suggesting the same findings.

3.11 Virion glycoproteins Gn and Gc

A Coomassie blue stained denaturing PAGE gel showed comparable protein levels between virus collected from Vero E6 or C6/36 cell lines, based on the intensity of stained protein bands (Figure 14). Two bands of approximately equal intensity are visible in the PEG insoluble fraction of Vero E6-grown RVFV. However, the C6/36-grown RVFV upper band is significantly more intense. Based on size, these two bands are most likely to be glycoproteins Gn (54 kDa) and Gc (56 kDa). In a side-by-side comparison (Figure 20), the N-doublet detected through immunoblotting is larger than the two protein bands visible in the Coomassie stained gel. These bands suggest that Gn may be expressed at a lower level than Gc in C6/36 insect cells, in comparison to the equal ratio heterodimer used to assemble virions in Vero E6 cells.

3.12 Electron microscopy of virions

Electron microscopy was used to examine the structure of RVFV virions assembled in Vero E6 and C6/36 cells. Electron microscopy was originally performed on virus samples that were purified through gradient ultracentrifugation. The detection of virions in these samples was also used to confirm the presence of virions in ultracentrifuged fractions. However, with concentration there was too high a background. Based on the high titres of RVFV reached during *in vitro* infection of

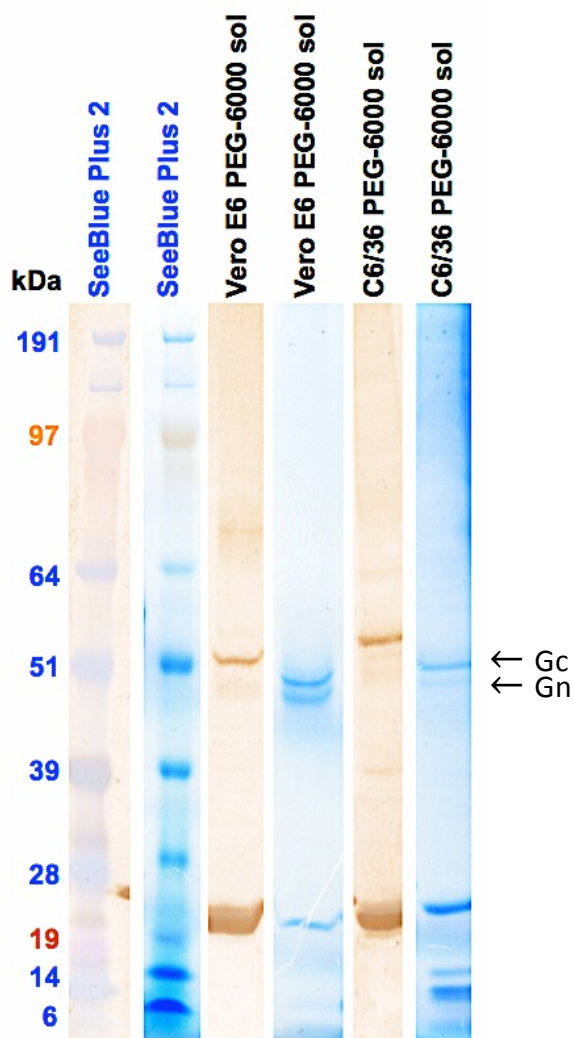


Figure 20. A composite of Figures 13A and 14A showing denaturing PAGE of Vero E6 RVFV and C6/36 RVFV following polyethylene glycol precipitation and resuspension. Blue lanes were stained using Coomassie G-250 SimplyBlue protein stain and tan lanes were immunoblotted using rabbit anti-nucleocapsid protein antibodies at 1:1000 dilution and secondary sheep anti-rabbit HRP at 1:1000 dilution. The two left-most lanes contain SeeBlue Plus2 pre-stained protein standard and were used for alignment of the gels. Arrows indicates glycoproteins Gc (56 kDa) and Gn (54 kDa), identified by size from purified virion preparations. The N-dimer is significantly larger than the protein bands believed to be glycoproteins Gn and Gc, showing that these bands are not the N-dimer.

Vero E6 and C6/36 cells, the attempts at electron microscopy were carried out without any steps being taken to concentrate the virus. Without concentration, there was a low virion particle yield, as seen in the results.

RVFV virions were PEG-precipitated and ultracentrifuged into a continuous iodixanol density gradient. Visible protein bands were collected through bottom-puncture aspiration, fixed in glutaraldehyde and removed from BSL-3E. The resulting images (not shown) contained virions in a background material, which is believed to have been a cross-reaction between the iodixanol and glutaraldehyde. Despite the lack of clear images of virions, these electron micrographs demonstrate the presence of RVFV virions in gradient ultracentrifuge fractions, supporting the results seen using immunoblots. Subsequent electron microscopy examinations were made using glutaraldehyde-fixed clarified infectious supernatant with no procedures employed to concentrate the virus; this resulted in a significantly lower number of virions per electron micrograph field than would be expected for concentrated virions but also low levels of background material.

Based on scale bars, virions amplified in Vero E6 cells appear to be approximately 90-100nm in diameter, while RVFV virions amplified in C6/36 cells appear significantly larger, approximately 105-115nm in diameter (Figure 21).

3.13 Comparative serum neutralization

Serum neutralization assays were performed to compare the ability of sheep serum raised against Vero E6-grown RVFV ZH501 to neutralize Vero E6-grown RVFV and C6/36-grown RVFV. If NSm1 is acting in place of Gc, it may affect the

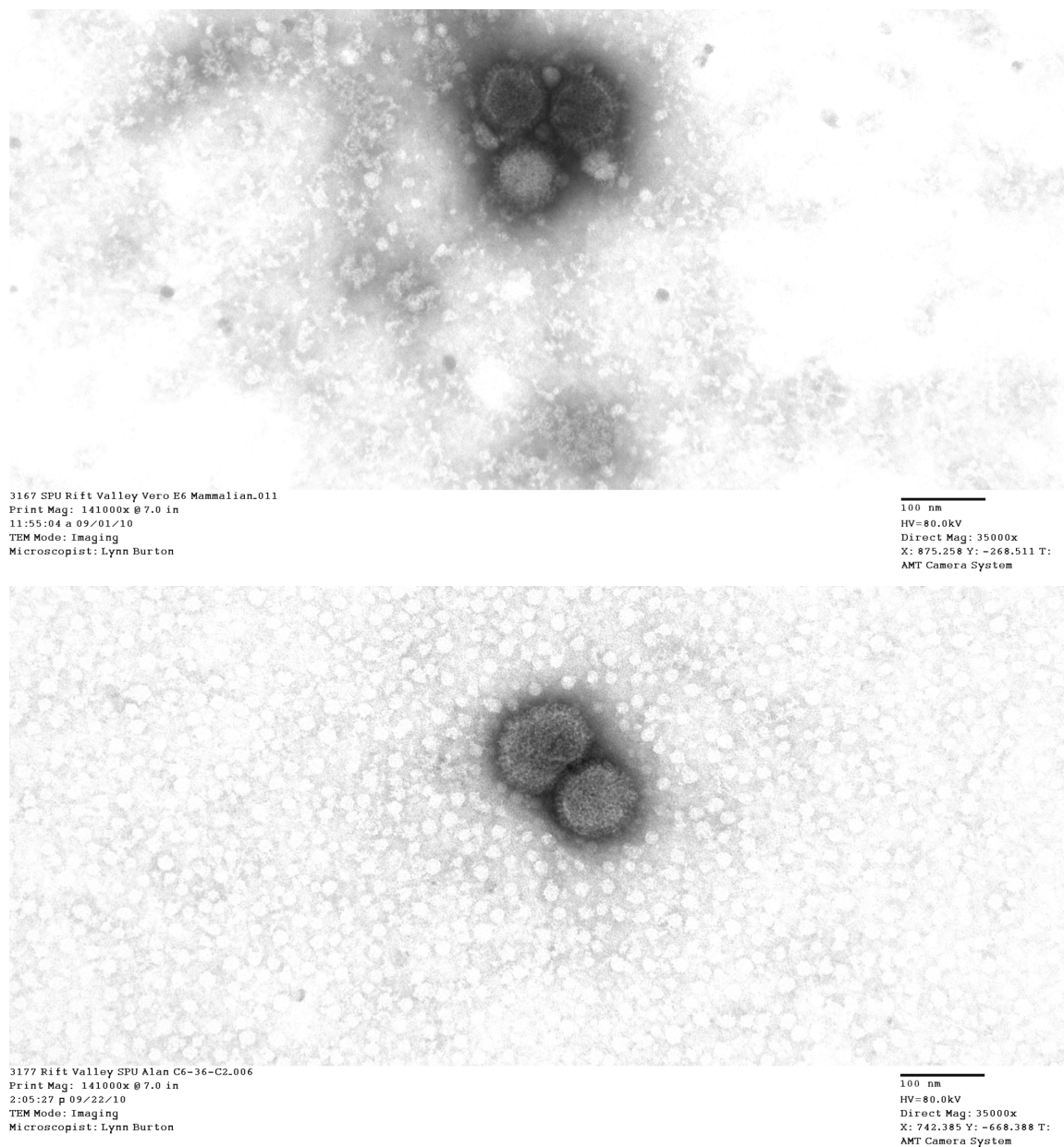


Figure 21. Electron micrographs of RVFV virions produced in Vero E6 (top) or C6/36 (bottom) cell cultures. Viruses were polyethylene glycol-precipitated and ultracentrifuged into an iodixanol gradient to produce purified samples. Based on scale bars, virions produced in Vero E6 appear to be approximately 90-100nm in diameter. Virions produced in C6/36 cells appear to be approximately 105-115nm in diameter.

surface antigens of the virion and thus change the way that antibodies bind the virion. Replacement of one surface glycoprotein with another could influence the outcome of serological assays such as virus neutralization or enzyme-linked immunosorbent assay (ELISA). Sheep sera were collected from two different experiments but, in both cases, were raised against RVFV grown in Vero E6 cells. Neutralizing titres varied between animals but were not significantly different for each individual animal between VE6-RVFV and C6/36-RVFV (Figure 22).

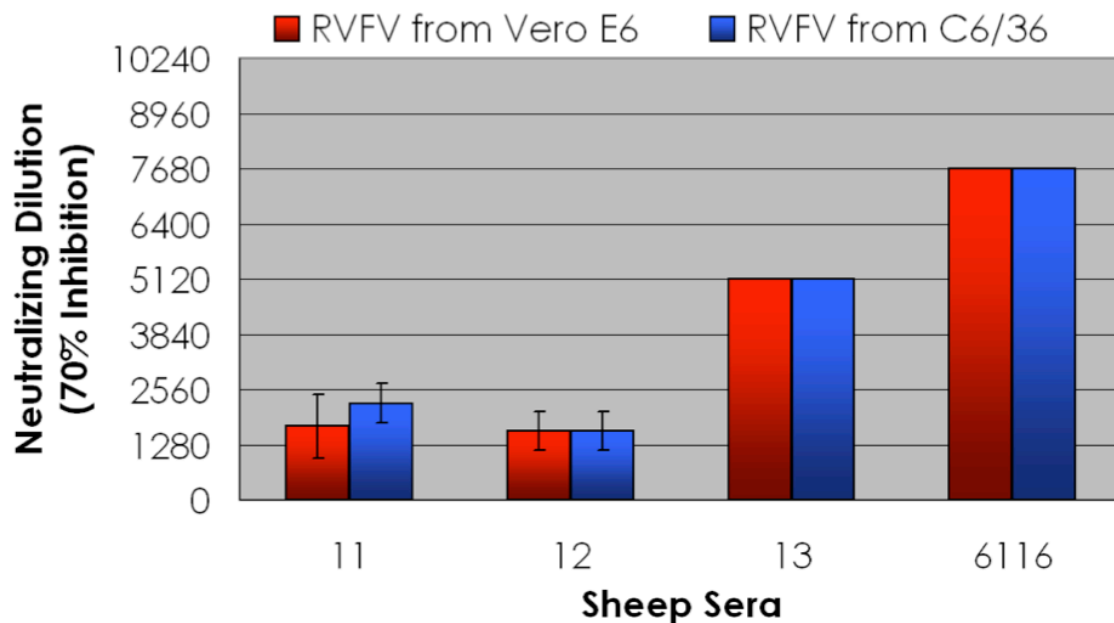


Figure 22. Serum neutralization assays of Vero E6 RVFV and C6/36 RVFV performed with final bleed polyclonal sheep sera raised against Vero E6 RVFV. Sera from sheep 11, 12 and 13 were collected at 29 dpi. Serum from sheep 6116 was collected at 38 dpi.

Chapter 4: Discussion

4.1 Summary of findings

NSm1 was not detected in Vero E6 or C6/36 cell lysate up to 21 hpi. Differences in the expression of virus nucleocapsid protein and NSs can be explained by the difference in incubation temperature between mammalian and insect cell lines. Immunoblots of ultracentrifuge-purified RVFV detected RVFV protein NSm1 in virions assembled in insect C6/36 cells but not in mammalian Vero E6 cells, which was confirmed through repeated full replicates. The detection of NSm1 using polyclonal anti-NSm1 sera was supported by mass spectrometry of samples excised from PAGE gels at the apparent molecular weight indicated on immunoblots. Serum neutralization of C6/36- and Vero E6-derived RVFV using polyclonal sheep sera showed no significant differences based on the cell line in which the virus had been grown. Based on a limited sample size, electron microscopy showed a size difference in virions, with C6/36-derived virions appearing slightly larger than Vero E6-derived virions. This size difference is consistent with other observations made of mammalian and insect RVFV virions purified using similar purification protocols (Burton, unpublished data).

4.2 RVFV production and titration

C6/36 production of RVFV appeared to plateau at approximately 5-6 dpi. In Vero E6 cells, viral titres appeared to plateau after 1-2d pi and remained constant through 8 dpi, despite complete cell lysis by 4 dpi. RVFV shows remarkable thermo-tolerance at 37°C (Turell, unpublished data), confirmed by the constant virus titre of

Vero E6 infectious supernatant through 8dpi. It is reasonable to assume that RVFV virions would have similar or greater longevity in C6/36 cultures, because the non-lytic infection would not promote the protease activity seen when a cell undergoes apoptosis or uncontrolled lysis and because the virus should be more stable at the lower incubation temperature of 28°C for C6/36 compared to 37°C for Vero E6. Despite RVFV infection in C6/36 being non-lytic, the lack of virus titre increase after 6dpi, with the long-term persistence of RVFV particles after Vero E6 cell death, suggests that C6/36 cells eventually become metabolically dead as a result of RVFV infection. The length of time to reach metabolic death following RVFV infection in C6/36 cells is not currently known.

Observations of RVFV replication in mammalian and insect cells were consistent with previously reported data (Vaughn *et al.* 2010). Reports that RVFV establishes a non-lytic infection in C6/36 cells (Vaughn *et al.* 2010) were consistent with micrograph images of C6/36 cells infected at MOI between 0.01 and 50 (Figure 9). For the purposes of maximizing virus production for virion purification and the analysis of protein composition, the virions were harvested at 2 dpi from Vero E6 cells and at 6 dpi from C6/36 cells. Virus cannot be titrated by plaque-forming assays on C6/36 cells, as C6/36 cells do not undergo lysis following RVFV infection. Because the focus of these experiments was the protein content of the virions, rather than the susceptibility of each cell line, all RVFV preparations were titrated on Vero E6 cells to provide a consistent procedure for titration.

4.3 RVFV replication in Vero E6 and C6/36 cells

Cell lysates were collected and analyzed using immunoblots to compare the protein profiles of RVFV during replication in Vero E6 and C6/36 cells during the first 21 hpi at three-hour intervals. This timeline was based on an established chronology of infection in Vero E6 cells that showed that one viral life cycle appears to take approximately 11 to 13 hpi (Ellis *et al.* 1988). To accommodate the potentially slower viral kinetics in mosquito cells grown at a lower temperature, this time window was almost doubled to 21 hpi. Shortly after this time point in Vero E6 cells, virus replication would be detectable in secondarily-infected cells. Because it is not possible to determine when secondary infection has taken place, but a second wave of infection could create detectable spikes in protein levels on immunoblots, the experiment was terminated before the majority of cells affected by secondary infection would finish virion assembly. A second wave of released virions was expected from Vero E6 cells at 25 hpi (Ellis *et al.* 1988).

Rabbit serum anti-N and anti-NSs immunoblots were able to detect RVFV proteins in Vero E6 and C6/36 cell lysates. In both cases, the proteins were detected one measurement interval (three hours) later in C6/36 than in Vero E6, which may be related to the slower virus replication observed in C6/36 cells (Figure 13). Because each cell line is adapted to a specific temperature within specific incubation conditions and media, it is not possible to control for all variables in virus replication. C6/36 cells are grown at 28°C, which is 9°C lower than the incubation temperature for Vero E6 cells; based on the Q10 rule of expected reaction kinetics in biological systems, an increase of 10°C should result in a doubling of the rate of

reaction. The results seen are consistent with the kinetics for a similar rate of reaction at the two given temperatures. Mammalian cells grown at the incubation temperature for insect cells continue to have higher expression of NSs than insect cells at the same temperature, suggesting that differences in protein expression level may be at least partially host-driven rather than being exclusively temperature-driven (Vaughn *et al.* 2010). Earlier research has demonstrated using non-structural protein NSs that a RVFV protein can have different expression levels (Billecocq *et al.* 2004), subcellular localization (Vaughn *et al.* 2010) and virulence *in vivo* when expressed in a mammalian or insect host (Billecocq *et al.* 2004, Crabtree *et al.* 2012). As there is a demonstrable mechanism for such modulation of NSs, it is possible that this has also occurred for other RVFV proteins.

A possible explanation for the differences in cell lysis observed between RVFV-infected Vero E6 and C6/36 cells may be the rate of virion release. As shown from viral growth curves, accumulation of VE6-RVFV virions in supernatant is quite rapid, with virus approaching peak concentrations at 1 dpi (Figure 13). In C6/36 cells, RVFV virion accumulation is significantly more gradual, reaching peak concentration at 6 dpi. Assuming that the accumulation of virions in supernatant is correlated with the release of virions from the host cells, this suggests a significant difference in the rate of virion release between the two cell lines. The rapid budding of enveloped virus through a host cell membrane release can destabilize the membrane and lead to cell lysis (Leonard *et al.* 1988), so differences in virus release could lead to differences in cytolysis between host species. RVFV's mechanism of

releasing virus-filled vesicles through fusion with the plasma membrane appears consistent for both Vero E6 and C6/36 cells, based on electron micrograph images.

4.4 RVFV virions produced in Vero E6 and C6/36 cells

Recombinant NSm1 was developed to act as a positive control for testing anti-NSm1 antibodies, and antibodies against NSm2 or Gn would also bind to it. Despite a frame shift mutation that resulted in a truncation at 80% of the recombinant protein's length, it remained functional as an immunoblot control because the N-terminal region targeted by rabbit anti-NSm1 antibodies was expressed correctly according to nucleotide sequencing. The rNSm1 expression was confirmed by detection with polyclonal sheep serum collected from RVFV-infected animals at 29 dpi. The 38 N-terminal amino acids are the only residues that are unique to NSm1 and thus, despite limited antigenicity, are the only candidates for a monospecific antibody that does not also bind NSm2 or Gn. Two rabbit anti-NSm1 antibodies developed against a synthetic polypeptide unique to this region showed high affinity for the truncated rNSm1. Because whole sera were used for immunoblotting, and not a monoclonal antibody, comments cannot be made on the specific avidity of the anti-NSm1 antibodies from rabbits R1108 and R1109. Generally, there was a higher background on immunoblots incubated with R1109 serum, but this is also seen in immunoblots performed using R1109 pre-bleed serum, suggesting that the animal had higher titres of antibodies that react non-specifically to proteins on the immunoblots prior to the animal's inoculation with

the synthesized peptide of the first 38 amino acids of NSm1. Both rabbit anti-NSm1 sera appeared to bind rNSm1 and purified virus C6-RVFV NSm1 in western blots.

As was observed with NSs, extensive cell lysis can allow non-structural proteins to reach detectable levels within the supernatant, particularly following protein concentration. By purifying the infectious supernatant using PEG precipitation and gradient ultracentrifugation, NSm1 was removed from Vero E6-derived samples but remained in C6/36 samples. The ultracentrifugation resulted in two distinct protein bands in both C6/36 and Vero E6 samples; the more dense bands were collected at the approximate iodixanol density expected for the purification of *Bunyaviridae* (AXIS-SHIELD 2011) and contained a strong nucleocapsid signal that was not seen in the upper band. NSm1 was detected using both R1108 and R1109 sera, with R1108 having a lower background but a higher detection threshold.

To further support the repeated detection of NSm1 in C6/36-derived virus but not in Vero E6-derived virus, mass spectrometric analysis of denatured PAGE-separated virion proteins was used to positively identify peptides unique to the NSm1/NSm2 region of the nested M segment polyprotein. Because of the relatively short fragment detected that was unique to NSm1, there is less statistical certainty in this identification. There is much greater confidence in the second fragment detected, which is found in both NSm1 and NSm2. The apparent molecular weight of the fragment excised, however, is more than double the molecular weight of NSm2. Therefore, using mono-specific immunoblots and mass spectrometry, NSm1

has been repeatedly detected in RVFV replicated in C6/36 cells but not in RVFV replicated in Vero E6 cells.

Earlier works on RVFV identified NSm1 as a virion-associated protein (Struthers *et al.* 1984), although other work with virus purification failed to detect it in virions produced in mammalian cells (Peters & Anderson 1982, Kakach *et al.* 1989). While it is possible that NSm1 is present in Vero E6-derived virions but that those levels are below the detection threshold for these immunoblots, Coomassie protein staining and anti-nucleocapsid protein immunoblots were performed and demonstrated comparable levels of protein between the two samples. If NSm1 is incorporated into virions following virus replication in both Vero E6 and C6/36 cell lines, it is present in virions at substantially higher levels in insect-derived virions.

Denaturing PAGE of virion preparations showed prominent protein bands that appear to be glycoproteins Gn and Gc, based on apparent molecular weight (Figure 22). In RVFV amplified in Vero E6 cells, these two bands were of approximately equal intensity. In C6/36-derived virus, however, the putative glycoprotein Gc was qualitatively more intense than Gn, suggesting that Gc is incorporated into the virion at higher levels than Gn and not the equal heterodimer seen in mammalian-derived virions (Huiskonen *et al.* 2009). Because the proteins of the M-segment arise from a single transcribed ORF, translation of the M-segment polyprotein from the first methionine codon, which results in the production of NSm1, would produce Gc but not Gn. If mosquito cells are more likely to begin translation from the first methionine in the RVFV M-segment, more M-segment transcriptions would be used to express NSm1 and fewer would be used to express

Gn but there would be no change in Gc expression. Other research has shown that Gn is expressed at lower levels in C6/36 cells than in mammalian and non-mosquito insect cell lines up to 48 hpi, but this work did not compare Gn expression to Gc expression (Vaughn *et al.* 2010).

From the size of prominent protein bands, there is an apparent molecular weight effect that varies between virion samples of the same type. The most obvious explanation is an artefact from polyethylene glycol precipitation of the proteins, which has been demonstrated to significantly affect the apparent molecular weight of proteins (Yan *et al.* 1984, Kurfürst 1992).

The detection of NSm1 in RVFV virions amplified in C6/36 cells but not Vero E6 cells would be consistent with the primary hypotheses of this thesis. Following further confirmation, this research could provide evidence of the presence of NSm1 in the virions as a functional protein during replication in insect, but not mammalian, cells.

4.5 Possible effects of incorporating NSm1 into C6/36-amplified virions

Based on the initial evidence that NSm1 is incorporated into RVFV virions assembled in C6/36 cells, experiments were performed to determine if these virions were significantly different from Vero E6-derived virions. Because glycoproteins Gn and Gc are essential to virus assembly and maturation, infected C6/36 cells were visualized using electron microscopy to attempt to detect virus maturation involving NSm1 occurring in sites other than the Golgi apparatus. Based on electron micrographs of virus maturation in Vero E6 and C6/36, which was consistent with

published literature, the virion release process does not appear to be significantly different between mammalian (Ellis *et al.* 1988) and insect cells (Rosomer *et al.* 2005). Maturation of RVFV in Vero E6 cells has been observed to be consistent with other *Bunyaviridae* (Ellis *et al.* 1988, Flick & Bouloy 2005). Virus budding in insect cells has not been researched as thoroughly, but recombinant glycoproteins Gn and Gc localize to the Golgi prior to budding in *Spodoptera frugiperda* Sf9 and Sf21 cells (Liu *et al.* 2008) and virus maturation in *Culex pipiens* mosquitoes *in vivo* was described as similar to what has been observed in rat hepatocytes (Lerdthusnee *et al.* 1995). The presence of NSm1 in C6/36-derived virions does not appear to be a product of a different site of virus assembly.

The current molecular model of the structure of RVFV amplified in mammalian cells is based on the surface glycoproteins forming equal heterodimers of Gn and Gc (Huiskonen *et al.* 2009). Gc and N are capable of forming VLPs without Gn, although the particles are more pleomorphic than when assembled in the presence of Gn (Liu *et al.* 2008). It is possible that the NSm1, which contains the entire amino acid sequence of Gn, may be incorporated into RVFV virions as a partial replacement of Gn during replication in mosquito cells. NSm1 is approximately 160 amino acids larger than Gn; depending on how these amino acids are incorporated into a glycoprotein polymer with Gc (and possibly also Gn), this could increase the size of the surface subunits on the icosahedral RVFV virion. This incorporation, in turn, could increase the overall size of the virion to the approximately 110 nm diameter particles seen under electron microscopy (Figure

21) compared to the 100 nm diameter that has been established for RVFV grown in Vero E6 cells (Ellis *et al.* 1988, Freiberg *et al.* 2008, Huiskonen *et al.* 2009).

The presence of NSm1 does not appear to affect neutralizing antibodies raised against RVFV. Serum neutralization assays showed no difference between virus derived from Vero E6 or C6/36 cells when incubated with sheep serum raised against Vero E6-derived RVFV. The differences between animals can be attributed to varied immune responses and no significant differences were observed for a single animal's serum neutralizing RVFV from Vero E6 or C6/36.

4.6 Significance of findings

All *Phlebovirus* species carry a non-structural protein at the N-terminus of the M-segment, generally referred to as NSm, which is produced through proteolytic cleavage from surface glycoproteins (Gerrard *et al.* 2007). However, not all of these proteins are homologues and generalizations cannot be made about the function of NSm1 and NSm2 (Bird *et al.* 2007a).

Recombinant RVFV lacking NSm1 and NSm2 has been used to examine systemic infection of *Aedes aegypti* and *Culex quinquefasciatus* mosquitoes (Crabtree *et al.* 2012) using an RVFV Δ NSm recombinant virus (Gerrard & Nichol 2007). No mechanism was proposed for the decreased infection rate in both types of mosquitoes using the Δ NSm RVFV, but it was assumed that the effect was due to the deletion of NSm2 and no mention was made of NSm1 (Crabtree *et al.* 2012). Research has shown that insect-amplified RVFV can induce increased host cell surface expression of NSm1 and a significantly different response in the innate

immune system (Nfon *et al.* 2012); thus, the assumption that all changes arising from a Δ NSm RVFV recombinant are due to the lack of NSm2 may be presumptuous.

Recent research has shown significant differences in the innate immune response in goats following infection with C6-RVFV or VE6-RVFV (Nfon *et al.* 2012). Insect-derived RVFV reached peak viremia faster and stimulated higher levels of cytokine release in goats than mammalian-derived RVFV (Nfon *et al.* 2012). Insect-derived RVFV was also associated with lower levels of neutralizing antibodies at the onset of seroconversion in goats than mammalian-derived RVFV, although the differences were no longer significant by 30 dpi (Nfon *et al.* 2012). These observations suggest that the differences between C6-RVFV and VE6-RVFV are more than cosmetic and may play a functional role in the life cycle of the virus.

4.7 Potential Future Directions

These experiments demonstrate the beginnings of a very promising line of research into the role of NSm1 and virion assembly in arboviruses. However, these data are not conclusive and additional research would be necessary before any firm conclusions can be drawn.

Because many of these experiments rely on the sensitivity and specificity of antibodies, monoclonal anti-NSm1 antibodies should be developed. To investigate the conditions leading to the incorporation of NSm1 into RVFV virions, it would be necessary to quantify intracellular NSm1 levels during virus replication in Vero E6 and C6/36 cells.

In order to draw conclusions on the RVFV virions derived from Vero E6 or C6/36 cells, the purity of the samples must be increased. Further purification can be accomplished by collecting particle bands from multiple rounds of gradient ultracentrifugation, combining them into a single run through a higher resolution gradient. This doubly-purified sample could then be dialyzed to remove iodixanol to calibrate immunoblots exactly based on total protein concentration, with a conserved host protein, such as β -actin, used as a control for protein degradation and immunoblotting. Successful dialysis should also remove the reduction and inconsistency in apparent molecular weight caused by PEG precipitation.

The purified and dialyzed virion preparations could also be used for electron microscopy. Immune-gold electron microscopy using anti-NSm1 monoclonal antibodies can provide evidence of the incorporation of NSm1 into the C6/36-derived virion. Cryo-electron microscopy can provide more accurate mapping of the surface glycoproteins of the virion to further explore the impact of the N-terminal tail of NSm1.

Using purified, dialyzed virions should also provide a sufficient concentration for electron micrographs to contain a large number of particles. One of the limitations of the electron micrographs presented here is the small sample size of virions observed. Additional replicates with larger sample sizes would be necessary to draw conclusions from these observations.

These robust experiments would serve to significantly increase confidence in the findings that NSm1 is incorporated into RVFV grown in C6/36 cells but not Vero E6 cells. In their absence, the presence of NSm1 has been detected, although

relatively weakly, in multiple full replicates of RVFV replication and ultracentrifuge purification from C6/36 cells and not from Vero E6 cells. The identity of the NSm1 protein has been supported by mass spectrometry. Finally, these findings are consistent with subsequent work showing quantifiable difference between insect- and mammalian-derived RVFV virions that has been carried out by other researchers concurrently to this (Nfon *et al.* 2012).

4.8 Conclusions

To our knowledge, this appears to be the first evidence of a virus that produces a demonstrably different protein composition of virions based on the host cell line. The evidence that NSm1 is specifically associated with mature virions when RVFV replicates in C6/36 insect cells but not when grown in Vero E6 cells suggests several experiments that can examine this feature. The function of NSm1 in insect cell infection, replication and release can be examined using NSm1-deletion mutants, as was done to investigate the function of NSm2 (Won *et al.* 2008).

The differences in RVFV virions between those produced in Vero E6 cells and C6/36 cells have not been demonstrated in any other cell lines. Both Vero E6 and C6/36 were selected for their permissiveness to virus infection and replication. Different insect cell lines have been shown to have different viral protein kinetics *in vitro* (Vaughn *et al.* 2010), so it is not fair to generalize that these results are representative of the behaviour of RVFV in all mammalian or all insect hosts.

West Nile virus, like RVFV, is a mosquito-borne single-stranded RNA arbovirus. In contrast to RVFV, it is a positive-stranded virus of the genus

Flaviviridae and it does not produce significantly different viral structural proteins or elicit different immune responses in mice when amplified in mammalian or insect hosts (Lim *et al.* 2010). Further research may elucidate whether the observed differences between mammalian and insect cell-line derived RVFV virions are common among arboviruses and under what conditions this may develop.

Rift Valley fever virus NSm1 protein has been detected in purified virions amplified in C6/36 mosquito cells but not in Vero E6 monkey cells. NSm1 has been identified through repeated immunoblots and confirmed with mass spectrometry. The identification of the differentiated virion production in RVFV illuminates not only structural distinctions in the virus, but also potential factors in virulence and the process of infection between hosts. These findings are supported by recent publications on RVFV infection in mosquito cells and suggest a possible role for the NSm1 protein.

References

- Altmann F, Staudacher E, Wilson IB, Marz L. Insect cells as hosts for the expression of recombinant glycoproteins. *Glycoconj J* 1999; 16, 109–123.
- Anderson GW Jr, Peters CJ. Viral determinants of virulence for Rift Valley fever (RVF) in rats. *Microb Pathog.* 1988 Oct;5(4):241-250.
- Anderson GW Jr, Rosebrock JA, Johnson AJ, Jennings GB, Peters CJ. Infection of inbred rat strains with Rift Valley fever virus: development of a congenic resistant strain and observations on age-dependence of resistance. *Am J Trop Med Hyg.* 1991 May;44(5):475-80.
- Anderson GW Jr, Slone TW Jr, Peters CJ. Pathogenesis of Rift Valley fever virus (RVFV) in inbred rats. *Microb Pathog.* 1987 Apr;2(4):283-193.
- Anderson GW Jr, Smith JF. Immunoelectron microscopy of Rift Valley fever viral morphogenesis in primary rat hepatocytes. *Virology.* 1987 Nov;161(1):91-100.
- AXIS SHIELD. Application Sheet V22: Purification and analysis of Group IV -ve sense RNA viruses: Bunyaviridae, 4th Edition [Internet]. 2011 July; cited 2012 Oct 15. available from: <http://www.axis-shield-density-gradient-media.com/V22.pdf>
- Billecocq A, Spiegel M, Vialat P, Kohl A, Weber F, Bouloy M, Haller O. NSs protein of Rift Valley fever virus blocks interferon production by inhibiting host gene transcription. *J Virol.* 2004 Sep;78(18):9798-806.
- Bird BH, Khristova ML, Rollin PE, Ksiazek TG, Nichol ST. Complete genome analysis of 33 ecologically and biologically diverse Rift Valley fever virus strains reveals widespread virus movement and low genetic diversity due to recent common ancestry. *J Virol.* 2007a Mar;81(6):2805-16.
- Bird BH, Albariño CG, Nichol ST. Rift Valley fever virus lacking NSm proteins retains high virulence in vivo and may provide a model of human delayed onset neurologic disease. *Virology.* 2007b May 25;362(1):10-5.
- Bird BH, Githinji JW, Macharia JM, Kasiiti JL, Muriithi RM, Gacheru SG, Musaa JO, Towner JS, Reeder SA, Oliver JB, Stevens TL, Erickson BR, Morgan LT, Khristova ML, Hartman AL, Comer JA, Rollin PE, Ksiazek TG, Nichol ST. Multiple virus lineages sharing recent common ancestry were associated with a Large Rift Valley fever outbreak among livestock in Kenya during 2006-2007. *J Virol.* 2008 Nov;82(22):11152-66.
- Bird BH, Ksiazek TG, Nichol ST, MacLachlan NJ. Rift Valley fever virus. *J Am Vet Med Assoc.* 2009 Apr 1;234(7):883-93.

- Bouloy M, Janzen C, Vialat P, Khun H, Pavlovic J, Huerre M, Haller O. Genetic evidence for an interferon-antagonistic function of rift valley fever virus nonstructural protein NSs. *J Virol*. 2001 Feb;75(3):1371-7.
- Brubaker JF, Turell MJ. Effect of environmental temperature on the susceptibility of *Culex pipiens* (Diptera: Culicidae) to Rift Valley fever virus. *J Med Entomol*. 1998 Nov;35(6):918-21.
- CDC. Outbreak of Rift Valley Fever – Yemen, August – October 2000. *MMWR* December 01, 2000/49(47);1065-6
- Chappell WA, Calisher CH, Toole RF, Maness KC, Sasso DR, Henderson BE. Comparison of three methods used to isolate dengue virus type 2. *Appl Microbiol*. 1971 Dec;22(6):1100-3.
- Collett MS, Purchio AF, Keegan K, Frazier S, Hays W, Anderson DK, Parker MD, Schmaljohn C, Schmidt J, Dalrymple JM. Complete nucleotide sequence of the M RNA segment of Rift Valley fever virus. *Virology*. 1985 Jul 15;144(1):228-45.
- Crabtree MB, Kent Crockett RJ, Bird BH, Nichol ST, Erickson BR, Biggerstaff BJ, Horiuchi K, Miller BR. Infection and transmission of Rift Valley fever viruses lacking the NSs and/or NSm genes in mosquitoes: potential role for NSm in mosquito infection. *PLoS Negl Trop Dis*. 2012;6(5):e1639.
- Daubney R, Hudson JR, Garnham PC. Enzootic hepatitis or Rift Valley fever: An undescribed virus disease of sheep, cattle and man from East Africa. *J Pathol Bacteriol*. 1931;34:545-579.
- Daubney R, Hudson JR, RIFT VALLEY FEVER. *Lancet*. 1932 Mar; 219(5664), 611-612.
- Davis CW, Nguyen HY, Hanna SL, Sanchez MD, Doms RW, Pierson TC. West Nile virus discriminates between DC-SIGN and DC-SIGNR for cellular attachment and infection. *J Virol* 2006; 80, 1290–1301.
- Desmyter J, Melnick JL, Rawls WE. Defectiveness of Interferon Production and of Rubella Virus Interference in a Line of African Green Monkey Kidney Cells (Vero). *J. Virol*. 1968 Oct;2(10):955–61.
- Drake JW, Holland JJ. Mutation rates among RNA viruses. *Proc Natl Acad Sci U S A*. 1999 Nov 3;96(24):13910-3.
- Ellis DS, Shirodaria PV, Fleming E, Simpson DI. Morphology and development of Rift Valley fever virus in Vero cell cultures. *J Med Virol*. 1988 Feb;24(2):161-74.

- Erasmus BJ, Coetzer JAW. The symptomatology and pathology of Rift Valley fever in domestic animals. *Contrib Epidemiol Biostat* 1981;3:77-82.
- Fagbo SF. The Evolving Transmission Pattern of Rift Valley Fever in the Arabic Peninsula. *Ann. N.Y. Acad. Sci.* 2002;961:201-204.
- Ferron F, Li Z, Danek EI, Luo D, Wong Y, Coutard B, Lantez V, Charrel R, Canard B, Walz T, Lescar J. The hexamer structure of Rift Valley fever virus nucleoprotein suggests a mechanism for its assembly into ribonucleoprotein complexes. *PLoS Pathog.* 2011 May;7(5):e1002030.
- Filone CM, Heise M, Doms RW, Bertolotti-Ciarlet A. Development and characterization of a Rift Valley fever virus cell-cell fusion assay using alphavirus replicon vectors. *Virology.* 2006 Dec 5-20;356(1-2):155-64. Epub 2006 Aug 30.
- Findlay G.M., Daubney R. The virus of Rift Valley Fever or Enzootic Hepatitis. *Lancet* 1931; ii: 1350.
- Flick R, Bouloy M. Rift Valley fever virus. *Curr Mol Med.* 2005 Dec;5(8):827-34.
- Freiberg AN, Sherman MB, Morais MC, Holbrook MR, Watowich SJ. Three-dimensional organization of Rift Valley fever virus revealed by cryoelectron tomography. *J Virol.* 2008 Nov;82(21):10341-8.
- Frese M, Kochs G, Feldmann H, Hertkorn C, Haller O. Inhibition of bunyaviruses, phleboviruses, and hantaviruses by human MxA protein. *J Virol.* 1996 Feb;70(2):915-23.
- Gargan TP 2nd, Bailey CL, Higbee GA, Gad A, El Said S. The effect of laboratory colonization on the vector-pathogen interactions of Egyptian *Culex pipiens* and Rift Valley fever virus. *Am J Trop Med Hyg.* 1983 Sep;32(5):1154-63.
- Garry CE, Garry RF. Proteomics computational analyses suggest that the carboxyl terminal glycoproteins of Bunyaviruses are class II viral fusion protein (beta-penetrenes). *Theor Biol Med Model.* 2004 Nov 15;1:10.
- Geisbert TW, Jahrling PB. Exotic emerging viral diseases: progress and challenges. *Nat Med.* 2004 Dec;10(12 Suppl):S110-21.
- Georges AJ, Wahid SA, Meunier DY, Georges MC, Saluzzo JF, Peters CJ, McCormick JB, Gonzalez JP. Serological evidence of endemic Zinga virus and Rift Valley Fever virus in Central African Republic. *Lancet.* 1983 Jun 11;1(8337):1338.
- Gerdes GH. Rift Valley fever. *Rev Sci Tech.* 2004 Aug;23(2):613-23.

- Gerrard SR, Bird BH, Albariño CG, Nichol ST. The NSm proteins of Rift Valley fever virus are dispensable for maturation, replication and infection. *Virology*. 2007 Mar 15;359(2):459-65.
- Gerrard SR, Nichol ST. Synthesis, proteolytic processing and complex formation of N-terminally nested precursor proteins of the Rift Valley fever virus glycoproteins. *Virology*. 2007 Jan 20;357(2):124-33.
- Habjan M, Penski N, Wagner V, Spiegel M, Overby AK, Kochs G, Huiskonen JT, Weber F. Efficient production of Rift Valley fever virus-like particles: The antiviral protein MxA can inhibit primary transcription of bunyaviruses. *Virology*. 2009 Mar 15;385(2):400-8.
- Habjan M, Pichlmair A, Elliott RM, Overby AK, Glatter T, Gstaiger M, Superti-Furga G, Unger H, Weber F. NSs protein of rift valley fever virus induces the specific degradation of the double-stranded RNA-dependent protein kinase. *J Virol*. 2009 May;83(9):4365-75.
- Huiskonen JT, Overby AK, Weber F, Grünewald K. Electron cryo-microscopy and single-particle averaging of Rift Valley fever virus: evidence for GN-GC glycoprotein heterodimers. *J Virol*. 2009 Apr;83(8):3762-9.
- Igarashi A. Isolation of a Singh's *Aedes albopictus* cell clone sensitive to Dengue and Chikungunya viruses. *J Gen Virol*. 1978 Sep;40(3):531-44.
- Ihara T, Akashi H, Bishop DHL. Novel coding strategy (ambisense genomic RNA) revealed by sequence analyses of Punta Toro phlebovirus SRNA. *Virology*. 1984;136:293-306.
- Ikegami T, Won S, Peters CJ, Makino S. Rift Valley fever virus NSs mRNA is transcribed from an incoming anti-viral-sense S RNA segment. *J Virol*. 2005 Sep;79(18):12106-11.
- Ikegami T, Won S, Peters CJ, Makino S. Rescue of infectious rift valley fever virus entirely from cDNA, analysis of virus lacking the NSs gene, and expression of a foreign gene. *J Virol*. 2006 Mar;80(6):2933-40.
- Jahriling PB, Marty AM, Geisbert TW. Viral Hemorrhagic Fevers. In: Dembek ZF, editor. *Medical Aspects of Biological Warfare*. Falls Church: Office of The Surgeon General; 2007. p. 271-310.
- Jenkins GM, Rambaut A, Pybus OG, Holmes EC. Rates of molecular evolution in RNA viruses: a quantitative phylogenetic analysis. *J Mol Evol*. 2002 Feb;54(2):156-65.

- Jupp PG, Kemp A, Grobbelaar A, Lema P, Burt FJ, Alahmed AM, Al Mujalli D, Al Khamees M, Swanepoel R. The 2000 epidemic of Rift Valley fever in Saudi Arabia: mosquito vector studies. *Med Vet Entomol*. 2002 Sep;16(3):245-52.
- Jupp PG, Cornel AJ. Vector competence tests with Rift Valley fever virus and five South African species of mosquito. *J Am Mosq Control Assoc*. 1988 Mar;4(1):4-8.
- Kakach LT, Suzich JA, Collett MS. Rift Valley fever virus M segment: phlebovirus expression strategy and protein glycosylation. *Virology*. 1989 Jun;170(2):505-10.
- Kakach LT, Wasmoen TL, Collett MS. Rift Valley fever virus M segment: use of recombinant vaccinia viruses to study Phlebovirus gene expression. *J Virol*. 1988 Mar;62(3):826-33.
- Kramer LD, Hardy JL, Presser SB, Houk EJ. Dissemination barriers for western equine encephalomyelitis virus in *Culex tarsalis* infected after ingestion of low viral doses. *Am J Trop Med Hyg*. 1981 Jan;30(1):190-7.
- Kurfürst MM. Detection and molecular weight determination of polyethylene glycol-modified hirudin by staining after sodium dodecyl sulfate-polyacrylamide gel electrophoresis. *Anal Biochem*. 1992 Feb 1;200(2):244-8.
- LaBeaud AD, Muchiri EM, Ndzovu M, Mwanje MT, Muiruri S, Peters CJ, King CH. Interepidemic Rift Valley fever virus seropositivity, northeastern Kenya. *Emerg Infect Dis*. 2008 Aug;14(8):1240-6.
- Le May N, Mansuroglu Z, Léger P, Josse T, Blot G, Billecocq A, Flick R, Jacob Y, Bonnefoy E, Bouloy M. A SAP30 complex inhibits IFN-beta expression in Rift Valley fever virus infected cells. *PLoS Pathog*. 2008 Jan;4(1):e13.
- Lerdthusnee K, Romoser WS, Faran ME, Dohm DJ. Rift Valley fever virus in the cardia of *Culex pipiens*: an immunocytochemical and ultrastructural study. *Am J Trop Med Hyg*. 1995 Oct;53(4):331-7.
- Leonard R, Zagury D, Desportes I, Bernard J, Zagury JF, Gallo RC. Cytopathic effect of human immunodeficiency virus in T4 cells is linked to the last stage of virus infection. *Proc Natl Acad Sci U S A*. 1988 May;85(10):3570-4.
- Levi M, ten Cate H. Disseminated intravascular coagulation. *N Engl J Med*. 1999 Aug 19;341(8):586-92.
- Lim PY, Louie KL, Styer LM, Shi PY, Bernard KA. Viral pathogenesis in mice is similar for West Nile virus derived from mosquito and mammalian cells. *Virology* 2010; 400 (1): 93-103.

- Linthicum KJ, Anyamba A, Tucker CJ, Kelley PW, Myers MF, Peters CJ. Climate and satellite indicators to forecast Rift Valley fever epidemics in Kenya. *Science*. 1999 Jul 16;285(5426):397-400.
- Linthicum KJ, Davies FG, Kairo A, Bailey CL. Rift Valley fever virus (family Bunyaviridae, genus Phlebovirus). Isolations from Diptera collected during an inter-epizootic period in Kenya. *J Hyg (Lond)*. 1985 Aug;95(1):197-209.
- Liu L, Celma CC, Roy P. Rift Valley fever virus structural proteins: expression, characterization and assembly of recombinant proteins. *Virology*. 2008 Jul 18;5:82.
- Lozach PY, Kühbacher A, Meier R, Mancini R, Bitto D, Bouloy M, Helenius A. DC-SIGN as a receptor for phleboviruses. *Cell Host Microbe*. 2011 Jul 21;10(1):75-88.
- Madani TA, Al-Mazrou YY, Al-Jeffri MH, Mishkhas AA, Al-Rabeah AM, Turkistani AM, Al-Sayed MO, Abodahish AA, Khan AS, Ksiazek TG, Shobokshi O. Rift Valley fever epidemic in Saudi Arabia: epidemiological, clinical, and laboratory characteristics. *Clin Infect Dis*. 2003 Oct 15;37(8):1084-92.
- Mansuroglu Z, Josse T, Gilleron J, Billecocq A, Leger P, Bouloy M, Bonnefoy E. Nonstructural NSs protein of rift valley fever virus interacts with pericentromeric DNA sequences of the host cell, inducing chromosome cohesion and segregation defects. *J Virol*. 2010 Jan;84(2):928-39.
- McGavran MH, Easterday BC. Rift Valley Fever Virus Hepatitis: Light and Electron Microscopic Studies in the Mouse. *Am J Pathol*. 1963 May;42(5):587-607.
- McIntosh BM, Jupp PG, dos Santos I, Barnard BJ. Vector studies on Rift Valley Fever virus in South Africa. *S Afr Med J*. 1980 Jul 19;58(3):127-32.
- Meegan JM, Digoutte JP, Peters CJ, Shope RE. MONOCLONAL ANTIBODIES TO IDENTIFY ZINGA VIRUS AS RIFT VALLEY FEVER VIRUS. *Lancet*. 1983 Mar 19;321(8325):641.
- Meegan JM, Hoogstraal H, Moussa MI. An epizootic of Rift Valley fever in Egypt in 1977. *Vet Rec* 1979;105:124-125.
- Meegan JM, Khalil GM, Hoogstraal H, Adham FK. Experimental transmission and field isolation studies implicating *Culex pipiens* as a vector of Rift Valley fever virus in Egypt. *Am J Trop Med Hyg*. 1980 Nov;29(6):1405-10.
- Meegan JM. Rift Valley fever in Egypt: an overview of the epizootics in 1977 and 1978. *Contrib Epidemiol Biostat* 1981;3:100-113.

- Muller R, Saluzzo JF, Lopez N, Dreier T, Turell M, Smith J, Bouloy M. Characterization of clone 13, a naturally attenuated avirulent isolate of Rift Valley fever virus, which is altered in the small segment. *Am J Trop Med Hyg.* 1995 Oct;53(4):405-11.
- Nabeth P, Kane Y, Abdalahi MO, Diallo M, Ndiaye K, Ba K, Schneegans F, Sall AA, Mathiot C. Rift Valley fever outbreak, Mauritania, 1998: seroepidemiologic, virologic, entomologic, and zoologic investigations. *Emerg Infect Dis.* 2001 Nov-Dec;7(6):1052-4.
- Nehyba J, Hrdlicková R, Bose HR. Dynamic evolution of immune system regulators: the history of the interferon regulatory factor family. *Mol Biol Evol.* 2009 Nov;26(11):2539-50.
- Nfon CK, Marszal P, Zhang S, Weingartl HM. Innate Immune Response to Rift Valley Fever Virus in Goats. *PLoS Negl Trop Dis* 2012 May;6(4):e1623.
- Parker MD, Smith JF, Dalrymple JM. 1984. Rift Valley fever virus intracellular RNA: a functional analysis, p. 21-28. In Compans RW and Bishop DHL (ed.), *Segmented negative strand viruses*. Academic Press, Inc., New York.
- Peters CJ, Jones D, Trotter R, Donaldson J, White J, Stephen E, Slone TW Jr. Experimental Rift Valley fever in rhesus macaques. *Arch Virol.* 1988;99(1-2):31-44.
- Peters CJ, Slone TW. Inbred rat strains mimic the disparate human response to Rift Valley fever virus infection. *J Med Virol.* 1982;10(1):45-54.
- Piper ME, Sorenson DR, Gerrard SR. Efficient cellular release of Rift Valley fever virus requires genomic RNA. *PLoS One.* 2011 Mar 21;6(3):e18070.
- Ritter M, Bouloy M, Vialat P, Janzen C, Haller O, Frese M. Resistance to Rift Valley fever virus in *Rattus norvegicus*: genetic variability within certain 'inbred' strains. *J Gen Virol.* 2000 Nov;81(Pt 11):2683-8.
- Robalino J, Browdy CL, Prior S, Metz A, Parnell P, Gross P, Warr G. Induction of antiviral immunity by double-stranded RNA in a marine invertebrate. *J Virol.* 2004 Oct;78(19):10442-8.
- Rönkä H, Hildén P, Von Bonsdorff CH, Kuismanen E. Homodimeric association of the spike glycoproteins G1 and G2 of Uukuniemi virus. *Virology.* 1995 Aug 1;211(1):241-50.

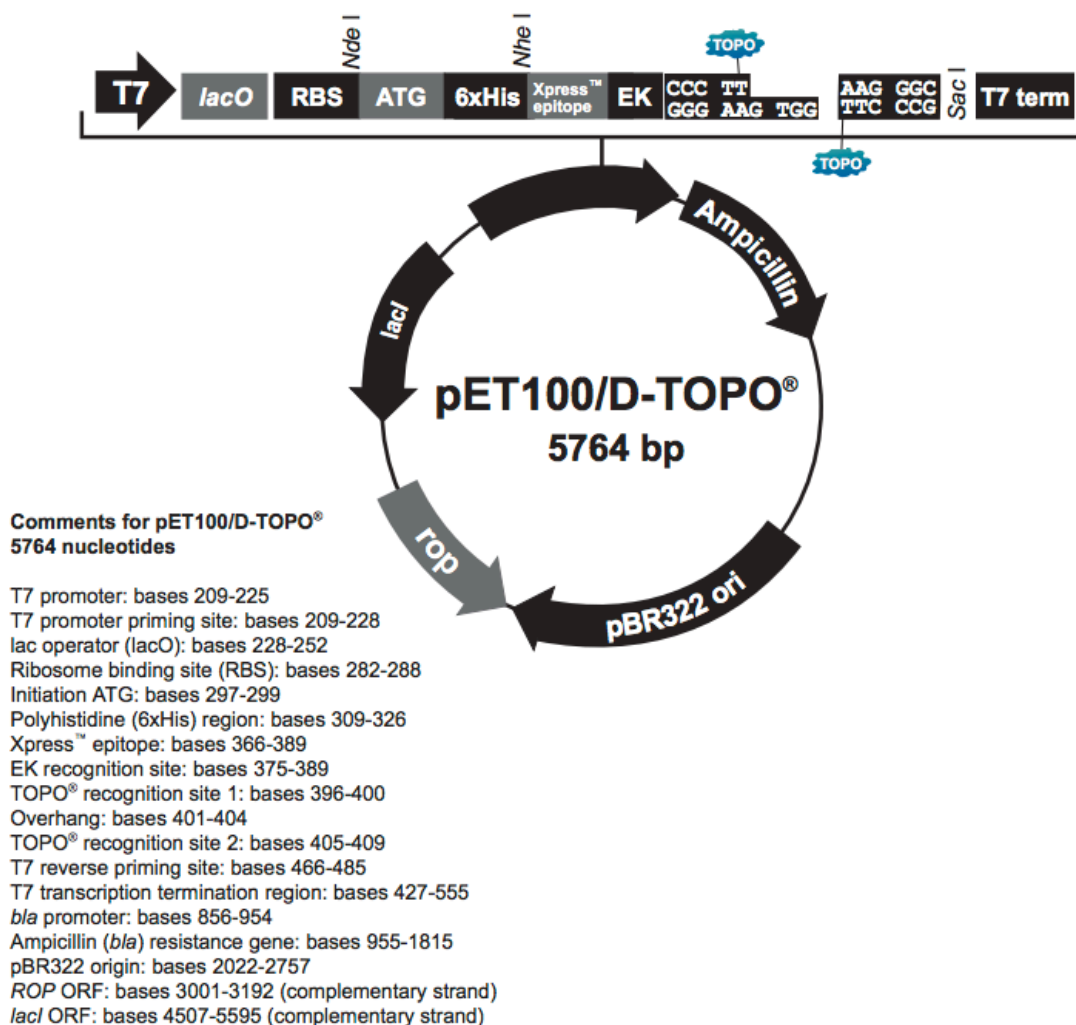
- Rosebrock, JA, Peters CJ. Cellular Resistance to Rift Valley Fever Virus (RVFV) Infection in Cultured Macrophages and Fibroblasts From Genetically Resistant and Susceptible Rats. *In Vitro*, Vol. 18, No. 3, Program Issue, Thirty-Third Annual Meeting of the Tissue Culture Association (Mar., 1982), pp. 274-330
- Rosomer WS, Turell MJ, Lerdthusnee K, Neira M, Dohm D, Ludwig G, Wasieleski L. Pathogenesis of Rift Valley fever virus in mosquitoes--tracheal conduits & the basal lamina as an extra-cellular barrier. *Arch Virol Suppl.* 2005;(19):89-100.
- Roulston A, Marcellus RC, Branton PE. Viruses and apoptosis. *Annu Rev Microbiol.* 1999;53:577-628.
- Scott GR, Coackley W, Roach RW, Cowdy NR. Rift Valley fever in camels. *J Pathol Bacteriol.* 1963 Jul;86:229-31.
- Sherman MB, Freiberg AN, Holbrook MR, Watowich SJ. Single-particle cryo-electron microscopy of Rift Valley fever virus. *Virology.* 2009 Apr 25;387(1):11-5.
- Shoemaker T, Boulianne C, Vincent MJ, Pezzanite L, Al-Qahtani MM, Al-Mazrou Y, Khan AS, Rollin PE, Swanepoel R, Ksiazek TG, Nichol ST. Genetic Analysis of Viruses Associated with the Emergence of Rift Valley Fever in Saudi Arabia and Yemen, 2000-01. *Emerg Infect Dis.* 2002 December; 8(12):1415-1420.
- Silva MC, Guerrero-Plata A, Gilfoy FD, Garofalo RP, Mason PW. Differential activation of human monocyte-derived and plasmacytoid dendritic cells by West Nile virus generated in different host cells. *J Virol* 2007 81, 13640-13648.
- Simonian MH, Smith JA. Spectrophotometric and Colorimetric Determination of Protein Concentration. *Curr Protoc Mol Biol.* 2006 Nov;Chapter 10:Unit 10.1A.
- Singh KR, Paul SD. Isolation of Dengue viruses in *Aedes albopictus* cell cultures. *Bull World Health Organ.* 1969;40(6):982-3.
- Struthers, J. K., R. Swanepoel, and S. P. Shepherd. 1984. Protein synthesis in Rift Valley fever virus-infected cells. *Virology* 134:118-124.
- Suzich JA, Kakach LT, Collett MS. Expression strategy of a phlebovirus: biogenesis of proteins from the Rift Valley fever virus M segment. *J Virol.* 1990 Apr;64(4):1549-55.
- Swanepoel R, Blackburn NK. Demonstration of nuclear immunofluorescence in Rift Valley fever infected cells. *J Gen Virol.* 1977 Mar;34(3):557-61.
- Turell MJ, Bailey CL, Rossi CA. Increased mosquito feeding on Rift Valley fever virus-infected lambs. *Am J Trop Med Hyg.* 1984b Nov;33(6):1232-8.

- Turell MJ, Dohm DJ, Mores CN, Terracina L, Walette DL Jr, Hribar LJ, Pecor JE, Blow JA. Potential for North American mosquitoes to transmit Rift Valley fever virus. *J Am Mosq Control Assoc.* 2008 Dec;24(4):502-7.
- Turell MJ, Faran ME, Cornet M, Bailey CL. Vector competence of Senegalese *Aedes fowleri* (Diptera: Culicidae) for Rift Valley fever virus. *J Med Entomol.* 1988 Jul;25(4):262-6
- Turell MJ, Gargan TP 2nd, Bailey CL. *Culex pipiens* (Diptera: Culicidae) morbidity and mortality associated with Rift Valley fever virus infection. *J Med Entomol.* 1985 May 24;22(3):332-7.
- Turell MJ, Gargan TP 2nd, Bailey CL. Replication and dissemination of Rift Valley fever virus in *Culex pipiens*. *Am J Trop Med Hyg.* 1984a Jan;33(1):176-81.
- Turell MJ, Rossi CA, Bailey CL. Effect of extrinsic incubation temperature on the ability of *Aedes taeniorhynchus* and *Culex pipiens* to transmit Rift Valley fever virus. *Am J Trop Med Hyg.* 1985 Nov;34(6):1211-8.
- Turell MJ, Saluzzo JF, Tammariello RF, Smith JF. Generation and transmission of Rift Valley fever viral reassortants by the mosquito *Culex pipiens*. *J Gen Virol.* 1990 Oct;71 (Pt 10):2307-12.
- Varfolomeev EE, Schuchmann M, Luria V, Chiannikulchai N, Beckmann JS, Mett IL. Targeted disruption of the mouse caspase 8 gene ablates cell death induction by the TNF receptors, Fas/Apo1, and DR3 and is lethal prenatally. *Immunity.* 1998 Aug; 9(2) 267-76.
- Vaughn VM, Streeter CC, Miller DJ, Gerrard SR. Restriction of Rift Valley Fever Virus Virulence in Mosquito Cells. *Viruses.* 2010; 2(2):655-675.
- Wasmoen TL, Kakach LT, Collett MS. Rift Valley fever virus M segment: cellular localization of M segment-encoded proteins. *Virology.* 1988 Sep;166(1):275-80.
- West J, Hernandez R, Ferreira D, Brown DT, White LA. Mutations in the endodomain of Sindbis virus glycoprotein E2 define sequences critical for virus assembly. *J Virol.* 2006 May;80(9):4458-68.
- White LA. Susceptibility of *Aedes albopictus* C6/36 cells to viral infection. *J Clin Microbiol.* 1987 Jul;25(7):1221-4.
- WHO. Rift Valley fever in Kenya, Somalia and the United Republic of Tanzania [Internet]. 2007 May 9; cited 2012 October 15. available from http://www.who.int/csr/don/2007_05_09/en/index.html

- WHO. Rift Valley fever in Sudan – update 5 [Internet]. 2008a Jan 22; cited 2012 October 15. available from http://www.who.int/csr/don/2008_01_22/en/index.html
- WHO. Rift Valley fever in Madagascar [Internet]. 2008b Apr 18; cited 2012 October 15. available from http://www.who.int/csr/don/2008_04_18a/en/index.html
- WHO. Rift Valley fever outbreaks forecasting models. Joint FAO - WHO experts consultation, Rome, Italy, 29 September-1October 2008 [Internet]. 2009; cited 2012 Oct 15. available from: http://whqlibdoc.who.int/hq/2009/WHO_HSE_GAR_BDP_2009.2_eng.pdf
- WHO. Rift Valley fever in South Africa- update 2 [Internet]. 2010 May 12; cited 2012 Oct 15. available from: http://www.who.int/csr/don/2010_05_12/en/index.html
- Won S, Ikegami T, Peters CJ, Makino S. NSm and 78-kilodalton proteins of Rift Valley fever virus are nonessential for viral replication in cell culture. *J Virol.* 2006 Aug;80(16):8274-8.
- Won S, Ikegami T, Peters CJ, Makino S. NSm protein of Rift Valley fever virus suppresses virus-induced apoptosis. *J Virol.* 2007 Dec;81(24):13335-45.
- Yan SB, Tuason DA, Tuason VB, Frey WH 2nd. Polyethylene glycol interferes with protein molecular weight determinations by gel filtration. *Anal Biochem.* 1984 Apr;138(1):137-40.
- Zamoto-Niikura A, Terasaki K, Ikegami T, Peters CJ, Makino S. Rift valley fever virus L protein forms a biologically active oligomer. *J Virol.* 2009 Dec;83(24):12779-89.

Appendix A. DNA sequences

pET-100/D-TOPO vector



DNA sequence of pET-100/D-TOPO RVFV ZH501 NSm1 clone 02.

A frameshift mutation occurred in a series of seven glutamine repeats at nt 1626 from the 3' end of RVFV M-segment or nt 1714 from ATG of pET-100 rNSm1. This resulted in a stop codon two amino acid residues downstream at nt 1630-1632 from the 3' end of RVFV M-segment or nt 1718-1720 from ATG of pET-100 rNSm1.

Lower case letters are plasmid sequence. Capital letters are RVFV M-segment sequence. Letters are separated onto three-character codons in-frame beginning with the plasmid expression start codon. Two triplets highlighted in yellow and bolded are frameshifted, resulting in a TAG stop codon. The remaining sequence following the stop codon is not transcribed and is not shown in triplets.



```

caaggagatggcgcccaacagtcccccgccacggggcctgccaccatacccacgccga
aacaagcgctcatgagcccgaagtggcgagcccgatcttccccatcggtgatgtcggcg
atataggcgccagcaaccgcacctgtggcgccgggtgatgccggccacgatgcgtccggc
gtagaggatcgagatctcgatcccgcgaaattaatacgactcactataggggaattgtg
agcggataacaattccccctctagaataattttgtttaactttaagaaggagatataca
t atg cgg ggt tct cat cat cat cat cat cat ggt atg gct agc
atg act ggt gga cag caa atg ggt cgg gat ctg tac gac gat gac
gat aag gat cat ccc ttc acc ATG TAT GTT TTA TTA ACA ATT CTA
ATC TCG GTT CTG GTG TGT GAA GCG GTT ATT AGA GTG TCT CTA AGC
TCC ACA AGA GAA GAG ACC TGC TTT GGT GAC TCC ACT AAC CCA GAG
ATG ATT GAA GGA GCT TGG GAT TCA CTC AGA GAG GAG GAG ATG CCG
GAG GAG CTC TCC TGT TCT ATA TCA GGC ATA AGA GAG GTT AAG ACC
TCA AGC CAG GAG TTA TAC AGG GCA TTA AAA GCC ATC ATT GCT GCT
GAT GGC TTG AAC AAC ATC ACC TGC CAT GGT AAG GAT CCT GAG GAC
AAG ATT TCC CTC ATA AAG GGT CCT CCT CAC AAA AAG CGG GTG GGG
ATA GTT CGG TGT GAG AGA CGA AGA GAT GCT AAG CAA ATA GGG AGA
GAA ACC ATG GCA GGG ATT GCA ATG ACA GTC CTT CCA GCC TTA GCA
GTT TTT GCT TTG GCA CCT GTT GTT TTT GCT GAA GAC CCC CAT CTC
AGA AAC AGA CCA GGG AAG GGG CAC AAC TAC ATT GAC GGG ATG ACT
CAG GAG GAT GCC ACA TGC AAA CCT GTG ACA TAT GCT GGG GCA TGT
AGC AGT TTT GAT GTC TTG CTT GAA AAG GGA AAA TTT CCC CTT TTC
CAG TCG TAT GCT CAT CAT AGA ACT CTA CTA GAG GCA GTT CAC GAC
ACC ATC ATT GCA AAG GCT GAT CCA CCT AGC TGT GAC CTT CAG AGT
GCT CAT GGG AAC CCC TGC ATG AAA GAG AAA CTC GTG ATG AAG ACA
CAC TGT CCA AAT GAC TAC CAG TCA GCT CAT TAC CTC AAC AAT GAC
GGG AAA ATG GCT TCA GTC AAG TGC CCT CCT AAG TAT GAG CTC ACT
GAG GAC TGC AAC TTT TGT AGG CAG ATG ACA GGT GCT AGC CTG AAG
AAG GGG TCT TAT CCT CTC CAA GAC TTG TTT TGT CAG TCA AGT GAG
GAT GAT GGA TCA AAA TTA AAA ACA AAA ATG AAA GGG GTC TGC GAA
GTG GGG GTT CAA GCA CTC AAA AAG TGT GAT GGC CAA CTC AGC ACT
GCA CAT GAG GTT GTG CCC TTT GCA GTG TTT AAG AAC TCA AAG AAG
GTT TAT CTT GAT AAG CTT GAC CTT AAG ACT GAG GAG AAT CTG CTA
CCA GAC TCA TTT GTC TGT TTC GAG CAT AAG GGA CAG TAC AAA GGA
ACA ATG GAC TCT GGT CAG ACT AAG AGG GAG CTC AAA AGC TTT GAT
ATC TCT CAG TGC CCC AAG ATT GGA GGA CAT GGT AGT AAG AAG TGC
ACT GGG GAC GCA GCA TTT TGC TCT GCT TAT GAG TGC ACT GCT CAG
TAC GCC AAT GCC TAT TGT TCA CAT GCT AAT GGG TCA GGG ATT GTG

```

CAG ATA CAA GTA TCA GGG GTC TGG AAG AAG CCT TTA TGT GTA GGG
 TAT GAG AGA GTG GTT GTG AAG AGA GAA CTC TCT GCC AAG CCC ATC
 CAG AGA GTT GAG CCT TGC ACA ACT TGT ATA ACC AAA TGT GAG CCT
 CAT GGA TTG GTT GTC CGA TCA ACA GGG TTC AAG ATA TCA TCA GCA
 GTT GCT TGT GCT AGC GGA GTT TGC GTC ACA GGA TCG CAG AGT CCT
 TCC ACC GAG ATT ACA CTC AAG TAT CCA GGG ATA TCC CAG TCT TCT
 GGG GGG **ACA TAG** GGGTTCACATGGCACACGATGATCAGTCAGTTAGCT
 CCAAAATAGTAGCTCACTGCCCTCCCCAGGACCCGTGCTTAGTGCATGGCTGCATAGTG
 TGTGCTCATGGCCTGATAAATTACCAGTGTCACTGCTCTCAGTGCCTTTGTTGTTGT
 GTTTGTATTCACTTCTATTGCAATAATTTGTTTAGCTGTTCTTTATAGGGTGCTTAAGT
 GCCTGAAGATTGCCCCAAGGAAAGTTCTGAATCCACTAATGTGGATCACAGCCTTCATC
 AGATGGATATATAAGAAGATGGTTGCCAGAGTGGCAGACAACATTAATCAAGTGAACAG
 GGAAATAGGATGGATGGAAGGAGGTCAGTTGGTTCTAGGGAACCCTGCCCCCTATTCCTC
 GTCATGCCCCAATCCCACGTTATAGCACATACCTGATGTTATTATTGATTGTCTCATAT
 GCATCAGCAaagggcgagctcaacgatccggctgctaacaaagcccgaaggaagctga
 gttggctgctgccaccgctgagcaataa

ExPASy ProtParam prediction of the molecular weight of rNSm1 with frameshift mutation.



ExPASy
 Bioinformatics Resource Portal

[Home](#) | [Contact](#)

ProtParam

User-provided sequence:

```

      10      20      30      40      50      60
MRGSHHHHHH GMASMTGGQQ MGRDLYDDDD KDHFFTMYVL LTLISVLVC EAVIRVSLSS

      70      80      90     100     110     120
TREETCFGDS TNPEMIEGAW DSLREEEMPE ELSCSISGIR EVKTSSQELY RALKAIIAAD

     130     140     150     160     170     180
GLNNITCHGK DPEDKISLIK GPPHKRVRGI VRCERRRDAK QIGRETMAGI AMTVLPALAV

     190     200     210     220     230     240
FALAPVVFAE DPHLRNRPGK GHNYIDGMTQ EDATCKPVTY AGACSSFDVL LEKGKFPLFQ

     250     260     270     280     290     300
SYAHHRTLLE AVHDTIIAKA DPPSCDLQSA HGNPCMKEKL VMKTHCPNDY QSAHYLNNDG

     310     320     330     340     350     360
KMASVKCPFK YELTEDCNFC RQMTGASLKK GSYPLQDLFC QSSEDGSKL KTKMKGVCEV

     370     380     390     400     410     420
GVQALKKCDG QLSTAHEVVP FAVFKNSKKV YLDKLDLKE ENLLPDSFVC FEHKGQYKGT

     430     440     450     460     470     480
MDSGQTKREL KSFDISQCPK IGGHGSKKCT GDAAFCSAYE CTAQYANAYC SHANGSGIVQ

     490     500     510     520     530     540
IQVSGVWKKP LCVGYERVVV KRELSAKPIQ RVEPCTTCIT KCEPHGLVVR STGFKISSAV

     550     560     570
ACASGVCVTG SQSPSTEITL KYPGISQSSG GT
  
```

[References](#) and [documentation](#) are available.

new Please note the [modified algorithm](#) for extinction coefficient.

Number of amino acids: 572

Molecular weight: 62596.5

Theoretical pI: 7.69

Mass Spectrometry confirmation of rNSm1 expression from pET-100/D-TOPO RVFV ZH501 NSm1 clone 02.

Match to: **ALAN_RVFV** Score: **662**

pET-100 RVFV NSm1 recombinant protein

Nominal mass (M_r): **84219**; Calculated pI value: **8.22**

Fixed modifications: Carbamidomethyl (C)

Variable modifications: Oxidation (M)

Cleavage by Trypsin: cuts C-term side of KR unless next residue is P

Sequence Coverage: **25%**

Matched peptides shown in **Bold Red**

1	MRGSHHHHHH	GMASMTGGQQ	MGRDLYDDDD	KDHPFTMYVL	LTILISVLVC
51	EAVIRVSLSS	TR EETCFGDS	TNPEMIEGAW	DSLREEEMPE	ELSCSISGIR
101	EVKTSSQELY	RALK AI IAAD	GLNNITCHGK	DPEDK ISLIK	GPPHKRVRGI
151	VRCERRRDAK	QIGRETMAGI	AMTVLPALAV	FALAPVVFAE	DPHLRNRP GK
201	GHNYIDGMTQ	EDATCKPVTY	AGACSSF DVL	LEK GKFPLFQ	SYAHHRTLLE
251	AVHDTI IAKA	DPPSCDLQSA	HGNPCMKEKL	VMKTHCPNDY	QSAHYLNNDG
301	KMASVK CPPK	YELTEDCNFC	RQMTGASLKK	GSYPLQDLFC	QSSEDDGSKL
351	KTKMKGVC EV	GVQALK KCDG	QLSTAHEVVP	FAVFKNSKKV	YLDK LDLKTE
401	ENLLPDSFVC	FEHKGQYKGT	MDSGQTKREL	KSFDISQCPK	IGGHGSKKCT
451	GDAAFCSAYE	CTAQYANAYC	SHANGSGIVQ	IQVSGVWKKP	LCVGYERVVV
501	KRELSAKPIQ	RVEPCTTCIT	KCEPHGLVVR	STGFK ISSAV	ACASGVCVTG
551	SQSPSTEITL	KYPGISQSSG	GDIGVHMAHD	DQSVSSKIVA	HCPPQDPCLV
601	HGCIVCAHGL	INYQCHTALS	AFVVVFVFSS	IAIICLAVLY	RVLKCLKIAP
651	RKVLNPLMWI	TAFIRWIYKK	MVARVADNIN	QVNREIGWME	GGQLVLGNPA
701	PIPRHAPIPR	YSTYLMLLLI	VSYASAKGEL	NDPAANKARK	EAELAAATAE
751	Q				

Appendix B. Buffers and Media

Preparation of carboxymethyl cellulose (CMC) overlay

400 mL required
1.75 % final concentration

Put magnetic stirring bar in a bottle

Add 306.27mL mQ water

Heat to almost boiling point.

Add slowly 7.00 g of CMC

Stir on a magnetic stirrer until CMC is dissolved.

Heat again if necessary. Do not boil.

Autoclave at 121°C for 15 minutes.

Cool to 37C

Add (mL): 40.00 10X DMEM
8.00 FBS
19.73 7.5% NaHCO₃
10.00 1M HEPES
4.00 0.4 g/L Folic Acid (100x)
4.00 200 mM L-Glutamine
4.00 100mM (11.0 mg/mL) Sodium Pyruvate
4.00 100x Penicillin/Streptomycin

Mix on magnetic stirrer in 37C incubator until ready to use.

Vero E6 *in vitro* growth medium

500 mL	DMEM
57 mL	FBS
5.7 mL	sodium pyruvate

C6/36 *in vitro* growth medium

46% Expression Systems Formula (ESF) 921 (Expression Systems 96-001)
 46% Eagle's minimum essential medium (EMEM) (Wisent 320-036-CL)
 2.5% heat-inactivated fetal bovine serum (FBS) (Wisent 080-450)
 1mM final concentration sodium pyruvate (Sigma Aldrich S8636)
 25mM final concentration HEPES (Sigma Aldrich H0887)
 2x non-essential amino acid solution (11.6 mL of 100x stock, Sigma Aldrich 58572C).

Media Preparation

1. Prepare "EMEM-3" growth media as follows
 - a. 500 mL EMEM (Wisent #320-036-CL)
 - b. 10% Fetal Bovine Serum (58 mL)
 - c. 25mM HEPES (14.5 mL of 1M stock)
 - d. 1mM Sodium Pyruvate (5.8 mL of 7.5% stock)
 - e. 2x non-essential amino acid solution (11.6 mL of 100x stock)
2. Mix 1:1 EMEM-3 with ESF-921 protein-free media (Expression Systems #96-001)
3. Final media formulation "ESF-MEM" (545 mL total volume)
 - a. 250 mL ESF-921 growth media
 - b. 250 mL Wisent EMEM
 - c. 5% Fetal Bovine Serum (29 mL)
 - d. 12.5mM HEPES (7.25 mL)
 - e. 500µM Sodium Pyruvate (2.9 mL)
 - f. 1x non-essential amino acid solution (6 mL)

TBE running buffer (0.5x stock concentration)

10.8 g Tris base (121.14 g/mol, 90mM final concentration)
 5.5 g Boric acid (61.83 g/mol, 90mM final concentration)
 0.58 g EDTA (292.24 g/mol, 2mM final concentration)
 H₂O to 1000 mL
 pH to 8.3

TN Buffer

1.576 g Tris-HCl (157.6 g/mol, 10mM final concentration)
 8.766 g NaCl (58.44 g/mol, 150mM final concentration)
 H₂O to 1000 mL total volume
 pH to 7.4

TNE Buffer

15.76 g Tris-HCl (157.6 g/mol, 100mM final concentration)
 5.84 g NaCl (58.44 g/mol, 100mM final concentration)
 0.29 g EDTA (292.241 g/mol, 1mM final concentration)
 H₂O to 1000 mL total volume
 pH to 7.4

PEG precipitate resuspension buffer (200 mL total volume)

3.152g Tris-HCl (157.6 g/mol, 100mM final concentration)
 H₂O to 200 mL total volume
 pH to 8.0

TBS-T

1.21 g Tris (121.14 g/mol, 50mM final concentration)
 8.76 g NaCl (58.44 g/mol, 150mM final concentration)
 1.0 mL Tween-20
 H₂O to 1000 mL

Blocking Buffer

0.12 g Tris (121.14 g/mol, 50mM final concentration)
 0.88 g NaCl (58.44g/mol, 150mM final concentration)
 0.1 mL Tween-20
 5.0 g Skim milk powder
 H₂O to 100 mL

Appendix C: Protocols

EvoQuest protocol for generating antibodies against synthetic peptides.

PolyQuik™ Protocol for Rabbit (Two animals):

Procedure	Time Relative to Placing Order	Time Relative to Injection of Animals	Description
Peptide synthesis	~2 weeks	-	-Proprietary
Peptide conjugation to carrier	~3 weeks	-	
Control serum collection	~3 weeks	Day 0	
Primary injection	~3 weeks	Day 0	
Serum collection	~8 weeks	Day 36	
ELISA and shipping	~9 weeks		

TriPure RNA Isolation Protocol

1. Extraction
 - a. Add 900 μ L TriPure to 100 μ L virus in 1.5mL tube
 - b. Remove from BSC, transfer into new tube
 - c. Remove from BSL-3E
2. RNA isolation
 - a. incubate 5 minutes at RT
 - b. Add 200 μ L chloroform, mix thoroughly
 - c. Spin at 12,000g for 15 minutes at 2-8C
 - d. Take 500 μ L of aqueous, clear phase
 - e. Add 1 μ L GlycoBlue
 - f. Add 750 μ L isopropanol, mix by inversion
 - g. Incubate 5 minutes at RT
 - h. Spin at 12,000g for 15 minutes at 2-8C
 - i. Wash pellet with 75% EtOH
 - j. Spin 7,500g for 5 minutes at 2-8C
 - k. Discard supernatant
3. RNA storage
 - a. Air dry pellet for 5-10 minutes
 - b. Resuspend in RNase-free water or DEPC-treated water by incubating 10-15 minutes at 60C
 - c. Store at -70C

RT-PCR of RVFV NSm1

Reagent	Vol (μL)	# tubes	Total Vol
Nuclease-free water	17.8	2	35.6
Template RNA	5	2	10
Reaction Mix (2X)	25	2	50
MgSO ₄	1	2	2
Forward Primer (100μM initial conc.)	0.1	2	0.2
Reverse Primer (100μM initial conc.)	0.1	2	0.2
RT-PCR polymerase	1	2	2
Total Volume	50	2	100

Thermal Cycler Program			
50°C 30m	94°C 2m	94°C 15s	57°C 35s
		68°C 2m30	68°C 10m
			4°C ∞
1X	40X	1X	

Agarose Gel Electrophoresis

1. Agarose Gel
 - a. 50 mL H₂O
 - b. 0.5g agarose for a 1% gel
 - c. 0.75g agarose for a 1.5% gel
 - d. 1 µL SYBR dye
2. Products
 - a. 1 µL DNA ladder, 2 µL Blue Juice, 13 µL H₂O
 - b. 10 µL PCR product, 2 µL BlueJuice, 3 µL H₂O
3. Running the Gel
 - a. 70 to 100 V
 - b. 45 to 80 minutes

Ligation and transformation protocol for TOP10 chemically competent *E. coli* cells

1. Ligation
 - a. Set up the ligation reaction in a 1.5mL tube
 - i. 2.5 μ L 2 \times Rapid Ligation Buffer
 - ii. 0.25 μ L Vector
 - iii. 0.5 μ L T4 DNA Ligase
 - iv. 1.75 μ L purified PCR product
 - b. Let the ligation proceed overnight at 4 °C
2. Transformation
 - a. Add 5 μ L ligation mix to 25 μ L competent cells
 - b. Transform cells on ice for 20 minutes
 - c. Heat-shock cells at 42°C for 50 seconds
 - d. Put cells back on ice for 2 minutes
 - e. Add 200 μ L sterile SOC media to each tube
 - i. Variation: Add 100 μ L sterile SOC media
 - f. Incubate in shaker for 1 to 1.5 hours at 37°C at 200 to 275 rpm
 - g. Plate 50-200 μ L cells on LB agar plate with antibiotic and incubate overnight
 - i. Variation: Plate all of the cells
3. PCR Screening of Colonies
 - a. Pick large, perfectly round colonies
 - b. Using a 0.5 μ L loop, pick the colony and transfer it into a PCR tube
 - c. Transfer the tube to a 1mL vial of LB media with antibiotic and grow at 37 °C high aeration for 8 hours
 - d. Run PCR on the tube
 - i. 95°C for 15 minute activation
 - ii. 35 cycles of
 1. 95°C for 30 seconds
 2. 50°C for 30 seconds
 3. 72°C for 30-60 seconds
 - iii. 72°C for 7 minutes
 - iv. 4°C indefinite hold

Restriction Endonuclease Digestion

5 µL	purified pET-100 RVFV NSm1 clone 02 plasmid (15.5 µg/µL)
2 µL	Restriction endonuclease (10,000 U/mL)
2 µL	10× stock reaction buffer
11 µL	H ₂ O

Incubate at 37°C overnight in a sterile 1.5 mL microcentrifuge tube. Store at 4°C until ready for use.

SDS-PAGE and semi-dry blotting transfer for the initial detection of rNSm1**Sodium Dodecyl Sulfate Polyacrylamide Gel Electrophoresis**

1. Resolving Gel
 - a. Pour resolving gel to bottom of loop
 - b. Add methanol layer
 - c. Allow to set for 30 minutes
2. Stacking Gel
 - a. Remove methanol layer by blotting with paper towel
 - b. Pour stacking gel to fill cassette
 - c. Add comb
 - d. Allow to set for 30 minutes
3. Sample Loading
 - a. Remove comb
 - b. Load into holder with wells facing in
 - c. Lock cassettes and place in tank
 - d. Fill area between wells with run buffer, area outside of wells half-full of run buffer
 - e. Load up to 30 μ L samples per well
 - f. run gel at 150V for 60 minutes or until the dye front begins to exit the gel

Protein Stain

1. Staining SDS-PAGE gel
 - a. Wash gel in H₂O on shaker platform for 5 minutes
 - b. Add Coomassie Brilliant Blue stain (pump may be powerful enough to tear gel)
 - c. Wash gel in stain for 30-60 minutes on shaker platform
 - d. Wash gel in H₂O overnight on shaker platform

Electrophoretic Transfer to Polyvinylidene Fluoride Membrane

1. Filter
 - a. Using gloves, cut filter to 5.5cm by 8.5cm
2. PVDF Membrane
 - a. Using gloves, cut membrane to 5.5cm by 8.5cm (in box under Greg's desk)
 - b. Immerse membrane in 100% methanol for 10 seconds
 - c. Soak in anode (bottom) buffer for 30 minutes on rocker platform
3. Gel
 - a. Wash gel in H₂O
 - b. Soak gel in cathode buffer for 5 minutes
4. Transfer
 - a. Immerse filter in anode buffer and place on transfer platform
 - b. Place membrane on top of anode filter
 - c. Place gel on top of membrane
 - d. Immerse filter (x2) in cathode buffer and place on top of gel
 - e. Roll with pipette tip to remove all air bubbles
 - f. Run at 0.07A (for one) or 0.14A (for two) for 60 minutes

SDS-PAGE and semi-dry blotting transfer for the initial detection of rNSm1 (without iBlot) continued – Western blotting

Transfer Protein Stain

1. Staining PVDF membrane
 - a. Wash membrane in H₂O
 - b. Submerge in Ponceau S stain
 - c. Wash in water to reveal stained proteins
 - d. Wash in ionic solution to remove Ponceau S stain

Western Blot

1. Blocking
 - a. Soak the membrane overnight in 5% skim milk or 3% BSA with Tween-20 detergent to saturate the protein binding of the membrane
 - b. Soak the membrane in blocking buffer at +4C
 - c. Freeze the membrane submerged in blocking buffer at -20C
2. Chromogenic Antibody Detection (Conjugate)
 - a. Wash the membrane 3 x 10 minutes in TBS-Tween
 - b. Wash the membrane in conjugate antibody in 20% strength blocking buffer for 1 hour
 - c. Wash the membrane 3 x 10 minutes in TBS-Tween
 - d. Mix one dose of Sigma-Fast DAB in 5mL H₂O, allow to react for up to one minute
 - e. Wash the membrane in H₂O to stop the reaction and dry on a paper towel
3. Chromogenic Antibody Detection (Primary and Secondary)
 - a. Wash the membrane 3 x 10 minutes in TBS-Tween
 - b. Wash the membrane in primary antibody in 20% strength blocking buffer for 1 hour
 - c. Wash the membrane 3 x 10 minutes in TBS-Tween
 - d. Wash the membrane in secondary antibody in 20% strength blocking buffer for 1 hour
 - e. Mix one dose of Sigma-Fast DAB in 5mL H₂O, allow to react for up to one minute
 - f. Wash the membrane in H₂O to stop the reaction and dry on a paper towel

Transformation protocol for BL21 Star (DE3) chemically competent *E. coli* cells

1. Transformation
 - a. Add 5 μL ligation mix to 25 μL competent cells
 - b. Transform cells on ice for 30 minutes
 - c. Heat-shock cells at 42°C for 30 seconds
 - d. Put cells back on ice for 2 minutes
 - e. Add 250 μL of 37°C sterile SOC media to each tube
 - f. Incubate in shaker for 1 hour at 37°C at 225 rpm
 - g. Plate 25 μL of the cells on one LB agar plate with ampicillin and plate the remaining volume of cells (approximately 200 μL) onto a second plate of LB agar. Incubate both plates overnight at 37°C.
2. PCR Screening of Colonies
 - a. Pick large, perfectly round colonies
 - b. Using a 0.5 μL loop, pick the colony and transfer it into a PCR tube
 - c. Transfer the tube to a 1mL vial of LB media with antibiotic and grow at 37 °C high aeration for 8 hours
 - d. Run PCR on the tube
 - i. 95°C for 15 minute activation
 - ii. 35 cycles of
 1. 95°C for 30 seconds
 2. 50°C for 30 seconds
 3. 72°C for 30-60 seconds
 - iii. 72°C for 7 minutes
 - iv. 4°C indefinite hold

rNSm1 Large Scale Production

- Overnight growth
 - 100uL seed culture
 - 100mL LB broth + ampicillin (50mg/mL final conc.) in a 500mL flask
- Large scale growth
 - 4 x 500mL in 2L flasks
 - 25mL overnight growth + 475mL LB broth + ampicillin
 - OD600 at 9:00 = 0.204
 - OD600 at 10:30 = 0.573
 - Induced with 1mM IPTG
 - 2 x 3mL cultures in 14mL dilution tubes grown separately, one uninduced
 - OD600 at 16:30 (6hpi)
 - IPTG = 1.627, Control = 1.731
- Process samples
 - Preliminary indicator
 - 16,000 x g for 10 minutes 4C for 1.5mL tubes
 - mass pellets for IPTG+ and uninduced control
 - spin down
 - 10,000 x g for 10 minutes 4C
 - resuspend in 5% culture volume of BugBuster (assume 10g/L cell paste)
 - 84.718g – 81.689g = 3.029g 85.989g – 82.756g = 3.233g
 - 85.649g – 82.363g = 3.286g 85.854g – 82.379g = 3.475g
 - 13.023g cell paste total
 - 25mL BugBuster for 500mL culture
 - combine into 100mL sample in one tube
 - add 1:1000 benzonase endonuclease (100uL for 2L culture)
 - add 1:100 HALT protease inhibitors (1mL for 2L culture)
 - incubate 20 minutes RT
 - spin 16,000 rpm, 20 minutes 4C
 - collect soluble and insoluble fractions
- insoluble fraction
 - resuspend pellet in 100mL BugBuster
 - add 100uL lysozyme
 - incubate 5 minutes
 - add 100mL 1:10 BugBuster
 - mix 1 minute
 - spin 5,000g, 15 minutes 4C
 - remove supernatant, keep pellet
 - resuspend pellet in 200mL 1:10 BugBuster
 - spin 5,000g, 15 minutes 4C
 - resuspend pellet in 200mL 1:10 BugBuster
 - spin 5,000g 15 minutes 4C
 - resuspend pellet in 200mL 1:10 BugBuster
 - spin 16,000g 15 minutes 4C
 - Freeze pellet at -70C

Vero E6 cell culture procedures

Freezing Cells

1. Split Cells
 - a. Split the cells into new flasks the day before you intend to freeze them
2. Prepare Freezing Solutions:
 - a. Solution A: 80% FBS, 20% culture medium
 - b. Solution B: 80% FBS, 20% DMSO
 - c. 0.5mL of each solution will be required per vial to be frozen
3. Count Cells
 - a. Ideally 1×10^7 cells should be frozen, expecting a survival rate of 50%
 - b. 1×10^7 cells/mL, diluted 1:2 with stain, would be a cell count of 500 per counting square ($1 \times 10^{-4} \text{ cm}^2$)
 - c. If the cells are trypsinized and resuspended in 10mL media, this would be a count of 50 per $1 \times 10^{-4} \text{ cm}^2$
 - d.
4. Pellet Cells
 - a. Pre-cool the centrifuge to +4C
 - b. Spin the cells at $500 \times g$ for 3 minutes and do not apply the brake to decelerate the centrifuge
 - c. Remove the supernatant
5. Freeze Cells
 - a. Gently resuspend the cells in 0.5mL of Solution A per 1×10^7 cells
 - b. Add 0.5mL Solution B
 - c. Begin freezing process within 30 minutes, placing the cells within a slow-freezing container overnight
 - d. Transfer cells to -150C for long-term storage

Thawing Cells

- a. Transfer the frozen vial from -150C to a water bath in less than 1 minute
- b. Sterilize the outside of the vial with ethanol
- c. Add 1mL media dropwise to frozen vial to gently resuspend cells
- d. Add the cell suspension dropwise to 10mL 4C growth media
OPTIONAL: Pellet cells as per Freezing Cells above to remove Freezing Solutions
- e. Add the cells to media for a final volume of 20mL before transferring to a T75 flask
- f. If the Freezing Solution was not removed as per above, change media within 4-12 hours

C6/36 cell culture procedures

Passaging Procedure

1. Remove all growth media from the flask
2. Use a cell scraper to remove adherent cells from the flask
 - a. Brown-handled scrapers work better than gray-handled Fisher brand scrapers
3. Collect the scraped cells in fresh media
4. Resuspend in 5x the original culture volume
5. Distribute into new unvented flasks

The cells can be passaged at this dilution twice per week.

Cryopreservation Procedure

Day 1

1. Change cell media 1 day prior to freezing

Day 2

2. Remove “conditioned” media to separate sterile container
3. Scrape cells from flask
4. Resuspend scraped cells in a reduced volume of conditioned media (~5 mL per T-75 flask)
5. Transfer cell suspension to centrifuge tube(s)
6. Stain and count cells in collected media
 - a. Recommended freezing concentration of 2.5×10^7 cells/vial
7. Pellet cells in centrifuge at 4°C, 800 g for 10 minutes with minimal deceleration
8. Remove conditioned media from cell pellet to a separate sterile container
9. Resuspend the cells in 1M DMSO freezing media
 - a. 465 µL conditioned media
 - b. 465 µL fresh media (4°C)
 - c. 70 µL DMSO
10. Cool the cells at 1°C per minute to -70°C

Day 3

11. Transfer the vials to -150°C within 24 hours

Thawing Procedure

1. Remove vial from -150°C freezer
 2. Completely thaw vial as quickly as possible
 3. Add cold (4°C) media dropwise to the cryovial until the cryovial is mostly full
 4. Transfer the contents of the cryovial to an unvented T-75 flask
 5. Add cold (4°C) media dropwise to the flask to a final volume of 20 mL
- Incubate at 28°C in the dark

Indirect immunofluorescent assays of RVFV maturation

1. Growth of cells
 - a. Autoclave IFA slides
 - b. Split confluent T75 flask into 40mL fresh media (1:1 dilution)
 - c. Add 20mL cells to 3 x IFA slides per square Petri plate
 - d. Incubate overnight
2. Infection of cells
 - a. Infect slides at MOI 10
 - b. After 1 hour, add FBS to a final concentration of 2%
3. Fixing cells
 - a. Remove 10mL media, replace with 10mL formalin
 - b. Incubate for a minimum of 1 hour at 37°C or overnight at 4°C
 - c. Remove slides from BSL-3E
4. Indirect immunofluorescent assays
 - a. Wash slides 3 × 10 minutes in PBS
 - b. Block slides in TBS-T overnight at 4°C to permeabilize cells
 - c. Wash slides 3 × 10 minutes in PBS
 - d. Add primary antibodies and incubate for 1 hour at 37°C
 - e. Wash slides 3 × 10 minutes in PBS
 - f. Add secondary antibodies and incubate for 1 hour at 37°C
 - g. Wash slides 3 × 10 minutes in PBS
 - h. Apply DAPI counterstain. Dilute DAPI stock solution (Component A) 1:300 into PBS to make a 0.2 µg/mL (600 nM) solution. Apply a sufficient amount of the 600 nM solution to cover cells, then incubate for 2 minutes.
 - i. Wash slides 3 × 10 minutes in PBS
 - j. Mount coverslip in ProLong Gold antifade reagent

Target	Reagent	Excitation	Emission
RVFV N	Rabbit anti-RVFV N polyclonal serum	—	—
RVFV NSm1	Rabbit anti-RVFV NSm1 polyclonal serum	—	—
RVFV NSs	Rabbit anti-RVFV NSs polyclonal serum	—	—
Rabbit IgG	Goat anti-rabbit IgG AlexaFluor 594	590	617
Nucleus	DAPI	358	461
Golgi	golgin-97 (human), mouse IgG1, monoclonal CDF4 (anti-Golgi)	—	—
Mouse IgG	Goat anti-mouse IgG AlexaFluor 488	495	519

Indirect immunofluorescent assays of RVFV maturation (continued)

Cell Type	RVFV infection	anti-N	anti-NSm1	anti-NSs	anti-Rabbit IgG	Nuclear stain (DAPI)	Golgi stain (golgin-97)
Vero	+	-	-	-	+	+	+
C6/36	+	-	-	-	+	+	+

Vero	+	+	-	-	+	+	+
Vero	-	+	-	-	+	+	+
C6/36	+	+	-	-	+	+	+
C6/36	-	+	-	-	+	+	+

Vero	+	-	+	-	+	+	+
Vero	-	-	+	-	+	+	+
C6/36	+	-	+	-	+	+	+
C6/36	-	-	+	-	+	+	+

Vero	+	-	-	+	+	+	+
Vero	-	-	-	+	+	+	+
C6/36	+	-	-	+	+	+	+
C6/36	-	-	-	+	+	+	+

Timecourse Comparison Western Blots

Gels 1 & 2: C6/36 timecourse

1. -
2. SeeBlue Plus 2 prestained protein standard
3. 10-03-04 C6/36 3hpi negative control
4. 10-03-04 C6/36 RVFV ZH501 3hpi
5. 10-03-04 C6/36 RVFV ZH501 6hpi
6. 10-03-04 C6/36 RVFV ZH501 9hpi
7. 10-03-04 C6/36 12hpi negative control
8. 10-03-04 C6/36 RVFV ZH501 12hpi
9. 10-03-05 C6/36 12hpi negative control
10. 10-03-05 C6/36 RVFV ZH501 12hpi
11. 10-03-05 C6/36 RVFV ZH501 15hpi
12. 10-03-05 C6/36 RVFV ZH501 18hpi
13. 10-03-05 C6/36 21hpi negative control
14. 10-03-05 C6/36 RVFV ZH501 21hpi
15. 10-02-26 RVFV ZH501 semi-purified from C6/36 cells

Gels 3 & 4: timecourse in mammalian or insect cells up to 12hpi

1. -
2. SeeBlue Plus 2 prestained protein standard
3. 09-09-30 RVFV ZH501 semi-purified from Vero E6 cells
4. 10-02-26 RVFV ZH501 semi-purified from C6/36 cells
5. 09-12-10 Vero E6 3hpi negative control
6. 10-03-04 C6/36 3hpi negative control
7. 09-12-10 Vero E6 RVFV ZH501 3hpi
8. 10-03-04 C6/36 RVFV ZH501 3hpi
9. 09-12-10 Vero E6 RVFV ZH501 6hpi
10. 10-03-04 C6/36 RVFV ZH501 6hpi
11. 09-12-10 Vero E6 RVFV ZH501 9hpi
12. 10-03-04 C6/36 RVFV ZH501 9hpi
13. 09-12-10 Vero E6 12hpi negative control
14. 10-03-04 C6/36 12hpi negative control
15. 09-12-10 Vero E6 RVFV ZH501 12hpi
16. 10-03-04 C6/36 RVFV ZH501 12hpi

Gels 3 & 4: timecourse in mammalian or insect cells 12 to 21hpi

1. -
2. SeeBlue Plus 2 prestained protein standard
3. 09-09-30 RVFV ZH501 semi-purified from Vero E6 cells
4. 10-02-26 RVFV ZH501 semi-purified from C6/36 cells
5. 09-12-11 Vero E6 12hpi negative control
6. 10-03-05 C6/36 12hpi negative control
7. 09-12-11 Vero E6 RVFV ZH501 12hpi
8. 10-03-05 C6/36 RVFV ZH501 12hpi
9. 09-12-11 Vero E6 RVFV ZH501 15hpi
10. 10-03-05 C6/36 RVFV ZH501 15hpi
11. 09-12-11 Vero E6 RVFV ZH501 18hpi
12. 10-03-05 C6/36 RVFV ZH501 18hpi
13. 09-12-11 Vero E6 21hpi negative control
14. 10-03-05 C6/36 21hpi negative control
15. 09-12-11 Vero E6 RVFV ZH501 21hpi
16. 10-03-05 C6/36 RVFV ZH501 21hpi

- NuPAGE bis-tris 4-12% 17-lane gel in MES buffer at 200V constant for 35 minutes, 10 uL per well
- Dry blot transfer at 20V 7 minutes using Invitrogen iBlot (program P3)

Blocking

- Membranes blocked overnight with gentle rocking in 10mL of 5% skim milk TBS-T at 4°C
- Antibodies
 - Antibodies suspended in 5mL of 5% skim milk TBS-T
 - Blots incubated with antibodies for one hour with gentle rocking at room temperature
 - Antibody incubation was followed by 3 washes for 10 minutes in TBS-T with gentle rocking at room temperature

	PRIMARY	SECONDARY
Gel 1	anti-HIS conjugate (1:1000)	—
Gel 2	rabbit anti-N (1:2500) rabbit anti-NSs (1:2500)	goat anti-rabbit IgG (1:2000) goat anti-rabbit IgG (1:2000)

Protocol for Figures 17 and 18.

Cell growth and infection

- Seed HYPERFlasks with VeroE6 or C6/36 cells
- Add 560mL media per Hyperflask
- Infect with C6/36-amplified RVFV at MOI 0.1
- After 1 h of absorption, remove media, add 2% FBS (10mL) and replace media
- Vero E6: collect supernatant at 2dpi
- C6/36: collect supernatant at 6dpi
- Clarify virus with 3,000g centrifugation for 20 minutes at 4°C

Pre-concentrate virus with polyethylene glycol (PEG 6000) precipitation

- Add NaCl to increase molarity 0.5 Molar (58.4g/L, 32.7g/560mL HYPERFlask). Stir to dissolve.
- Refrigerate at 4°C for 2 hours
- Add PEG 6000 slowly while stirring to a final concentration of 10% w/v (56.0g/560mL HYPERFlask)
- Add glycerol to a final concentration of 3% v/v (16.8mL/560mL HYPERFlask)
- Stir overnight at 4°C
- Centrifuge at 3,000g × 60 minutes
- Discard supernatant and suspend pellet in 10mL 100mM NaCl 10mM HEPES (PEG-6000 solution)
- Some solid material could not be dissolved and was discarded (PEG-6000 precipitate)

Sucrose gradient ultracentrifugation

- Beckman Coulter Ultra-Clear 14mm x 89mm tubes (13.2mL volume)
- 1mL each of 10, 20, 30, 40, 50% sucrose (w/v) in TN buffer

Opti-Prep (iodixanol) gradient ultracentrifugation

- Beckman Coulter Ultra-Clear 14mm x 89mm tubes (13.2mL volume)
- 1.5mL each of 10, 20, 30, 40% in 0.1 M NaCl, 1 mM EDTA, 0.01 M Tris-HCl, pH 7.4

Ultracentrifugation

- Remaining volume of all tubes filled with clear resuspension of PEG-precipitated virus
- All tubes were balanced within 0.05g
- Samples were centrifuged in an SW41 Ti rotor at 40,000 rpm for two hours at 4°C, exerting between 200,000g and 275,000g down the length of the tube
- Visible protein bands were collected by top-entry syringe aspiration

Sample extraction from BSL-3+

- 75uL samples were mixed with 25uL NuPAGE sample buffer in 1.5mL microcentrifuge tubes and heated to 95 °C for 30 minutes

NuPAGE bis-tris 4-12% 17-lane gel in MOPS buffer at 150V constant for 60 minutes,

- 2 slides at 5 uL sample per well
- 2 slides at 10 uL sample per well

Dry blot transfer at 20V for 7 minutes using Invitrogen iBlot (program P3)

Blocking

- Membranes blocked in 10mL of 5% skim milk TBS-T for 1 hour at room temperature with gentle rocking

Antibody incubations

- Antibodies suspended in 5mL of 5% skim milk TBS-T
- Blots were incubated with primary antibodies overnight at 4°C with gentle rocking
- Antibody incubation was followed by 3 washes for 10 minutes each in TBS-T at room temperature with gentle rocking

Primary antibodies

- Rabbit anti-N (1:1000, previously used at 1:5000)
- Rabbit anti-NSs (1:1000)
- Rabbit anti-NSm1 R1108 (1:1000, previously used at 1:200)

Secondary antibodies

- Goat anti-rabbit IgG (1:2000)

Chromogenic detection of signal

- Unit of of Sigma FastDAB in 5mL milli-Q H₂O per membrane

Immunoblots with ECL Detection

1 × NuPAGE 4-12% Bis-Tris 1.0mm thick 15-well gel

Lane		Sample (μ L)	Buffer (μ L)	DTT (μ L)	Water (μ L)	Total (μ L)
1						
2	Novex Sharp protein standard	-	-	-	-	10.0
3	MagicMark XP protein standard	-	-	-	-	10.0
4	2010-09-30 rNSm1 (1:64 dilution)	0.15	2.5	1.0	6.35	10.0
5	Vero E6 low band	6.5	2.5	1.0	-	10.0
6	C6/36 low band 2	6.5	2.5	1.0	-	10.0
7	MagicMark XP protein standard	-	-	-	-	10.0
8						
9	Novex Sharp protein standard	-	-	-	-	10.0
10	MagicMark XP protein standard	-	-	-	-	10.0
11	2010-09-30 rNSm1 (1:64 dilution)	0.15	2.5	1.0	6.35	10.0
12	Vero E6 low band	6.5	2.5	1.0	-	10.0
13	C6/36 low band 2	6.5	2.5	1.0	-	10.0
14	MagicMark XP protein standard	-	-	-	-	10.0
15						

1 × NuPAGE 4-12% Bis-Tris 1.0mm thick 12-well gel

Lane		Sample (μ L)	Buffer (μ L)	DTT (μ L)	Water (μ L)	Total (μ L)
1	Novex Sharp protein standard	-	-	-	-	10.0
2	MagicMark XP protein standard	-	-	-	-	10.0
3	2010-09-30 rNSm1 (1:64 dilution)	0.15	2.5	1.0	6.35	10.0
4	Vero E6 low band	6.5	2.5	1.0	-	10.0
5	C6/36 low band 2	6.5	2.5	1.0	-	10.0
6	MagicMark XP protein standard	-	-	-	-	10.0
7	Novex Sharp protein standard	-	-	-	-	10.0
8	MagicMark XP protein standard	-	-	-	-	10.0
9	2010-09-30 rNSm1 (1:64 dilution)	0.15	2.5	1.0	6.35	10.0
10	Vero E6 low band	6.5	2.5	1.0	-	10.0
11	C6/36 low band 2	6.5	2.5	1.0	-	10.0
12	MagicMark XP protein standard	-	-	-	-	10.0

Immunoblots with ECL Detection (continued)

790mL MOPS buffer was prepared. The 200mL volume in the upper reservoir of the western blot also had 0.5mL NuPAGE antioxidant.

Run in MOPS buffer at 150V constant for 1 hour.

Transferred to PVDF membranes on iBlot at 20V constant for 13 minutes.

Blocked in 10mL of 5% skim milk TBS-T per membrane for 1 hour at room temperature with gentle rocking.

Primary antibodies were applied in 5mL of 5% skim milk TBS-T per membrane overnight at 4°C with gentle rocking.

R1109 rabbit anti-NSm1 (1:100)

Sheep 11, 12, 13, 14 anti-RVFPV 29dpi (1:100)

Blots were washed 3 × 10 minutes in 10mL TBS-T per membrane at room temperature with gentle rocking.

Secondary antibodies were applied in 5mL of 5% skim milk TBS-T per membrane overnight at 4°C with gentle rocking.

KPL goat anti-rabbit IgG conjugate HRP (1:500)

KPL rabbit anti-sheep IgG conjugate HRP (1:1000)

Blots were washed 3 × 10 minutes in 10mL TBS-T per membrane at room temperature with gentle rocking.

Amersham ECL reagents A and B were mixed in equal volumes. Blots were covered with approximately 1.5mL each and incubated at room temperature for 4 minutes.

ECL was imaged using BioRad ChemiDoc to determine approximate exposure times.

ECL was imaged at higher resolution using Kodak BioMax light film.

Plaque Assay Titration of Rift Valley Fever Virus

Dilution tubes

- 16 × 5mL dilution tubes
 - 2.25mL DMEM each
- 150mL 2% CMC overlay

Plates

- Vero E6 cells were grown to passage 61
- 4 × P24 plates were seeded at 125,000 cells/cm²
- Plates were seeded with 1mL DMEM +10% FBS media per well at 250,000 cells/mL into each 2cm² well

Virus Titration

Cell Preparation

- Remove media from 4 confluent P24 plates of Vero E6 cells
- Wash cells twice with 0.5mL serum-free DMEM per well

Virus Dilution

- Add 250μL VE6-RVFPV stock virus into 2.25mL DMEM to create 10⁻¹ dilution
 - Mix thoroughly
 - Move 250μL to another tube containing 2.25mL DMEM (10⁻² dilution)
 - Repeat to 10⁻⁸ dilution
- Repeat for C6/36-RVFPV stock virus

Virus/Plaque Growth

- Add 250μL of infectious media per well
- Incubate 1 hour at 37°C
- Remove infectious media
- Add 1mL of 2% CMC overlay
- Incubate at 37°C

Fixing & Staining

- Add 10% buffered formalin to the wells containing CMC
- Incubate in formalin at room temperature for at least 30 minutes, up to overnight
- Remove CMC/formalin mixture inactivate with 1 part Formalex to 4 parts Formalin
- Wash cells gently under running water until all CMC is removed
- Add 5% crystal violet in ethanol
- Incubate at RT for 30 minutes
- Wash cells gently under running water
- Let dry
- Count plaques

Plaque Assay Titration of Rift Valley Fever Virus (continued)

Plate Layout

10^{-3}	10^{-4}	10^{-5}	10^{-6}	10^{-7}	Cell Control
10^{-3}	10^{-4}	10^{-5}	10^{-6}	10^{-7}	Cell Control
10^{-3}	10^{-4}	10^{-5}	10^{-6}	10^{-7}	Cell Control
10^{-3}	10^{-4}	10^{-5}	10^{-6}	10^{-7}	Cell Control

10^{-4}	10^{-5}	10^{-6}	10^{-7}	10^{-8}	Cell Control
10^{-4}	10^{-5}	10^{-6}	10^{-7}	10^{-8}	Cell Control
10^{-4}	10^{-5}	10^{-6}	10^{-7}	10^{-8}	Cell Control
10^{-4}	10^{-5}	10^{-6}	10^{-7}	10^{-8}	Cell Control

Sheep Serum RVFV Neutralization Assay

Overview

This assay will investigate differences in neutralization binding by sheep serum, raised against Vero E6-derived RVFV, against Vero E6

Materials per 2 sera

- 8 confluent P24 plates of Vero E6 cells
- 42 × 5mL dilution tubes (serum dilution)
 - 2 × 1.8mL DMEM
 - 40 × 1mL DMEM
- 9 × 14mL dilution tubes (virus dilution)
 - 8 × 9mL DMEM
 - 1 × 10mL DMEM
- 24 × 1.5mL microcentrifuge tubes
 - 12 × 450 µL DMEM (serum control)
 - 2 × empty (virus 10⁰ back-titration)
 - 2 × 900 µL DMEM (virus 10⁻¹, 10⁻² back-titration)
 - 8 × 400 µL DMEM (virus back-titration)
- 48 × 1.5mL microcentrifuge tubes (serum/virus neutralization)
- 200mL 1.5% CMC overlay

Sera

- Sheep 13, 27dpi
- Sheep 14, 27dpi

Plates

- Vero E6 cells were grown
- 8 × P24 plates were seeded at 120,000 cells/cm² (5.76 × 10⁶ cells per plate) on 2010-10-24
- Plates were seeded with 1mL DMEM +10% FBS media per well at 240,000 cells/mL into each 2cm² well

Serum Dilution

- Add 200 µL serum into 1.8mL DMEM to create 1/10 dilution (1/20 with virus)
 - Move 1mL to tube containing 1mL DMEM
 - Repeat 11 times (12 tubes total)
 - Discard 1mL from last tube
- Add 200 µL of 1/10 dilution serum into 1 mL DMEM to create 1/60 dilution (1/120 with virus)
 - Move 1mL to tube containing 1mL DMEM
 - Repeat 8 times (9 tubes total)
 - Discard 1mL from last tube

Starting dilution 1:1 serial dilution	$1/20$	$1/120$
1	20	120
2	40	240
3	80	480
4	160	960
5	320	1920
6	640	3840
7	1280	7680
8	2560	
9	5120	
10	10240	
11		
12		

Dilution values after mixing 1:1 with virus.

Dilutions in **red** will be plated.

Serum Control

- 6 × 450 µL DMEM in 1.5mL microcentrifuge tubes
- Add 150 µL of the following serum dilutions: $1/480$, $1/640$, $1/960$, $1/1,280$, $1/1,920$, $1/2,560$

Virus Dilution

- Vero E6-amplified virus
 - On ice, dilute virus in serum-free DMEM to 200pfu/250µL (800pfu/mL, $10^{2.9}$ pfu/mL)
 - RVFV stock $10^{6.6}$ pfu/mL
 - 1mL + 9mL serum-free DMEM = $10^{5.68}$ pfu/mL
 - 1mL + 9mL serum-free DMEM = $10^{4.68}$ pfu/mL
 - 1mL + 9mL serum-free DMEM = $10^{3.68}$ pfu/mL
 - 2mL + 10mL serum-free DMEM = $10^{2.90}$ pfu/mL
 - Dilution in serum-free DMEM (800pfu/mL) for back titration
 - 1mL of $10^{2.90}$ pfu/mL (10^0)
 - 100µL + 900µL serum-free DMEM = $10^{1.90}$ pfu/mL (10^{-1})
- C6/36-amplified virus
 - On ice, dilute virus in serum-free DMEM to 200pfu/250µL (800pfu/mL, $10^{2.9}$ pfu/mL)
 - RVFV stock $10^{7.5}$ pfu/mL
 - 1mL + 9mL serum-free DMEM = $10^{6.50}$ pfu/mL
 - 1mL + 9mL serum-free DMEM = $10^{5.50}$ pfu/mL
 - 1mL + 9mL serum-free DMEM = $10^{4.50}$ pfu/mL
 - 1mL + 9mL serum-free DMEM = $10^{3.50}$ pfu/mL
 - 3mL + 9mL serum-free DMEM = $10^{2.90}$ pfu/mL

- Dilution in serum-free DMEM (200pfu/mL) for "10⁻¹" column of back titration
 - 1mL of 10^{2.90} pfu/mL (10⁰)
 - 100μL + 900μL serum-free DMEM = 10^{1.90} pfu/mL (10⁻¹)
- Keep on ice until ready to use

Back Titration

- 12 × 400 DMEM in 1.5mL microcentrifuge tubes
- Add 400 μL of 10⁰ or 10⁻¹ virus dilutions from 10^{2.9} pfu/mL working stock of each virus

Virus Neutralization

- 12 × 400 μL Vero E6-virus (10^{2.9} pfu/mL) placed in 1.5mL microcentrifuge tube
- Add 400 μL of the following serum dilutions: 1/960, 1/1,280, 1/1,920, 1/2,560, 1/3,840, 1/5,120, 1/7,680, 1/10,240, 1/15,360, 1/20,480, 1/30,720, 1/40,960.
- Repeat for C6/36-virus
- Incubate virus and serum for 1 hour at 37°C

Cell Preparation

- Remove media from 4 confluent P24 plates of Vero E6 cells
- Wash cells with PBS

Virus/Plaque Growth

- Add 250μL of virus/serum mixture directly to cells (100pfu/well)
- Incubate 1 hour at 37°C
- Remove infectious media
- Add 1.5% CMC overlay
- Incubate 4 days at 37°C

Fixing & Staining

- Add 10% buffered formalin to the wells containing CMC
- Incubate in formalin at room temperature for at least 30 minutes, up to overnight
- Remove CMC/formalin mixture inactivate with 1 part Formalex to 4 parts Formalin
- Wash cells gently under running water until all CMC is removed
- Add 5% crystal violet in ethanol
- Incubate at RT for 15 to 30 minutes
- Wash cells gently under running water
- Let dry
- Count plaques

Plate layout

	Sheep Serum & C6/36 RVFV (100 pfu/well)			Sheep Serum control
$1/_{240}$				
$1/_{320}$				
$1/_{480}$				10^0
$1/_{640}$				10^0
$1/_{960}$				10^{-1}
$1/_{1,280}$				10^{-1}

	Sheep Serum & C6/36 RVFV (100 pfu/well)			Back Titration
$1/_{1,920}$				10^0
$1/_{2,560}$				10^0
$1/_{3,840}$				10^0
$1/_{5,120}$				10^{-1}
$1/_{7,680}$				10^{-1}
$1/_{10,240}$				10^{-1}

Appendix D. Supplemental Figures

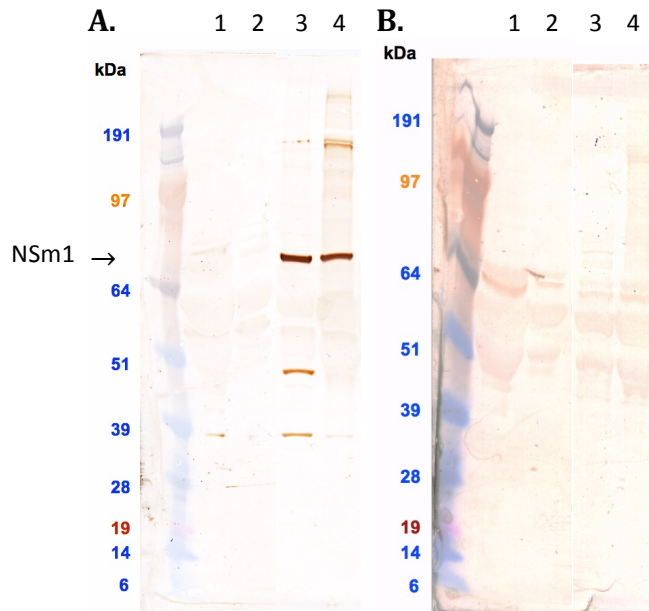


Figure D1. Immunoblot detection of NSm1 in RVFV concentrated supernatant and cell infected cell lysate, run on a denaturing NuPAGE 4-12% bis-tris gel in MOPS buffer with SeeBlue Plus 2 pre-stained protein standard. Lanes, left to right: 1. Vero E3 mock-infected control media. 2. C6/36 mock-infected control media. 3. RVFV-infected Vero E6 clarified supernatant concentrated using a 100kDa NMWL retention filter. 4. RVFV-infected C6/36 clarified supernatant concentrated using a 100kDa NMWL retention filter. All samples were diluted to 2.0 $\mu\text{g}/\mu\text{L}$ based on absorbance measured on a spectrophotometer at 280nm wavelength. **A.** Immunoblotted with rabbit R1108 anti-NSm1 serum (1:1000 dilution) and secondary goat anti-rabbit IgG HRP (1:2000 dilution). **B.** Immunoblotted with rabbit R1108 pre-bleed serum (1:200 dilution) and secondary goat anti-rabbit IgG HRP (1:2000 dilution). These blots show that NSm1 is produced in both Vero E6 and C6/36 cells, as it can be found in concentrated infectious supernatant but not in concentrated control supernatant. Other nonspecific binding seen in A can also be found in the uninfected control lanes of Figure D2 but a positive identification of each protein band would require mass spectrometry.

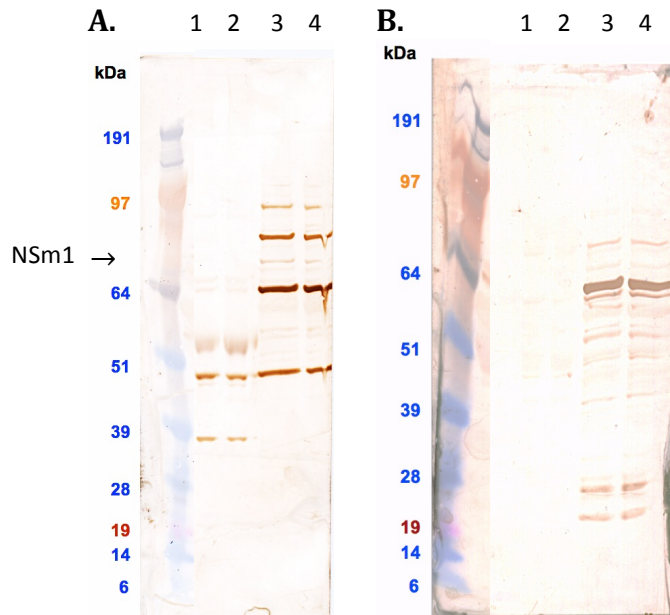


Figure D2. Immunoblot detection of NSm1 in RVFV concentrated supernatant and cell infected cell lysate, run on a denaturing NuPAGE 4-12% bis-tris gel in MOPS buffer. Lanes, left to right: 1. Mock-infected Vero E6 cell lysate collected 21 hpi. 2. RVFV-infected Vero E6 cell lysate collected 21 hpi. 3. Mock-infected C6/36 cell lysate collected 21 hpi. 4. RVFV-infected C6/36 cell lysate collected 21 hpi. All samples were diluted to 2.0 $\mu\text{g}/\mu\text{L}$ based on absorbance measured on a spectrophotometer at 280nm wavelength. Apparent molecular weights were compared with SeeBlue Plus 2 pre-stained protein standard. **A.** Immunoblotted with rabbit R1108 anti-NSm1 serum (1:1000 dilution) and secondary goat anti-rabbit IgG HRP (1:2000 dilution). **B.** Immunoblotted with rabbit R1108 pre-bleed serum (1:200 dilution) and secondary goat anti-rabbit IgG HRP (1:2000 dilution). These blots show that the R1108 anti-NSm1 serum is unable to detect any bands at 21hpi that are not also found in the uninfected control cells, but a positive identification of each protein band would require mass spectrometry.